REDOX-ACTIVE MOLECULES AS ANTIMICROBIALS: MECHANISMS AND RESISTANCE

EDITED BY: Martin C. H. Gruhlke, Jong H. Kim, Kirkwood M. Land and Luisa Cheng

PUBLISHED IN: Frontiers in Microbiology

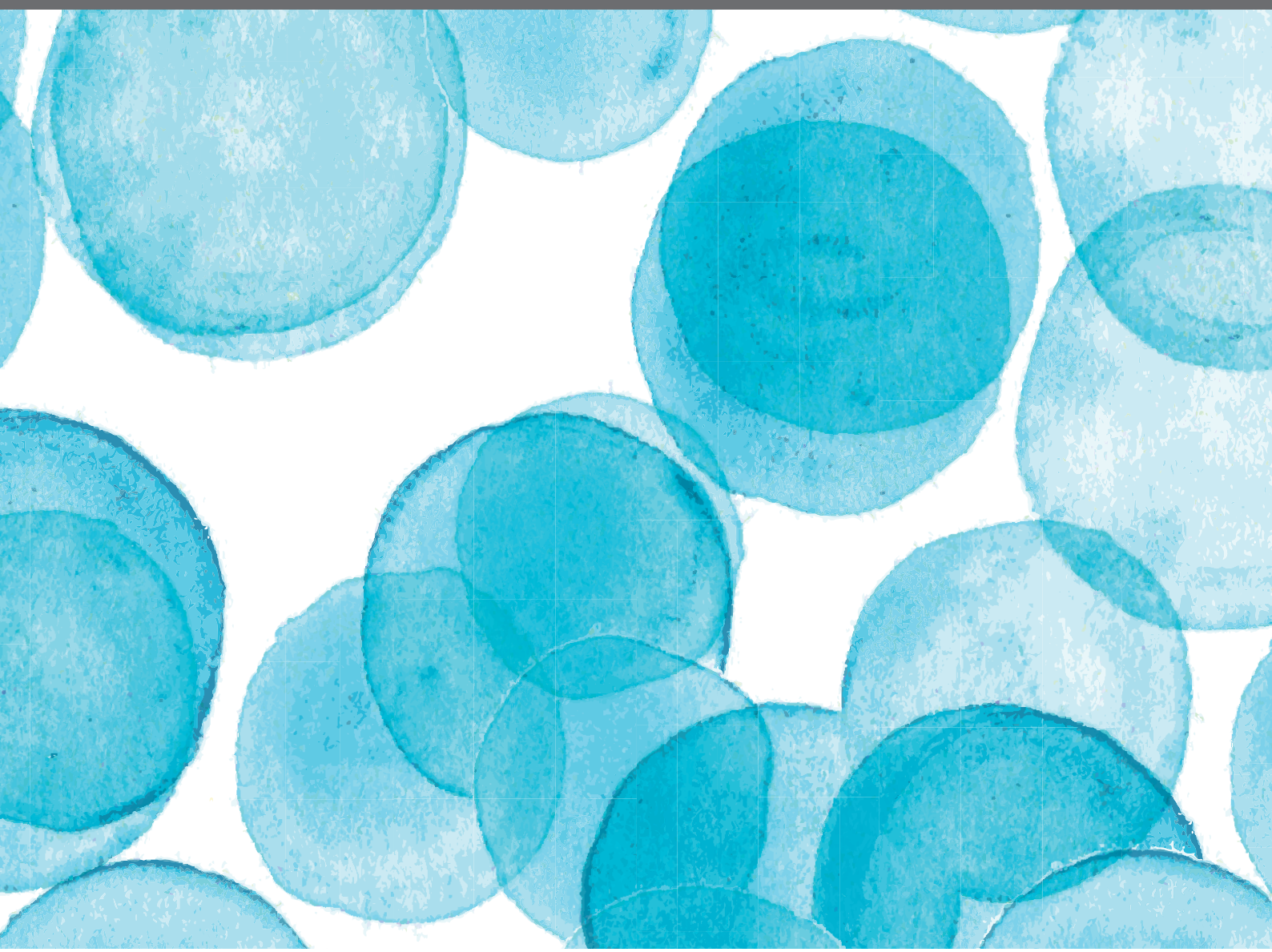

frontiers Research Topics

ISSN 1664-8714
ISBN 978-2-88971-637-1
DOI 10.3389/978-2-88971-637-1

About Frontiers

Frontiers is more than just an open-access publisher of scholarly articles: it is a pioneering approach to the world of academia, radically improving the way scholarly research is managed. The grand vision of Frontiers is a world where all people have an equal opportunity to seek, share and generate knowledge. Frontiers provides immediate and permanent online open access to all its publications, but this alone is not enough to realize our grand goals.

Frontiers Journal Series

The Frontiers Journal Series is a multi-tier and interdisciplinary set of open-access, online journals, promising a paradigm shift from the current review, selection and dissemination processes in academic publishing. All Frontiers journals are driven by researchers for researchers; therefore, they constitute a service to the scholarly community. At the same time, the Frontiers Journal Series operates on a revolutionary invention, the tiered publishing system, initially addressing specific communities of scholars, and gradually climbing up to broader public understanding, thus serving the interests of the lay society, too.

Dedication to Quality

Each Frontiers article is a landmark of the highest quality, thanks to genuinely collaborative interactions between authors and review editors, who include some of the world's best academicians. Research must be certified by peers before entering a stream of knowledge that may eventually reach the public - and shape society; therefore, Frontiers only applies the most rigorous and unbiased reviews.
Frontiers revolutionizes research publishing by freely delivering the most outstanding research, evaluated with no bias from both the academic and social point of view. By applying the most advanced information technologies, Frontiers is catapulting scholarly publishing into a new generation.

What are Frontiers Research Topics?

Frontiers Research Topics are very popular trademarks of the Frontiers Journals Series: they are collections of at least ten articles, all centered on a particular subject. With their unique mix of varied contributions from Original Research to Review Articles, Frontiers Research Topics unify the most influential researchers, the latest key findings and historical advances in a hot research area! Find out more on how to host your own Frontiers Research Topic or contribute to one as an author by contacting the Frontiers Editorial Office: frontiersin.org/about/contact

REDOX-ACTIVE MOLECULES AS ANTIMICROBIALS: MECHANISMS AND RESISTANCE

Topic Editors:
Martin C. H. Gruhlke, RWTH Aachen University, Germany
Jong H. Kim, Agricultural Research Service, United States
Kirkwood M. Land, The University of the Pacific, United States
Luisa Cheng, United States Department of Agriculture (USDA), United States

Citation: Gruhlke, M. C. H., Kim, J. H., Land, K. M., Cheng, L., eds. (2021). Redox-Active Molecules as Antimicrobials: Mechanisms and Resistance. Lausanne: Frontiers Media SA. doi: 10.3389/978-2-88971-637-1

Table of Contents

frontiers in Microbiology

EDITORIAL
published: 10 September 2021
doi: 10.3389/fmicb.2021.758750

Editorial: Redox-Active Molecules as Antimicrobials: Mechanisms and Resistance

Jong H. Kim[1]*, *Luisa W. Cheng*[1]*, *Kirkwood M. Land*[2]* and *Martin C. H. Gruhlke*[3,4]*

[1] Western Regional Research Center, Agricultural Research Service, Foodborne Toxin Detection and Prevention Research Unit, United States Department of Agriculture, Albany, CA, United States, [2] Department of Biological Sciences, University of the Pacific, Stockton, CA, United States, [3] Department of Plant Physiology, Rheinisch-Westfälische Technische Hochschule Aachen University, Aachen, Germany, [4] GENAWIF e.V. – Society for Natural Compound and Active Substance Research, Aachen, Germany

Keywords: antimicrobials, drug resistance, mode of action, redox molecules, sulfur compounds

OPEN ACCESS

Edited by:
Rustam Aminov, University of Aberdeen, United Kingdom

Reviewed by:
Alvaro Mourenza Flórez, University of Southern California, United States

***Correspondence:**
Jong H. Kim
jongheon.kim@usda.gov
Luisa W. Cheng
luisa.cheng@usda.gov
Kirkwood M. Land
kland@pacific.edu
Martin C. H. Gruhlke
martin.gruhlke@rwth-aachen.de

Specialty section:
This article was submitted to Antimicrobials, Resistance and Chemotherapy, a section of the journal Frontiers in Microbiology

Received: *14 August 2021*
Accepted: *20 August 2021*
Published: *10 September 2021*

Citation:
Kim JH, Cheng LW, Land KM and Gruhlke MCH (2021) Editorial: Redox-Active Molecules as Antimicrobials: Mechanisms and Resistance. Front. Microbiol. 12:758750. doi: 10.3389/fmicb.2021.758750

Editorial on the Research Topic

Redox-Active Molecules as Antimicrobials: Mechanisms and Resistance

Current drugs for treating microbial infections have limited efficiency, especially for eliminating drug resistant pathogens. Although high-throughput screenings have been investigated for identifying novel antimicrobial drug candidates, stagnation in development of new, safe antimicrobial agents is a persistent public health concern (Tillotson and Tillotson, 2015). Recent investigations have determined that the antimicrobial mechanisms of certain drugs involve oxidative stress/damage in pathogens, and therefore, those drugs are further defined as oxidative stress drugs. For example, ciprofloxacin is a fluoroquinolone antibiotic inhibiting the function of DNA topoisomerases. Of note, when bacteria are treated with ciprofloxacin, the level of reactive oxygen species (ROS) increases in the pathogens. However, application of antioxidant molecules or transfection of superoxide dismutase gene into bacteria reversed fluoroquinolone toxicity (Goswami et al., 2006). Various sulfur compounds as natural substances belong to the class of reactive sulfur species and lead to a modification of cysteine protein residues by oxidative means, which leads to antimicrobial capability in pathogenic bacteria (for example, in the case of the natural substance allicin; Loi et al., 2019). The anti-parasitic drug albendazole (ABZ) is commonly used for treating the parasitic protozoan *Giardia duodenalis*. Besides binding to β-tubulin, ABZ also induces oxidative stress and DNA damage in *G. duodenalis* (Martínez-Espinosa et al., 2015). Amphotericin B (AMB) is a polyene antifungal drug that binds to ergosterol in cell membrane. While AMB binding results in membrane depolarization, alteration in permeability, and cellular leakage/rupture, induction of cellular oxidative damage is another antifungal action of AMB (Jukic et al., 2017).

ROS-generating antimicrobials is an important subject in antimicrobial resistance study, where modern sensors are employed to accurately analyze the levels of ROS generated by redox-active antimicrobials against different pathogens. For instance, to target the bacterial pathogen *Pseudomonas aeruginosa* via exogenous ROS generation system, a glycomimetic-decorated fluorescent nanobiocide was developed which mediates ROS release from the functionalized CuInS/ZnS quantum dots (Li et al., 2021). This system simultaneously fulfilled a fluorescent monitoring and sterilization, where the fluorescence intensity was determined at 525 nm by the microplate reader. The natural naphthoquinone lapachol induced oxidative stress (ROS formation) against *Staphylococcus aureus*, a human pathogen rapidly acquiring multidrug resistance. The level of oxidation by lapachol was determined using *S. aureus* expressing the biosensor plasmids (Linzner et al., 2020), where the biosensor fluorescence emission was measured at 510 nm;

a similar biosensor was further applied against a mycoredoxin-null mutant of *Rhodococcus equi* (mammalian pathogen) to screen ROS-generating antibiotics exerting drug synergism (Mourenza et al., 2020). Meanwhile, the use of photosensitizers was investigated in photodynamic therapy against the yeast pathogen *Candida albicans*, where the production of ROS was determined using an electron paramagnetic resonance spectrometer (Kanpittaya et al., 2021). While all photosensitizers tested exhibited no toxicity on the fibroblast cells, selected photosensitizers inhibited *C. albicans* like the polyene drug nystatin. Further studies utilizing sensors to investigate ROS-generating antimicrobials include: (a) real-time single-cell fluorescence on *Escherichia coli* stained with a fluorogenic probe measuring lipid peroxyl radicals after ciprofloxacin treatment (Martínez et al., 2020), and (b) aggregation-induced emission (AIE) luminogens possessing high ROS generating capacity as a probe, which simultaneously detecting and performing photodynamic ablation of macrophage-engulfed Gram-positive bacteria (Lee et al., 2020).

In this Research Topic, six works (four original research articles, one review and one hypothesis and theory) were published on the use of redox-active molecules as antimicrobials, providing oxidative mechanisms and resistance management tools.

Thioredoxin reductase (TrxR) maintains systemic redox homeostasis in Gram-positive bacteria, limited number of Gram-negative bacteria and several parasites, hence TrxR can serve as a potential therapeutic target. In their Hypothesis and Theory paper, Felix et al. described that TrxR is a potential target for auranofin, ebselen, shikonin, and allicin, where auranofin is the most potent drug. Auranofin has been used as an anti-rheumatoid/arthritis drug but is recently repurposed to treat microbial infection. Auranofin interacts with TrxR in Gram-positive bacteria, where the CXXC motif could be the target. However, most Gram-negative bacteria can use another antioxidant system, glutathione-glutaredoxin (GSH), to scavenge reactive oxygen/nitrogen species and maintain redox homeostasis. GSH-independent pathogens, notably the clinically important *Mycobacterium tuberculosis* and Gram-negative *Helicobacter pylori*, remain susceptible to TrxR inhibitory drugs.

In a related study, Gong et al. investigated the effect of increased temperature on metronidazole resistance in *H. pylori*, where RNA-sequencing based transcriptomic profiling identified differentially expressed genes when the pathogen was grown at 41°C. Resistance to metronidazole was reduced at the higher temperature. Redox pathways seemed the potential drivers of metronidazole resistance at higher temperature; the expression of superoxide dismutase (*Sod*) gene was down-regulated at 41°C, and accompanied by the enhancement of a negative regulator of *Sod*. However, the transcriptional changes in TrxR system were not determined in the study.

The antibacterial mechanism of lysozyme-coated silver nanoparticles (AgNPs) was investigated in a multi-drug resistant *Klebsiella pneumonia* (Pareek et al.). AgNPs provide a greater surface area, leading to an enhanced controlled release of silver ion (Ag^+) to the target. Biochemical and transcriptional analyses (RNA sequencing) revealed AgNPs induced a *triclosan-like* bactericidal effect, thus inhibiting the expression of the type II fatty acid biosynthesis genes. Of note, the released Ag ion triggered oxidative stress in *K. pneumonia*, where Δ*soxS* mutant exhibited increased susceptibility to AgNPs compared to the wild type.

The protozoan parasite *Trypanosoma cruzi* is a causative agent of Chagas disease. Although benznidazole is currently the main therapeutic agent, this drug causes severe side effects while possessing low efficacy against the chronic phase of the disease. Macedo et al. examined the trypanocidal efficacy of novel phenyl-*tert*-butyl-nitrone (PBN) derivate LQB303 against *T. cruzi*, where this compound exhibited a potent trypanocidal activity against intra-/extracellular amastigotes *in vitro*. LQB303 caused mitochondrial dysfunction, which resulted in impaired oxygen consumption and the spare respiratory capacity of amastigotes. Of note, one of the PBN derivatives *alpha*-phenyl-*N*-*tert*-butylnitrone (PBN) nitrone possesses free radical spin trap capacity, thus exhibiting low toxicity to the host.

Certain azole fungicides applied to crop fields have the same mode of antifungal action as clinical azole drugs. Hence, long-term application of azole fungicides to agricultural fields provides a selection pressure for the emergence of pan-azole-resistant fungal pathogens. Meanwhile, thymol is a redox-active secondary metabolite that can induce oxidative stress in pathogens or impair fungal antioxidant systems. Shcherbakova et al. recently investigated the chemosensitizing capability of thymol to the azole fungicides difenoconazole and tebuconazole. In both seed and foliar treatments, co-application of thymol with azole fungicides synergistically inhibited the growth of the phytopathogens *Bipolaris sorokiniana*, *Parastagonospora nodorum* and *Fusarium culmorum*, while thymol did not enhance the production of mycotoxins (deoxynivalenol, zearalenone). A chemosensitizer, such as thymol, causes the target pathogen to become more susceptible to the co-applied drug by negatively modulating the pathogen's defense system.

Finally, Li et al. reviewed the involvement of ROS in antibiotic- and host-mediated pathogen killing. For example, quinolones-induced killing of bacterial pathogens is accompanied by the generation of endogenous hydroxyl radicals; primary damage caused by antibiotics stimulates a pathway that leads to ROS accumulation as a secondary damage. Exogenous ROS are generated from NADPH oxidase *via* phagocytes in the host cells, and could directly kill pathogens. It remains unknown precisely how phagocytic ROS inhibits pathogen growth. Li et al. described exogenous ROS-induced killing depends on a variety of innate mechanisms.

In summary, the antioxidant system of microbes could be an effective target for pathogen control. Redox-active molecules (natural or synthetic) can function as potent redox-cyclers in microbes, which contributes to the inhibition of pathogen growth by disrupting cellular redox homeostasis or the function of redox-sensitive cellular components. Identification of new, safe redox-active molecules and elucidation of their oxidative mechanisms will further the control of microbial pathogens, especially those resistant to current therapeutic agents.

AUTHOR CONTRIBUTIONS

JK, LC, KL, and MG were joint co-editors of this Research Topic. All authors contributed equally to the article and approved the submitted version.

FUNDING

JK and LC were supported by USDA-ARS CRIS Project 5325-42000-054-00D.

ACKNOWLEDGMENTS

The editors would like to acknowledge and thank the authors for their contributions, and all the reviewers for their effort, expertise and constructive suggestions that significantly contributed to the quality of this Research Topic. We would also like to thank Kathleen L. Chan, Foodborne Toxin Detection and Prevention Research Unit, Western Regional Research Center, USDA-ARS, for technical assistance.

REFERENCES

Goswami, M., Mangoli, S. H., and Jawali, N. (2006). Involvement of reactive oxygen species in the action of ciprofloxacin against *Escherichia coli*. *Antimicrob. Agents Chemother.* 50, 949–954. doi: 10.1128/AAC.50.3.949-954.2006

Jukic, E., Blatzer, M., Posch, W., Steger, M., Binder, U., Lass-Flörl, C., et al. (2017). Oxidative stress response tips the balance in *Aspergillus terreus* amphotericin B resistance. *Antimicrob. Agents Chemother.* 61, e00670–e00617. doi: 10.1128/AAC.00670-17

Kanpittaya, K., Teerakapong, A., Morales, N. P., Hormdee, D., Priprem, A., Weera-archakul, W., et al. (2021). Inhibitory effects of erythrosine/curcumin derivatives/nano-titanium dioxide-mediated photodynamic therapy on *Candida albicans*. *Molecules* 26:2405. doi: 10.3390/molecules26092405

Lee, M. M. S., Yan, D., Chau, J. H. C., Park, H., Ma, C. C. H., Kwok, R. T. K., et al. (2020). Highly efficient phototheranostics of macrophage-engulfed Gram-positive bacteria using a NIR luminogen with aggregation-induced emission characteristics. *Biomaterials* 261:120340. doi: 10.1016/j.biomaterials.2020.120340

Li, J., Wei, X., Hu, Y., Gao, Y., Zhang, Y., and Zhang, X. (2021). A fluorescent nanobiocide based on ROS generation for eliminating pathogenic and multidrug-resistant bacteria. *J. Mater. Chem. B.* 9, 3689–3695. doi: 10.1039/D1TB00273B

Linzner, N., Fritsch, V. N., Busche, T., Tung, Q. N., Loi, V. V., Bernhardt, J., et al. (2020). The plant-derived naphthoquinone lapachol causes an oxidative stress response in *Staphylococcus aureus*. *Free Radic. Biol. Med.* 158, 126–136. doi: 10.1016/j.freeradbiomed.2020.07.025

Loi, V. V., Huyen, N. T. T., Busche, T., Tung, Q. N., Gruhlke, M. C. H., Kalinowski, J., et al. (2019). *Staphylococcus aureus* responds to allicin by global *S*-thioallylation – role of the Brx/BSH/YpdA pathway and the disulfide reductase MerA to overcome allicin stress. *Free Radic. Biol. Med.* 139, 55–69. doi: 10.1016/j.freeradbiomed.2019.05.018

Martínez, S. R., Durantini, A. M., Becerra, M. C., and Cosa, G. (2020). Real-time single-cell imaging reveals accelerating lipid peroxyl radical formation in *Escherichia coli* triggered by a fluoroquinolone antibiotic. *ACS Infect. Dis.* 6, 2468–2477. doi: 10.1021/acsinfecdis.0c00317

Martínez-Espinosa, R., Argüello-García, R., Saavedra, E., and Ortega-Pierres, G. (2015). Albendazole induces oxidative stress and DNA damage in the parasitic protozoan *Giardia duodenalis*. *Front. Microbiol.* 6:800. doi: 10.3389/fmicb.2015.00800

Mourenza, Á., Gil, J. A., Mateos, L. M., and Letek, M. (2020). A novel screening strategy reveals ROS-generating antimicrobials that act synergistically against the intracellular veterinary pathogen *Rhodococcus equi*. *Antioxidants* 9:114. doi: 10.3390/antiox9020114

Tillotson, J., and Tillotson, G. S. (2015). The regulatory pathway for antifungal drugs: a US perspective. *Clin. Infect. Dis.* 61, S678–S683. doi: 10.1093/cid/civ819

Conflict of Interest: The authors declare that the research was conducted in the absence of any commercial or financial relationships that could be construed as a potential conflict of interest.

Publisher's Note: All claims expressed in this article are solely those of the authors and do not necessarily represent those of their affiliated organizations, or those of the publisher, the editors and the reviewers. Any product that may be evaluated in this article, or claim that may be made by its manufacturer, is not guaranteed or endorsed by the publisher.

frontiers in Microbiology

MINI REVIEW
published: 04 February 2021
doi: 10.3389/fmicb.2020.622534

Reactive Oxygen Species in Pathogen Clearance: The Killing Mechanisms, the Adaption Response, and the Side Effects

Hao Li, Xuedong Zhou, Yuyao Huang, Binyou Liao, Lei Cheng and Biao Ren**

State Key Laboratory of Oral Diseases, National Clinical Research Center for Oral Diseases, West China Hospital of Stomatology, Sichuan University, Chengdu, China

OPEN ACCESS

Edited by:
Kirkwood M. Land, University of the Pacific, United States

Reviewed by:
Tim Maisch, University of Regensburg, Germany
Kristin M. Burkholder, University of New England, United States

***Correspondence:**
Lei Cheng
chenglei@scu.edu.cn
Biao Ren
renbiao@scu.edu.cn

Specialty section:
This article was submitted to Antimicrobials, Resistance and Chemotherapy, a section of the journal Frontiers in Microbiology

Received: *28 October 2020*
Accepted: *28 December 2020*
Published: *04 February 2021*

Citation:
Li H, Zhou X, Huang Y, Liao B, Cheng L and Ren B (2021) Reactive Oxygen Species in Pathogen Clearance: The Killing Mechanisms, the Adaption Response, and the Side Effects. Front. Microbiol. 11:622534. doi: 10.3389/fmicb.2020.622534

Reactive oxygen species (ROS) are attractive weapons in both antibiotic-mediated killing and host-mediated killing. However, the involvement of ROS in antibiotic-mediated killing and complexities in host environments challenge the paradigm. In the case of bacterial pathogens, the examples of some certain pathogens thriving under ROS conditions prompt us to focus on the adaption mechanism that pathogens evolve to cope with ROS. Based on these, we here summarized the mechanisms of ROS-mediated killing of either antibiotics or the host, the examples of bacterial adaption that successful pathogens evolved to defend or thrive under ROS conditions, and the potential side effects of ROS in pathogen clearance. A brief section for new antibacterial strategies centered around ROS was also addressed.

Keywords: reactive oxygen species, secondary damage, metabolism remodeling, virulence, antibiotic resistance, antibiotic tolerance

INTRODUCTION

Reactive oxygen species (ROS), including hydrogen peroxide (H_2O_2), hydroxyl radical (OH-), singlet oxygen ($^1O_2$), and superoxide anion ($\cdot O_2^-$), are produced by the pathogen itself (endogenous) as a byproduct of aerobic respiration; they can also be encountered in the host environment (exogenous). ROS have been called "double-edged swords of life" (Mittler, 2017) in pathogen clearance. First, since ROS can directly damage DNA, lipids, and proteins, they are thought to be the weapon used by both antibiotics and the host immune system. However, controversies challenge the paradigm. Second, successful pathogens exploit ROS for their own adaption. This minireview aims to summarize the mechanisms of ROS-mediated killing by either antibiotics or the host, examples of pathogens that cope with the ROS conditions, the potential side effects of ROS in pathogen clearance, and novel antibacterial strategies centered around ROS.

ENDOGENOUS ROS, AS SECONDARY DAMAGE, FORMED IN RESPONSE TO ANTIBIOTIC EXPOSURE

In general, antibiotics are thought to kill microbes through interaction with specific intracellular targets (Kohanski et al., 2010b). However, in 2007, Collins group proposed a novel mechanism of quinolones-induced killing by the generation of endogenous hydroxyl radicals (Dwyer et al., 2007). Since then, ROS have been shown to play a central role in lethality of numerous classes of bactericidal antibiotics, regardless of their specific targets (Kohanski et al., 2007). However, the role of ROS in antibiotic lethality became controversial and has been challenged (Keren et al., 2013; Imlay, 2015), since antibiotics can kill in the absence of ROS. The paradox contained in these statements can be solved by the idea that killing can derive from the primary damage of antibiotic or from a secondary, lethal stress response mediated by ROS (Zhao and Drlica, 2014; Zhao et al., 2015; Luan et al., 2018). If primary damage with specific targets is severe enough, it can result in death directly. Otherwise, primary damage stimulates a pathway that leads to ROS accumulation as secondary damage. New evidence for this hypothesis was provided in *Escherichia coli*. Hong et al. (2019) described a novel experimental system in which the role of secondary ROS damage could be tested in isolation. In this case, even after complete removal of quinolones, ROS accumulation and cell death continued to occur, indicating that when secondary ROS damage exceeds a critical threshold, it becomes a self-amplifying process and the terminal stage when bacteria responds to antibiotics.

However, how primary damage leads to ROS accumulation remained unclear. Since target-specific damage occurs in antibiotic killing, pathways leading to ROS accumulation most probably have drug-specific context as well. While different studies suggest that primary drug-target damage may activate processes such as envelopes stress response and programmed cell death, leading to ROS accumulation (Lobritz et al., 2015; Van Acker and Coenye, 2017; Stokes et al., 2019), most evidence is provided for aminoglycosides. Misfolded proteins induced by gentamicin first insert into the membrane in *E. coli* and lead the activation of the response regulator ArcA through CpxA, the envelope stress response sensor. ArcA then activates the tricarboxylic acid (TCA) cycle enzymes, leading to dysfunction of TCA cycle and the hyperactivation of respiration (Kohanski et al., 2008). Similar dysfunction of TCA cycle can also be observed in quinolones and β-lactams treatments, suggesting that such metabolic flux could be a shared mechanism pushing the cell into a state that provokes oxidative stress in antibiotic treatments (Kohanski et al., 2008; Belenky et al., 2015). While β-lactams may directly activate envelope stress response by affecting membrane integrity, specific triggers for quinolones remain to be worked out. Several studies found that programmed cell death mediated by YihE kinase and MazF toxin was linked to a ROS cascade in quinolone treatment (Drlica et al., 2008; Dorsey-Oresto et al., 2013). Recently, additional evidence suggested that quinolones disrupted the nucleotide pool, leading to the increase of ATP demand (Yang et al., 2019). The increasing ATP demand elevates TCA cycle activity and cellular respiration and enhances antibiotic lethality.

EXOGENOUS ROS-INDUCED KILLING DEPENDS ON A VARIETY OF INNATE MECHANISMS

Exogenous ROS, as an antimicrobial weapon wielded by phagocytes, are generated from NADPH oxidase (NOX2) in response to microbe recognition (Panday et al., 2015). However, it has been surprisingly difficult to figure out exactly how phagocytic ROS production suppresses microbial growth (Imlay, 2019). Some indirect evidence support the notion that phagocytic ROS directly kill pathogens. Chronic granulomatous disease (CGD) is a genetic disorder in which patients lack functional NOX2 protein and therefore are associated with impaired respiratory burst (Nguyen et al., 2017). Indeed, a severe neutrophil killing defect was reported in CGD patients (Dinauer, 2005; Klebanoff, 2005). The host susceptibility to various pathogens including *Salmonella enterica*, *Staphylococcus aureus*, and *Burkholderia cepacia* in CGD patients highlights the importance of the respiratory burst to infectious diseases. However, whether host-derived ROS could directly kill pathogens is still a matter of debate, since several studies argued that intracellular ROS level in phagosomes was insufficient to kill pathogens (Slauch, 2011; Li and Imlay, 2018; Imlay, 2019).

Alternatively, ROS generated by NOX, as a signal, promote pathogen elimination via activating a variety of innate and adaptive mechanisms in the host cell. For example, ROS are commonly believed to be required in autophagy. NOX-derived ROS are indispensable for the recruitment of the autophagy protein light chain 3 (LC3), promoting antibacterial autophagy (Huang et al., 2009; de Luca et al., 2014). In addition, during infection, neutrophils and phagocytes can activate an additional antimicrobial mechanism, referred to as neutrophil extracellular traps (NETs) (Stoiber et al., 2015). NETs, formed by chromatin and associated proteins, trap and kill various extracellular pathogens. NET formation requires the production of ROS (Papayannopoulos et al., 2010) and is impaired in NOX2-deficient neutrophils (Stoiber et al., 2015). Another study suggested that fosfomycin, a broad-spectrum antibacterial agent, could enhance NET-mediated killing of *S. aureus* via NOX2-dependent ROS accumulation in mouse model (Shen et al., 2016).

In addition to the NOX complex, the mitochondrion is another cellular source of ROS in immune cells (Abuaita et al., 2018). Upon macrophage activation, mitochondrial conditions favor reverse electron transport in the electron transport chain and thus generate ROS (Garaude et al., 2016; Pinegin et al., 2018). Mice deficient in proteins responsible for generation of mitoROS are highly susceptible to infections caused by *Salmonella typhimurium* and *Listeria monocytogenes* (Sonoda et al., 2007; West et al., 2011). During methicillin-resistant *S. aureus* (MRSA) infection, mitoROS were generated and

delivered directly to the phagosome by mitochondrial-derived vesicles (MDVs) in a Toll-like receptor signaling-dependent manner (Abuaita et al., 2018). Of note, like NOX-mediated ROS, which can modulate IL-1β expression (Warnatsch et al., 2017), mitoROS can also modulate the antimicrobial functions of innate immune cells by regulating production of multiple cytokines both *in vitro* and *in vivo* (Mills et al., 2016; Herb et al., 2019).

BACTERIAL RESPONSE TO OXIDATIVE STRESS: ANTIOXIDANT AND METABOLIC DEFENSES

The systems in bacteria that regulate the expression of antioxidant defense networks have been extensively reviewed (Ezraty et al., 2017; Reniere, 2018). The ROS response is under the control of the master regulators. Transcription factors such as OxyR (i.e., in *S. enterica*, *Francisella tularensis*, and *Porphyromonas gingivalis*), PerR (i.e., in *S. aureus* and *Bacillus subtilis*), OhrR (i.e., in *B. subtilis* and *Mycobacterium smegmatis*), and SoxRS (i.e., in *E. coli* and *S. aureus*) can be activated by direct oxidation of their sensor proteins and then adjusting the bacterial response appropriately (Chiang and Schellhorn, 2012). Although the particulars vary among different species, in general, these regulons regulate genes required for antioxidant defense, including superoxide dismutase, catalase, thioredoxins, heme biosynthesis machinery, glutathione reductases, ferric uptake regulator (Fur), ferritin, and bacterioferritin (Imlay, 2008; Chiang and Schellhorn, 2012; Reniere, 2018). In addition, iron homeostasis is also critical to mitigate redox damage induced by Fenton reaction. Therefore, in pathogenic bacteria (i.e., *E. coli*, *S. aureus*, and *Salmonella*), the iron-sensing transcriptional repressors, such as Fur and DtxR (diphtheria toxin repressor), can also be utilized to sustain redox homeostasis by controlling the expression of genes encoding iron acquisition systems and iron-dependent enzymes (Troxell and Hassan, 2013).

Apart from antioxidant defense systems, metabolism remodeling also plays a pivotal role in mitigating oxidative damage (**Figure 1**). Metabolic adaptions can reduce oxidative burden by retarding respiration. For example, the glyoxylate shunt (GS) is an anaplerotic reaction of the TCA cycle developed in numerous species, which bypasses two NADH-generating steps (Lemire et al., 2017; Dolan and Welch, 2018). In *B. cepacia*, GS genes were upregulated in cells surviving aminoglycoside treatment (Van Acker et al., 2013). Similarly, in *Mycobacterium tuberculosis* (MTB), GS enzyme isocitrate lyase deficient mutants were significantly more susceptible than wild-type strain toward isoniazid, rifampicin, and streptomycin (Nandakumar et al., 2014). Consistent with these observations, the Collins group found that glyoxylate could serve as a direct biochemical inducer of aminoglycoside tolerance via reducing cellular respiration. Meanwhile, TCA cycle intermediates, such as fumarate, significantly potentiate tobramycin lethality (Meylan et al., 2017).

Replenishment of antioxidants can also be achieved by metabolic modulation. Pentose phosphate (PP) pathway is an important target to mitigate ROS damage, since NADPH is the cofactor for antioxidant systems. In *E. coli*, by increased abundance of glucose-6-phosphate dehydrogenase, the metabolic flux can be rerouted toward the PP pathway, leading to increased ROS tolerance (Christodoulou et al., 2018).

Ketoacids including α-ketoglutarate (KG) and pyruvate can undergo non-enzymatic decarboxylation in the presence of ROS, generate non-toxic byproducts, and thus alleviate the ROS damage. Bacteria like *E. coli* and *Pseudomonas fluorescens* tend to pool ketoacids both inside the cell and in the extracellular matrix under ROS conditions. For example, the increased generation of KG can be achieved by the modulation of TCA cycle enzymes like isocitrate dehydrogenase when using citrate, glucose, and malate as carbon sources (Alhasawi et al., 2016). It can also be achieved by the deamination of glutamate when glutamate or histidine is supplied as the carbon source (Lemire et al., 2010, 2017). When exposed to H_2O_2, *P. fluorescens* can go through a metabolic reconfiguration with enhanced activity of substrate-level phosphorylation as well as impaired activity of the TCA cycle, leading to evident pyruvate synthesis with glucose or glycerol as the carbon source (Bignucolo et al., 2013; Alhasawi et al., 2016).

INDUCTION OF BACTERIAL VIRULENCE UNDER ROS CONDITIONS

In addition to antioxidant defenses, activations of the oxidative defense regulators are also required for full virulence in pathogens. For example, OxyR contributes to the virulence of *E. coli* and *Pseudomonas aeruginosa* (Lau et al., 2005; Wei et al., 2012; Fang et al., 2016). Similarly, SoxRS has been shown to act as a positive regulator in *Salmonella* pathogenicity island (SPI)-2 mediated virulence in *S. enterica* (Wang P. et al., 2020). In *S. aureus*, after oxidation of the sensor protein by ROS, the redox-signaling regulator AirSR positively regulates the biosynthesis of staphyloxanthin (STX), an important virulence factor of *S. aureus* (Hall et al., 2017). MntR, a member of the DtxR family, is required for *S. aureus* pathogenesis via maintaining manganese homeostasis (Grunenwald et al., 2019).

In host conditions, virulence modulation can be achieved by ROS indirectly. During ROS generation, phagocytes simultaneously produce glutathione (GSH) to sustain intracellular redox homeostasis. Certain intracellular pathogens have even evolved to exploit the host GSH for adaptions. In *Burkholderia pseudomallei*, virulence is completely dependent on the expression of a type VI secretion system (T6SS). During the exit from phagosome, *B. pseudomallei* senses host GSH via sensor protein VirA, which then activates the expression of the T6SS (Wong et al., 2015). In *L. monocytogenes*, the extracellular host GSH can trigger the production of bacterial GSH. Both host GSH and bacterial GSH bind to the master virulence regulator PrfA and function as an allosteric activator (Reniere et al., 2015; Portman et al., 2017).

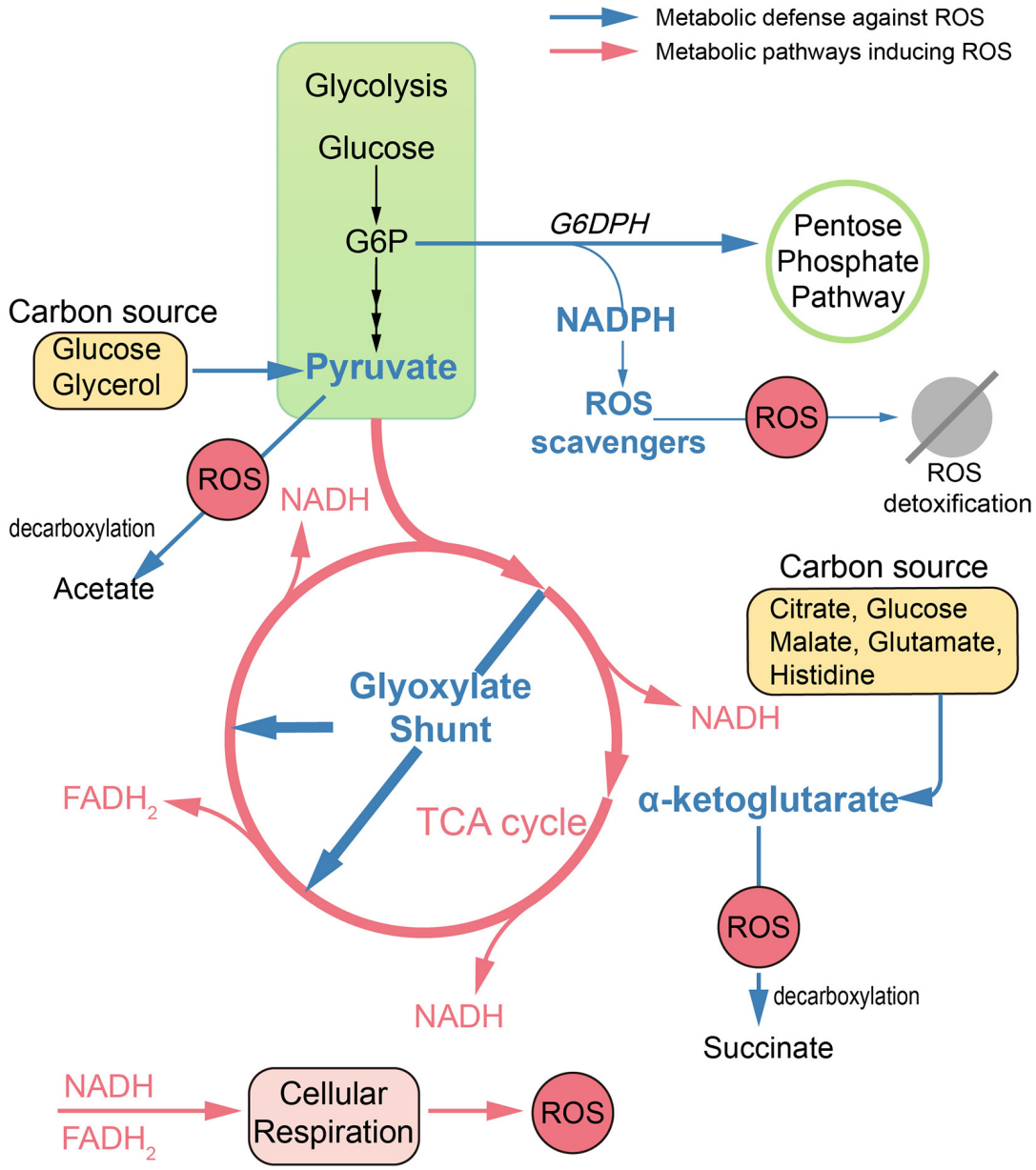

FIGURE 1 | Metabolic remodeling designed to reduce oxidative damage. In antibiotic treatments, dysfunction of TCA cycle and hyperactivation of cell respiration lead to ROS accumulation in bacteria. Defense against ROS can be achieved by metabolic remodeling. Reduced endogenous ROS formation can be achieved by upregulation of the glyoxylate shunt, which bypasses two NADH-generating steps. Replenishment of antioxidants can be achieved by rerouting metabolism toward the pentose phosphate pathway and enhancing production of cofactor NADPH. Also, ketoacids, including pyruvate and α-ketoglutarate, can mitigate oxidative damage via non-enzymatic decarboxylation in the presence of numerous carbon sources. G6P, glucose 6-phosphate; G6DPH, glucose-6-phosphate dehydrogenase.

THRIVE UNDER ROS CONDITIONS BY METABOLIC REMODELING

While pathogens can be eliminated by ROS, it is quite clear that certain pathogens exploit ROS to coordinate metabolism to thrive. For example, *S. typhimurium* evidently makes use of host-derived ROS during intestinal inflammation. ROS generated by phagocytes convert thiosulfate to tetrathionate, which in turn can be used as a respiratory electron sink by *S. typhimurium*, allowing it to outcompete the native microbiota (Winter et al., 2010; Bäumler and Sperandio, 2016). Another example comes from *E. coli*. In the intestinal lumen, oxygen from the epithelium collides with sulfide generated by luminal bacteria, potentially generating H_2O_2 through direct reaction. Also, lactic-acid bacteria excrete H_2O_2 as a direct metabolic product. Under such circumstances, cytochrome *c* peroxidase (Ccp) regulated

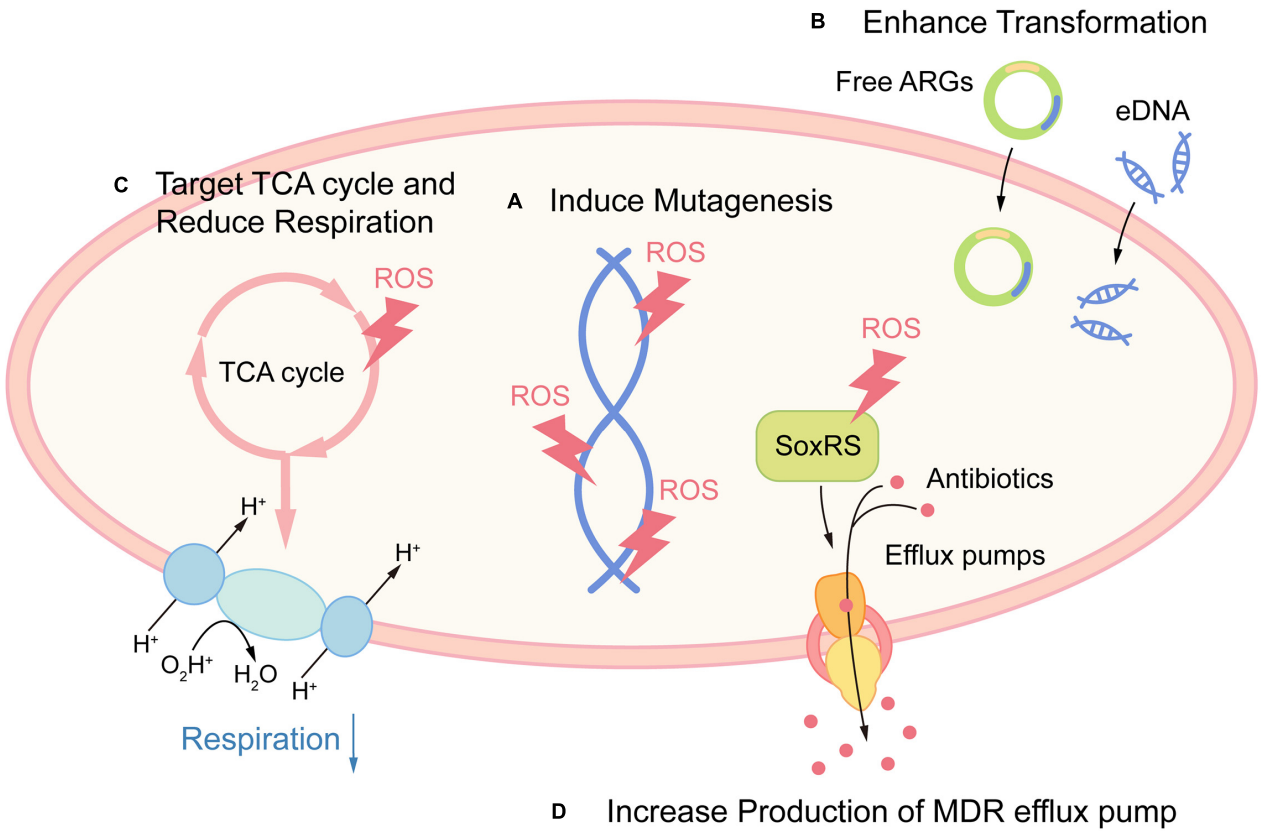

FIGURE 2 | Promoting antibiotic resistance and tolerance as potential side effects of ROS. **(A)** ROS promote resistance by directly damaging DNA and leading to mutagenesis. **(B)** ROS act as a signal for gene transformation, by promoting the transformation of antibiotic resistance genes (ARGs) and eDNA in certain species. **(C)** Host-derived ROS promote antibiotic tolerance by targeting TCA cycle and retarding cellular respiration in *S. aureus*. **(D)** Host-derived ROS promote antibiotic tolerance by increased production of MDR efflux pump via activation of redox regulon SoxRS.

by OxyR allows *E. coli* to employ H_2O_2 as a terminal oxidant for respiration (Khademian and Imlay, 2017). *Helicobacter pylori* is well known as a ROS-inducing gastric pathogen. It utilizes chemotaxis to seek sites optimal for efficient colonization. Recent studies showed that ROS could be sensed in *H. pylori* by the chemoreceptor TlpD. Host oxidants hypochlorous acid (HOCl) could act as a chemoattractant by reversibly oxidizing TlpD that inactivates the chemotransduction signaling complex (Perkins et al., 2019). While H_2O_2 could act as a chemorepellent which initiates chemotaxis through TlpD to promote gastric gland colonization (Collins et al., 2018).

BACTERIAL RESISTANCE AND TOLERANCE AS SIDE EFFECTS OF ROS

Recently, the radical-based theory in pathogen clearance has been questioned for the protective role of ROS against antimicrobial killing (Burger and Drlica, 2009; Mosel et al., 2013). ROS can directly damage DNA, leading to genetic mutations. Indeed, ROS produced by non-lethal antibiotics induce mutations in specific antibiotic targets and promote the development of multi-drug resistance (Kohanski et al., 2010a; Takahashi et al., 2017). If ROS is a shared mechanism in antibiotic lethality, then it is to be expected that protection against ROS can be one of the shared traits for bacterial resistance against antibiotics as well. Indeed, bactericidal antibiotic mediates *de novo* acquisition of resistance, which then provides protection against ROS accumulation upon exposure to a different type of antibiotics (Hoeksema et al., 2018). In addition, it was recently demonstrated that non-lethal exposure to H_2O_2 boosted evolvability of bacterial populations by enhancing survival under oxidative stress (Rodriguez-Rojas et al., 2020).

ROS also act as a signal for gene transformation. H_2O_2 is a metabolic product of certain oral streptococci such as *Streptococcus gordonii* under aerobic conditions. In H_2O_2-producing streptococci, the release of extracellular DNA (eDNA) is entirely dependent on H_2O_2. Also, numerous H_2O_2-non-producing species like *Streptococcus mutans* and *Streptococcus pyogenes* release eDNA in a H_2O_2-dependent manner (Itzek et al., 2011), suggesting that ROS serve as an important environmental signal in oral biofilm (Redanz et al., 2018). Intriguingly, a recent study shows that non-antibiotic pharmaceuticals including non-steroidal anti-inflammatory drugs (NSAIDs) and the lipid-lowering drug also induce significant ROS accumulation in *Acinetobacter baylyi*, which is closely related to the enhanced transformation of antibiotic resistance genes (ARGs) (Wang Y. et al., 2020).

ROS are key weapons in host cells, while recent evidence suggests that host ROS induce antibiotic tolerance during infection. ROS generated by macrophages target TCA enzymes aconitase and succinate dehydrogenase and coerce *S. aureus* into a metabolic state with reduced respiration, which is incompatible with the killing mechanism of most bactericidal antibiotics (Rowe et al., 2019). The persister is an extreme case of tolerance for the high levels of multi-drug tolerance (Brauner et al., 2016). Host ROS can also modulate persister formation in *E. coli*. The activation of redox regulators SoxRS results in increasing expression of the AcrAB-TolC multidrug-resistant (MDR) pump, which in turn lowers the fluoroquinolones concentration and promotes antibiotic tolerance (Wu et al., 2012).

Together, these examples indicate that ROS may potentiate the emergence of bacterial resistance and tolerance (**Figure 2**). Although there is currently no clinical evidence proving this hypothesis, contradictory evidence favoring these potential side effects have been indicated in several studies. Early study suggested that *S. aureus* internalized in leucocytes isolated from patients with CGD (with impaired respiratory burst) were more susceptible to rifampicin, when compared with wild-type leucocytes (Jacobs and Wilson, 1983). Also, elevated levels of oxidation products are related to MTB infection in pulmonary tuberculosis (PTB) patients (Amaral et al., 2016). While there is scarce demonstration that the use of antioxidants can increase pathogen burden, a study showed that the antioxidant resveratrol reduced *Serratia marcescens* burden in mice (Lu et al., 2008). Surprisingly, the use of antioxidant N-acetyl cysteine (NAC) as an adjuvant to directly observed treatment short course significantly caused early sputum negativity in PTB patients (Mahakalkar et al., 2017).

NOVEL ANTIMICROBIAL STRATEGIES CENTERED AROUND ROS

The efficacy of antibiotics has been endangered by the rapid emergence of resistant pathogens. Therefore, new approaches to fight against pathogens, including antimicrobial photodynamic therapy (aPDT) and cold atmospheric plasma (CAP), have been suggested as efficient alternative approaches. Although their antibacterial efficacy also centered around ROS, the modes of action for these new techniques are distinct from conventional antibiotics, as ROS-mediated damage in such therapies is the primary stress-induced damage (Wilson and Patterson, 2008; Vatansever et al., 2013). For example, aPDT uses photosensitizers (PS) to generate ROS upon irradiation by visible light at specific wavelength, and CAPs are partly ionized gases producing a reactive mix by interacting with oxygen, generating a cocktail of ROS (Brany et al., 2020). Due to direct redox-active properties, aPDT and CAP can cause multi-target oxidative damage to pathogens (Melo et al., 2013; Hu et al., 2018) as well as direct oxidation of polysaccharides in biofilm (Beirão et al., 2014; Jiao et al., 2019). Due to their multi-target mode of action and large quantities of ROS production which overwhelm the antioxidant defenses in pathogens, the additional advantage of these new techniques is the lack of development of resistance mechanisms (Tavares et al., 2010; Kvam et al., 2012). As novel ROS-inducing strategies, aPDT and CAP showed excellent potential to tackle difficult-to-eradicate infections as alternative treatments in wound healing, dental cure, and food decontamination (Wilson and Patterson, 2008; Rao et al., 2020).

CONCLUDING REMARKS

ROS are attractive weapons to kill pathogenic microbial cells. However, ROS, as a double-edged sword, should be regulated with care since under non-lethal ROS, certain pathogens have evolved delicate mechanisms to utilize ROS for their adaption to thrive. Also, numerous pathogens can use ROS as a stepstone for the evolution of antibiotic tolerance and resistance. Efforts to target bacterial adaptive pathways, as well as the use of novel ROS-inducing antibacterial strategies, will be promising approaches for antibacterial therapy.

AUTHOR CONTRIBUTIONS

HL, XZ, YH, BL, LC, and BR: conception/design of the work, agreement to be accountable for all aspects of the work. HL, LC, and BR: drafting the work. XZ, LC, and BR: final approval of the manuscript to be published. All authors contributed to the article and approved the submitted version.

FUNDING

This study was supported by the National Natural Science Foundation of China grants 81870778 (BR), 81600858 (BR), and 82071106 (LC) and the Applied Basic Research Programs of Sichuan Province 2020YJ0227 (BR).

REFERENCES

Abuaita, B. H., Schultz, T. L., and O'Riordan, M. X. (2018). Mitochondria-derived vesicles deliver antimicrobial reactive oxygen species to control phagosome-localized *Staphylococcus aureus*. *Cell Host Microbe* 24, 625–636.e5. doi: 10.1016/j.chom.2018.10.005

Alhasawi, A., Thomas, S. C., and Appanna, V. D. (2016). Metabolic networks to generate pyruvate, PEP and ATP from glycerol in *Pseudomonas fluorescens*. *Enzyme Microb. Technol.* 85, 51–56. doi: 10.1016/j.enzmictec.2016.01.007

Amaral, E. P., Conceição, E. L., Costa, D. L., Rocha, M. S., Marinho, J. M., Cordeiro-Santos, M., et al. (2016). N-acetyl-cysteine exhibits potent anti-mycobacterial activity in addition to its known anti-oxidative functions. *BMC Microbiol.* 16:251. doi: 10.1186/s12866-016-0872-7

Bäumler, A. J., and Sperandio, V. (2016). Interactions between the microbiota and pathogenic bacteria in the gut. *Nature* 535, 85–93. doi: 10.1038/nature18849

Beirão, S., Fernandes, S., Coelho, J., Faustino, M. A., Tomé, J. P., Neves, M. G., et al. (2014). Photodynamic inactivation of bacterial and yeast biofilms with a cationic porphyrin. *Photochem. Photobiol.* 90, 1387–1396. doi: 10.1111/php.12331

Belenky, P., Ye, J. D., Porter, C. B., Cohen, N. R., Lobritz, M. A., Ferrante, T., et al. (2015). Bactericidal antibiotics induce toxic metabolic perturbations that lead to cellular damage. *Cell Rep.* 13, 968–980. doi: 10.1016/j.celrep.2015.09.059

Bignucolo, A., Appanna, V. P., Thomas, S. C., Auger, C., Han, S., Omri, A., et al. (2013). Hydrogen peroxide stress provokes a metabolic reprogramming in *Pseudomonas fluorescens*: enhanced production of pyruvate. *J. Biotechnol.* 167, 309–315. doi: 10.1016/j.jbiotec.2013.07.002

Brany, D., Dvorska, D., Halasova, E., and Skovierova, H. (2020). Cold atmospheric plasma: a powerful tool for modern medicine. *Int. J. Mol. Sci.* 21:2932. doi: 10.3390/ijms21082932

Brauner, A., Fridman, O., Gefen, O., and Balaban, N. Q. (2016). Distinguishing between resistance, tolerance and persistence to antibiotic treatment. *Nat. Rev. Microbiol.* 14, 320–330. doi: 10.1038/nrmicro.2016.34

Burger, R. M., and Drlica, K. (2009). Superoxide protects *Escherichia coli* from bleomycin mediated lethality. *J. Inorg. Biochem.* 103, 1273–1277. doi: 10.1016/j.jinorgbio.2009.07.009

Chiang, S. M., and Schellhorn, H. E. (2012). Regulators of oxidative stress response genes in *Escherichia coli* and their functional conservation in bacteria. *Arch. Biochem. Biophys.* 525, 161–169. doi: 10.1016/j.abb.2012.02.007

Christodoulou, D., Link, H., Fuhrer, T., Kochanowski, K., Gerosa, L., and Sauer, U. (2018). Reserve flux capacity in the pentose phosphate pathway enables *Escherichia coli*'s rapid response to oxidative stress. *Cell Syst.* 6, 569–578.e7. doi: 10.1016/j.cels.2018.04.009

Collins, K. D., Hu, S., Grasberger, H., Kao, J. Y., and Ottemann, K. M. (2018). Chemotaxis allows bacteria to overcome host-generated reactive oxygen species that constrain gland colonization. *Infect. Immun.* 86:e00878-17.

de Luca, A., Smeekens, S. P., Casagrande, A., Iannitti, R., Conway, K. L., Gresnigt, M. S., et al. (2014). IL-1 receptor blockade restores autophagy and reduces inflammation in chronic granulomatous disease in mice and in humans. *Proc. Natl. Acad. Sci. U.S.A.* 111, 3526–3531. doi: 10.1073/pnas.1322831111

Dinauer, M. C. (2005). Chronic granulomatous disease and other disorders of phagocyte function. *Hematology Am. Soc. Hematol. Educ. Program* 2005, 89–95. doi: 10.1182/asheducation-2005.1.89

Dolan, S. K., and Welch, M. (2018). The glyoxylate shunt, 60 years on. *Annu. Rev. Microbiol.* 72, 309–330. doi: 10.1146/annurev-micro-090817-062257

Dorsey-Oresto, A., Lu, T., Mosel, M., Wang, X., Salz, T., Drlica, K., et al. (2013). YihE kinase is a central regulator of programmed cell death in bacteria. *Cell Rep.* 3, 528–537. doi: 10.1016/j.celrep.2013.01.026

Drlica, K., Malik, M., Kerns, R. J., and Zhao, X. (2008). Quinolone-mediated bacterial death. *Antimicrob. Agents Chemother.* 52, 385–392. doi: 10.1128/aac.01617-06

Dwyer, D. J., Kohanski, M. A., Hayete, B., and Collins, J. J. (2007). Gyrase inhibitors induce an oxidative damage cellular death pathway in *Escherichia coli*. *Mol. Syst. Biol.* 3:91. doi: 10.1038/msb4100135

Ezraty, B., Gennaris, A., Barras, F., and Collet, J. F. (2017). Oxidative stress, protein damage and repair in bacteria. *Nat. Rev. Microbiol.* 15, 385–396. doi: 10.1038/nrmicro.2017.26

Fang, F. C., Frawley, E. R., Tapscott, T., and Vazquez-Torres, A. (2016). Bacterial stress responses during host infection. *Cell Host Microbe* 20, 133–143. doi: 10.1016/j.chom.2016.07.009

Garaude, J., Acín-Pérez, R., Martínez-Cano, S., Enamorado, M., Ugolini, M., Nistal-Villán, E., et al. (2016). Mitochondrial respiratory-chain adaptations in macrophages contribute to antibacterial host defense. *Nat. Immunol.* 17, 1037–1045. doi: 10.1038/ni.3509

Grunenwald, C. M., Choby, J. E., Juttukonda, L. J., Beavers, W. N., Weiss, A., Torres, V. J., et al. (2019). Manganese detoxification by MntE is critical for resistance to oxidative stress and virulence of *Staphylococcus aureus*. *mBio* 10:e02915-18.

Hall, J. W., Yang, J., Guo, H., and Ji, Y. (2017). The *Staphylococcus aureus* AirSR two-component system mediates reactive oxygen species resistance via transcriptional regulation of staphyloxanthin production. *Infect. Immun.* 85:e00838-16.

Herb, M., Gluschko, A., Wiegmann, K., Farid, A., Wolf, A., Utermöhlen, O., et al. (2019). Mitochondrial reactive oxygen species enable proinflammatory signaling through disulfide linkage of NEMO. *Sci. Signal.* 12:eaar5926. doi: 10.1126/scisignal.aar5926

Hoeksema, M., Brul, S., and Ter Kuile, B. H. (2018). Influence of reactive oxygen species on *de novo* acquisition of resistance to bactericidal antibiotics. *Antimicrob. Agents Chemother.* 62:e02354-17.

Hong, Y., Zeng, J., Wang, X., Drlica, K., and Zhao, X. (2019). Post-stress bacterial cell death mediated by reactive oxygen species. *Proc. Natl. Acad. Sci. U.S.A.* 116, 10064–10071. doi: 10.1073/pnas.1901730116

Hu, X., Huang, Y.-Y., Wang, Y., Wang, X., and Hamblin, M. R. (2018). Antimicrobial photodynamic therapy to control clinically relevant biofilm infections. *Front. Microbiol.* 9:1299. doi: 10.3389/fmicb.2018.01299

Huang, J., Canadien, V., Lam, G. Y., Steinberg, B. E., Dinauer, M. C., Magalhaes, M. A., et al. (2009). Activation of antibacterial autophagy by NADPH oxidases. *Proc. Natl. Acad. Sci. U.S.A.* 106, 6226–6231. doi: 10.1073/pnas.0811045106

Imlay, J. A. (2008). Cellular defenses against superoxide and hydrogen peroxide. *Annu. Rev. Biochem.* 77, 755–776. doi: 10.1146/annurev.biochem.77.061606.161055

Imlay, J. A. (2015). Diagnosing oxidative stress in bacteria: not as easy as you might think. *Curr. Opin. Microbiol.* 24, 124–131. doi: 10.1016/j.mib.2015.01.004

Imlay, J. A. (2019). Where in the world do bacteria experience oxidative stress? *Environ. Microbiol.* 21, 521–530. doi: 10.1111/1462-2920.14445

Itzek, A., Zheng, L., Chen, Z., Merritt, J., and Kreth, J. (2011). Hydrogen peroxide-dependent DNA release and transfer of antibiotic resistance genes in *Streptococcus gordonii*. *J. Bacteriol.* 193, 6912–6922. doi: 10.1128/jb.05791-11

Jacobs, R. F., and Wilson, C. B. (1983). Activity of antibiotics in chronic granulomatous disease leukocytes. *Pediatr. Res.* 17, 916–919. doi: 10.1203/00006450-198311000-00016

Jiao, Y., Tay, F. R., Niu, L. N., and Chen, J. H. (2019). Advancing antimicrobial strategies for managing oral biofilm infections. *Int. J. Oral Sci.* 11:28.

Keren, I., Wu, Y., Inocencio, J., Mulcahy, L. R., and Lewis, K. (2013). Killing by bactericidal antibiotics does not depend on reactive oxygen species. *Science* 339, 1213–1216. doi: 10.1126/science.1232688

Khademian, M., and Imlay, J. A. (2017). *Escherichia coli* cytochrome c peroxidase is a respiratory oxidase that enables the use of hydrogen peroxide as a terminal electron acceptor. *Proc. Natl. Acad. Sci. U.S.A.* 114, E6922–E6931. doi: 10.1073/pnas.1701587114

Klebanoff, S. J. (2005). Myeloperoxidase: friend and foe. *J. Leukoc. Biol.* 77, 598–625. doi: 10.1189/jlb.1204697

Kohanski, M. A., DePristo, M. A., and Collins, J. J. (2010a). Sublethal antibiotic treatment leads to multidrug resistance via radical-induced mutagenesis. *Mol. Cell* 37, 311–320. doi: 10.1016/j.molcel.2010.01.003

Kohanski, M. A., Dwyer, D. J., and Collins, J. J. (2010b). How antibiotics kill bacteria: from targets to networks. *Nat. Rev. Microbiol.* 8, 423–435. doi: 10.1038/nrmicro2333

Kohanski, M. A., Dwyer, D. J., Hayete, B., Lawrence, C. A., and Collins, J. J. (2007). A common mechanism of cellular death induced by bactericidal antibiotics. *Cell* 130, 797–810. doi: 10.1016/j.cell.2007.06.049

Kohanski, M. A., Dwyer, D. J., Wierzbowski, J., Cottarel, G., and Collins, J. J. (2008). Mistranslation of membrane proteins and two-component system activation trigger antibiotic-mediated cell death. *Cell* 135, 679–690. doi: 10.1016/j.cell.2008.09.038

Kvam, E., Davis, B., Mondello, F., and Garner, A. L. (2012). Nonthermal atmospheric plasma rapidly disinfects multidrug-resistant microbes by inducing cell surface damage. *Antimicrob. Agents Chemother.* 56, 2028–2036. doi: 10.1128/aac.05642-11

Lau, G. W., Britigan, B. E., and Hassett, D. J. (2005). *Pseudomonas aeruginosa* OxyR is required for full virulence in rodent and insect models of infection and for resistance to human neutrophils. *Infect. Immun.* 73, 2550–2553. doi: 10.1128/iai.73.4.2550-2553.2005

Lemire, J., Alhasawi, A., Appanna, V. P., Tharmalingam, S., and Appanna, V. D. (2017). Metabolic defence against oxidative stress: the road less travelled so far. *J. Appl. Microbiol.* 123, 798–809. doi: 10.1111/jam.13509

Lemire, J., Milandu, Y., Auger, C., Bignucolo, A., Appanna, V. P., and Appanna, V. D. (2010). Histidine is a source of the antioxidant, alpha-ketoglutarate, in *Pseudomonas fluorescens* challenged by oxidative stress. *FEMS Microbiol. Lett.* 309, 170–177. doi: 10.1111/j.1574-6968.2010.02034.x

Li, X., and Imlay, J. A. (2018). Improved measurements of scant hydrogen peroxide enable experiments that define its threshold of toxicity for *Escherichia coli*. *Free Radic. Biol. Med.* 120, 217–227. doi: 10.1016/j.freeradbiomed.2018.03.025

Lobritz, M. A., Belenky, P., Porter, C. B., Gutierrez, A., Yang, J. H., Schwarz, E. G., et al. (2015). Antibiotic efficacy is linked to bacterial cellular respiration. *Proc. Natl. Acad. Sci. U.S.A.* 112, 8173–8180. doi: 10.1073/pnas.1509743112

Lu, C. C., Lai, H. C., Hsieh, S. C., and Chen, J. K. (2008). Resveratrol ameliorates *Serratia marcescens*-induced acute pneumonia in rats. *J. Leukoc. Biol.* 83, 1028–1037. doi: 10.1189/jlb.0907647

Luan, G., Hong, Y., Drlica, K., and Zhao, X. (2018). Suppression of reactive oxygen species accumulation accounts for paradoxical bacterial survival at high quinolone concentration. *Antimicrob. Agents Chemother.* 62:e01622-17.

Mahakalkar, S. M., Nagrale, D., Gaur, S., Urade, C., Murhar, B., and Turankar, A. (2017). N-acetylcysteine as an add-on to Directly Observed Therapy Short-I therapy in fresh pulmonary tuberculosis patients: a randomized, placebo-controlled, double-blinded study. *Perspect. Clin. Res.* 8, 132–136. doi: 10.4103/2229-3485.210450

Melo, T., Santos, N., Lopes, D., Alves, E., Maciel, E., Faustino, M. A., et al. (2013). Photosensitized oxidation of phosphatidylethanolamines monitored by electrospray tandem mass spectrometry. *J. Mass Spectrom.* 48, 1357–1365. doi: 10.1002/jms.3301

Meylan, S., Porter, C. B. M., Yang, J. H., Belenky, P., Gutierrez, A., Lobritz, M. A., et al. (2017). Carbon sources tune antibiotic susceptibility in *Pseudomonas aeruginosa* via tricarboxylic acid cycle control. *Cell Chem. Biol.* 24, 195–206. doi: 10.1016/j.chembiol.2016.12.015

Mills, E. L., Kelly, B., Logan, A., Costa, A. S. H., Varma, M., Bryant, C. E., et al. (2016). Succinate dehydrogenase supports metabolic repurposing of mitochondria to drive inflammatory macrophages. *Cell* 167, 457–470.e13. doi: 10.1016/j.cell.2016.08.064

Mittler, R. (2017). ROS are good. *Trends Plant Sci.* 22, 11–19. doi: 10.1016/j.tplants.2016.08.002

Mosel, M., Li, L., Drlica, K., and Zhao, X. (2013). Superoxide-mediated protection of *Escherichia coli* from antimicrobials. *Antimicrob. Agents Chemother.* 57, 5755–5759. doi: 10.1128/aac.00754-13

Nandakumar, M., Nathan, C., and Rhee, K. Y. (2014). Isocitrate lyase mediates broad antibiotic tolerance in *Mycobacterium tuberculosis*. *Nat. Commun.* 5:4306. doi: 10.1038/ncomms5306

Nguyen, G. T., Green, E. R., and Mecsas, J. (2017). Neutrophils to the ROScue: mechanisms of NADPH oxidase activation and bacterial resistance. *Front. Cell. Infect. Microbiol.* 7:373. doi: 10.3389/fcimb.2017.00373

Panday, A., Sahoo, M. K., Osorio, D., and Batra, S. (2015). NADPH oxidases: an overview from structure to innate immunity-associated pathologies. *Cell. Mol. Immunol.* 12, 5–23. doi: 10.1038/cmi.2014.89

Papayannopoulos, V., Metzler, K. D., Hakkim, A., and Zychlinsky, A. (2010). Neutrophil elastase and myeloperoxidase regulate the formation of neutrophil extracellular traps. *J. Cell Biol.* 191, 677–691. doi: 10.1083/jcb.201006052

Perkins, A., Tudorica, D. A., Amieva, M. R., Remington, S. J., and Guillemin, K. (2019). *Helicobacter pylori* senses bleach (HOCl) as a chemoattractant using a cytosolic chemoreceptor. *PLoS Biol.* 17:e3000395. doi: 10.1371/journal.pbio.3000395

Pinegin, B., Vorobjeva, N., Pashenkov, M., and Chernyak, B. (2018). The role of mitochondrial ROS in antibacterial immunity. *J. Cell. Physiol.* 233, 3745–3754. doi: 10.1002/jcp.26117

Portman, J. L., Dubensky, S. B., Peterson, B. N., Whiteley, A. T., and Portnoy, D. A. (2017). Activation of the *Listeria monocytogenes* virulence program by a reducing environment. *mBio* 8:e01595-17.

Rao, Y., Shang, W., Yang, Y., Zhou, R., and Rao, X. (2020). Fighting mixed-species microbial biofilms with cold atmospheric plasma. *Front. Microbiol.* 11:1000. doi: 10.3389/fmicb.2020.01000

Redanz, S., Cheng, X., Giacaman, R. A., Pfeifer, C. S., Merritt, J., and Kreth, J. (2018). Live and let die: hydrogen peroxide production by the commensal flora and its role in maintaining a symbiotic microbiome. *Mol. Oral Microbiol.* 33, 337–352. doi: 10.1111/omi.12231

Reniere, M. L. (2018). Reduce, induce, thrive: bacterial redox sensing during pathogenesis. *J. Bacteriol.* 200:e00128-18.

Reniere, M. L., Whiteley, A. T., Hamilton, K. L., John, S. M., Lauer, P., Brennan, R. G., et al. (2015). Glutathione activates virulence gene expression of an intracellular pathogen. *Nature* 517, 170–173. doi: 10.1038/nature14029

Rodriguez-Rojas, A., Kim, J. J., Johnston, P. R., Makarova, O., Eravci, M., Weise, C., et al. (2020). Non-lethal exposure to H2O2 boosts bacterial survival and evolvability against oxidative stress. *PLoS Genet.* 16:e1008649. doi: 10.1371/journal.pgen.1008649

Rowe, S. E., Wagner, N. J., Li, L., Beam, J. E., Wilkinson, A. D., Radlinski, L. C., et al. (2019). Reactive oxygen species induce antibiotic tolerance during systemic *Staphylococcus aureus* infection. *Nat. Microbiol.* 5, 282–290. doi: 10.1038/s41564-019-0627-y

Shen, F., Tang, X., Cheng, W., Wang, Y., Wang, C., Shi, X., et al. (2016). Fosfomycin enhances phagocyte-mediated killing of *Staphylococcus aureus* by extracellular traps and reactive oxygen species. *Sci. Rep.* 6:19262. doi: 10.1038/srep19262

Slauch, J. M. (2011). How does the oxidative burst of macrophages kill bacteria? Still an open question. *Mol. Microbiol.* 80, 580–583. doi: 10.1111/j.1365-2958.2011.07612.x

Sonoda, J., Laganière, J., Mehl, I. R., Barish, G. D., Chong, L. W., Li, X., et al. (2007). Nuclear receptor ERR alpha and coactivator PGC-1 beta are effectors of IFN-gamma-induced host defense. *Genes Dev.* 21, 1909–1920. doi: 10.1101/gad.1553007

Stoiber, W., Obermayer, A., Steinbacher, P., and Krautgartner, W. D. (2015). The role of reactive oxygen species (ROS) in the formation of extracellular traps (ETs) in humans. *Biomolecules* 5, 702–723. doi: 10.3390/biom5020702

Stokes, J. M., Lopatkin, A. J., Lobritz, M. A., and Collins, J. J. (2019). Bacterial metabolism and antibiotic efficacy. *Cell Metab.* 30, 251–259. doi: 10.1016/j.cmet.2019.06.009

Takahashi, N., Gruber, C. C., Yang, J. H., Liu, X., Braff, D., Yashaswini, C. N., et al. (2017). Lethality of MalE-LacZ hybrid protein shares mechanistic attributes with oxidative component of antibiotic lethality. *Proc. Natl. Acad. Sci. U.S.A.* 114, 9164–9169. doi: 10.1073/pnas.1707466114

Tavares, A., Carvalho, C. M., Faustino, M. A., Neves, M. G., Tomé, J. P., Tomé, A. C., et al. (2010). Antimicrobial photodynamic therapy: study of bacterial recovery viability and potential development of resistance after treatment. *Mar. Drugs* 8, 91–105. doi: 10.3390/md8010091

Troxell, B., and Hassan, H. M. (2013). Transcriptional regulation by ferric uptake regulator (Fur) in pathogenic bacteria. *Front. Cell. Infect. Microbiol.* 3:59. doi: 10.3389/fcimb.2013.00059

Van Acker, H., and Coenye, T. (2017). The role of reactive oxygen species in antibiotic-mediated killing of bacteria. *Trends Microbiol.* 25, 456–466. doi: 10.1016/j.tim.2016.12.008

Van Acker, H., Sass, A., Bazzini, S., De Roy, K., Udine, C., Messiaen, T., et al. (2013). Biofilm-grown *Burkholderia cepacia* complex cells survive antibiotic treatment by avoiding production of reactive oxygen species. *PLoS One* 8:e58943. doi: 10.1371/journal.pone.0058943

Vatansever, F., de Melo, W. C., Avci, P., Vecchio, D., Sadasivam, M., Gupta, A., et al. (2013). Antimicrobial strategies centered around reactive oxygen species–bactericidal antibiotics, photodynamic therapy, and beyond. *FEMS Microbiol. Rev.* 37, 955–989. doi: 10.1111/1574-6976.12026

Wang, P., Zhang, H., Liu, Y., Lv, R., Liu, X., Song, X., et al. (2020). SoxS is a positive regulator of key pathogenesis genes and promotes intracellular replication and virulence of *Salmonella* Typhimurium. *Microb. Pathog.* 139:103925. doi: 10.1016/j.micpath.2019.103925

Wang, Y., Lu, J., Engelstadter, J., Zhang, S., Ding, P., Mao, L., et al. (2020). Non-antibiotic pharmaceuticals enhance the transmission of exogenous antibiotic resistance genes through bacterial transformation. *ISME J.* 14, 2179–2196. doi: 10.1038/s41396-020-0679-2

Warnatsch, A., Tsourouktsoglou, T. D., Branzk, N., Wang, Q., Reincke, S., Herbst, S., et al. (2017). Reactive oxygen species localization programs inflammation to clear microbes of different size. *Immunity* 46, 421–432. doi: 10.1016/j.immuni.2017.02.013

Wei, Q., Le Minh, P. N., Dötsch, A., Hildebrand, F., Panmanee, W., Elfarash, A., et al. (2012). Global regulation of gene expression by OxyR in an important human opportunistic pathogen. *Nucleic Acids Res.* 40, 4320–4333. doi: 10.1093/nar/gks017

West, A. P., Brodsky, I. E., Rahner, C., Woo, D. K., Erdjument-Bromage, H., Tempst, P., et al. (2011). TLR signalling augments macrophage bactericidal activity through mitochondrial ROS. *Nature* 472, 476–480. doi: 10.1038/nature09973

Wilson, B. C., and Patterson, M. S. (2008). The physics, biophysics and technology of photodynamic therapy. *Phys. Med. Biol.* 53, R61–R109. doi: 10.1088/0031-9155/53/9/r01

Winter, S. E., Thiennimitr, P., Winter, M. G., Butler, B. P., Huseby, D. L., Crawford, R. W., et al. (2010). Gut inflammation provides a respiratory electron acceptor for *Salmonella*. *Nature* 467, 426–429. doi: 10.1038/nature09415

Wong, J., Chen, Y., and Gan, Y. H. (2015). Host cytosolic glutathione sensing by a membrane histidine kinase activates the type VI secretion system in an intracellular bacterium. *Cell Host Microbe* 18, 38–48. doi: 10.1016/j.chom.2015.06.002

Wu, Y., Vulic, M., Keren, I., and Lewis, K. (2012). Role of oxidative stress in persister tolerance. *Antimicrob. Agents Chemother.* 56, 4922–4926. doi: 10.1128/aac.00921-12

Yang, J. H., Wright, S. N., Hamblin, M., McCloskey, D., Alcantar, M. A., Schrubbers, L., et al. (2019). A white-box machine learning approach for revealing antibiotic mechanisms of action. *Cell* 177, 1649–1661.e9. doi: 10.1016/j.cell.2019.04.016

Zhao, X., and Drlica, K. (2014). Reactive oxygen species and the bacterial response to lethal stress. *Curr. Opin. Microbiol.* 21, 1–6. doi: 10.1016/j.mib.2014.06.008

Zhao, X., Hong, Y., and Drlica, K. (2015). Moving forward with reactive oxygen species involvement in antimicrobial lethality. *J. Antimicrob. Chemother.* 70, 639–642. doi: 10.1093/jac/dku463

Conflict of Interest: The authors declare that the research was conducted in the absence of any commercial or financial relationships that could be construed as a potential conflict of interest.

frontiers in Microbiology

CORRECTION
published: 13 May 2021
doi: 10.3389/fmicb.2021.685133

Corrigendum: Reactive Oxygen Species in Pathogen Clearance: The Killing Mechanisms, the Adaption Response, and the Side Effects

Hao Li, Xuedong Zhou, Yuyao Huang, Binyou Liao, Lei Cheng and Biao Ren**

State Key Laboratory of Oral Diseases, National Clinical Research Center for Oral Diseases, West China Hospital of Stomatology, Sichuan University, Chengdu, China

Keywords: reactive oxygen species, secondary damage, metabolism remodeling, virulence, antibiotic resistance, antibiotic tolerance

A Corrigendum on

Reactive Oxygen Species in Pathogen Clearance: The Killing Mechanisms, the Adaption Response, and the Side Effects

by Li, H., Zhou, X., Huang, Y., Liao, B., Cheng, L., and Ren, B. (2021). Front. Microbiol. 11:622534. doi: 10.3389/fmicb.2020.622534

In the original article, there was an error. The original article read: Recent study shows that host ROS can be sensed as a chemorepellent in *H. pylori* by the chemoreceptor TlpD, which initiates chemotaxis to promote gastric gland colonization (Collins et al., 2018; Perkins et al., 2019).

A correction has been made to the section, ***Thrive Under ROS Conditions by Metabolic Remodeling.*** The corrected sentence is below:

Recent studies showed that ROS could be sensed in *H. pylori* by the chemoreceptor TlpD. Host oxidants hypochlorous acid (HOCl) could act as a chemoattractant by reversibly oxidizing TlpD that inactivates the chemotransduction signaling complex (Perkins et al., 2019). While H_2O_2 could act as a chemorepellent which initiates chemotaxis through TlpD to promote gastric gland colonization (Collins et al., 2018).

The authors apologize for this error and state that this does not change the scientific conclusions of the article in any way. The original article has been updated.

REFERENCES

Collins, K. D., Hu, S., Grasberger, H., Kao, J. Y., and Ottemann, K. M. (2018). Chemotaxis allows bacteria to overcome host-generated reactive oxygen species that constrain gland colonization. *Infect. Immun.* 86:e00878-17.

Perkins, A., Tudorica, D. A., Amieva, M. R., Remington, S. J., and Guillemin, K. (2019). *Helicobacter pylori* senses bleach (HOCl) as a chemoattractant using a cytosolic chemoreceptor. *PLoS Biol.* 17:e3000395. doi: 10.1371/journal.pbio.3000395

OPEN ACCESS

Edited and reviewed by:
Kirkwood M. Land, University of the Pacific, United States

***Correspondence:**
Lei Cheng
chenglei@scu.edu.cn
Biao Ren
renbiao@scu.edu.cn

Specialty section:
This article was submitted to Antimicrobials, Resistance and Chemotherapy, a section of the journal Frontiers in Microbiology

Received: *24 March 2021*
Accepted: *23 April 2021*
Published: *13 May 2021*

Citation:
Li H, Zhou X, Huang Y, Liao B, Cheng L and Ren B (2021) Corrigendum: Reactive Oxygen Species in Pathogen Clearance: The Killing Mechanisms, the Adaption Response, and the Side Effects. Front. Microbiol. 12:685133. doi: 10.3389/fmicb.2021.685133

frontiers in Microbiology

ORIGINAL RESEARCH
published: 15 February 2021
doi: 10.3389/fmicb.2021.638640

Silver Nanoparticles Induce a *Triclosan-Like* Antibacterial Action Mechanism in Multi-Drug Resistant *Klebsiella pneumoniae*

Vikram Pareek[1,2†], Stéphanie Devineau[3†], Sathesh K. Sivasankaran[4†], Arpit Bhargava[2†], Jitendra Panwar[2†], Shabarinath Srikumar[5†] and Séamus Fanning[1,6*†]*

[1] UCD-Centre for Food Safety, UCD School of Public Health, Physiotherapy and Sports Science, University College Dublin, Dublin, Ireland, [2] Department of Biological Sciences, Birla Institute of Technology and Science, Pilani, India, [3] Université de Paris, BFA, UMR 8251, CNRS, Paris, France, [4] Genome Informatics Facility, Iowa State University, Ames, IA, United States, [5] Department of Food, Nutrition and Health, College of Food and Agriculture, UAE University, Al Ain, United Arab Emirates, [6] Institute for Global Food Security, Queen's University Belfast, Belfast, United Kingdom

Infections associated with antimicrobial-resistant bacteria now represent a significant threat to human health using conventional therapy, necessitating the development of alternate and more effective antibacterial compounds. Silver nanoparticles (Ag NPs) have been proposed as potential antimicrobial agents to combat infections. A complete understanding of their antimicrobial activity is required before these molecules can be used in therapy. Lysozyme coated Ag NPs were synthesized and characterized by TEM-EDS, XRD, UV-vis, FTIR spectroscopy, zeta potential, and oxidative potential assay. Biochemical assays and deep level transcriptional analysis using RNA sequencing were used to decipher how Ag NPs exert their antibacterial action against multi-drug resistant *Klebsiella pneumoniae* MGH78578. RNAseq data revealed that Ag NPs induced a *triclosan-like* bactericidal mechanism responsible for the inhibition of the type II fatty acid biosynthesis. Additionally, released Ag^{+} generated oxidative stress both extra- and intracellularly in *K. pneumoniae*. The data showed that *triclosan-like* activity and oxidative stress cumulatively underpinned the antibacterial activity of Ag NPs. This result was confirmed by the analysis of the bactericidal effect of Ag NPs against the isogenic *K. pneumoniae* MGH78578 Δ*soxS* mutant, which exhibits a compromised oxidative stress response compared to the wild type. Silver nanoparticles induce a *triclosan-like* antibacterial action mechanism in multi-drug resistant *K. pneumoniae*. This study extends our understanding of anti-*Klebsiella* mechanisms associated with exposure to Ag NPs. This allowed us to model how bacteria might develop resistance against silver nanoparticles, should the latter be used in therapy.

Keywords: *Klebsiella pneumoniae*, silver nanoparticles, RNA sequencing, soxS, triclosan

OPEN ACCESS

Edited by:
Jong H. Kim, Agricultural Research Service, United States

Reviewed by:
Anima Nanda, Sathyabama Institute of Science and Technology, India
Sanjay Kumar Singh Patel, Konkuk University, South Korea

***Correspondence:**
Jitendra Panwar
jpanwar@pilani.bits-pilani.ac.in
Séamus Fanning
sfanning@ucd.ie

†ORCID:
Vikram Pareek
orcid.org/0000-0003-3980-1238
Stéphanie Devineau
orcid.org/0000-0002-1133-5223
Sathesh K. Sivasankaran
orcid.org/0000-0003-3037-6001
Arpit Bhargava
orcid.org/0000-0001-6450-6551
Jitendra Panwar
orcid.org/0000-0002-0750-9745
Shabarinath Srikumar
orcid.org/0000-0003-3775-2831
Séamus Fanning
orcid.org/0000-0002-1922-8836

Specialty section:
This article was submitted to Antimicrobials, Resistance and Chemotherapy, a section of the journal Frontiers in Microbiology

Received: *07 December 2020*
Accepted: *20 January 2021*
Published: *15 February 2021*

Citation:
Pareek V, Devineau S, Sivasankaran SK, Bhargava A, Panwar J, Srikumar S and Fanning S (2021) Silver Nanoparticles Induce a Triclosan-Like Antibacterial Action Mechanism in Multi-Drug Resistant Klebsiella pneumoniae. Front. Microbiol. 12:638640. doi: 10.3389/fmicb.2021.638640

INTRODUCTION

Antimicrobial resistance (AMR) is responsible for approximately 700,000 deaths annually across the globe and this number is expected to increase further if new measures are not adopted and antibacterial compounds discovered (World Health Organization, 2019). The emergence of multi-drug resistance (MDR) in various pathogenic bacterial species represents a serious public health

challenge (Logan and Weinstein, 2017; Cassini et al., 2019), leading to hospital- and community-acquired infections, which are difficult to treat and control (Pendleton et al., 2013; Klemm et al., 2018). Since AMR is estimated to overtake cancer as the main cause of death in 50 years, innovative approaches including the development of novel antimicrobial strategies using silver nanoparticles (Ag NPs) are required (Huh and Kwon, 2011; Gupta et al., 2019; Kalia et al., 2019).

Klebsiella pneumoniae is one of the members of the ESKAPE pathogens (representing *Enterococcus faecium, Staphylococcus aureus, Klebsiella pneumoniae, Acinetobacter baumannii, Pseudomonas aeruginosa*, and *Enterobacter* spp.) (Pendleton et al., 2013). It is a member of Enterobacteriaceae family—Gram-negative, non-motile, and rod-shaped. This bacterium is considered an opportunistic pathogen commonly found in the intestine, mouth, and skin of humans. It is mainly associated with hospital-acquired infections (nosocomial infections) and responsible for respiratory/urinary tract infections, pneumonia, and sepsis (Podschun and Ullmann, 1998; Lee and Burgess, 2012; World Health Organization, 2019). This pathogen can also form biofilms on indwelling medical devices leading to persistent nosocomial infection (Jagnow and Clegg, 2003; Li et al., 2014). About 25% of nosocomial *K. pneumoniae* were found to be resistant to carbapenem-based compounds (Han et al., 2016; Anes et al., 2017). *K. pneumoniae* were also found to be resistant to colistin, a last-line antibiotic (Antoniadou et al., 2007; Neuner et al., 2011). The emergence of AMR in *K. pneumoniae* against critically important classes of antibiotics represents a major threat to conventional clinical therapy (Li et al., 2014; Hu et al., 2020). Novel antibacterial strategies are required to overcome this challenge (Adamo and Margarit, 2018; Mulani et al., 2019).

Silver and other metals such as copper and zinc have historically been used as potential antibacterial agents (Alexander, 2009; Rai et al., 2012). Antibacterial activity of silver can vary depending on its chemical form (Mijnendonckx et al., 2013; Li et al., 2016; Zheng et al., 2018). Metallic forms continuously release small numbers of ions, which makes it a slow-acting agent, whilst the ionic form is more efficient. Although Ag^+ is reported to exhibit better antibacterial activity (Randall et al., 2012), direct exposure to mammalian cells has toxic side effects that limit its application in therapy (Chernousova and Epple, 2013; Vimbela et al., 2017). In contrast, Ag NPs provide a greater surface area, leading to a more controlled release of Ag^+ (Durán et al., 2016). Hence, this form has potential as an antibacterial compound (Roe et al., 2008; Kang et al., 2019). Green synthesis of silver NPs was also developed by different groups (Sharma et al., 2009; Chowdhury et al., 2014; Otari et al., 2017). Despite these advantages, little is known about the antibacterial action mechanisms of Ag NP based formulations.

We synthesized lysozyme coated Ag NPs (L-Ag NPs) and characterized their antibacterial mechanism against MDR *K. pneumonia* MGH78578 using chemical analysis, biochemical assays and deep-level RNA sequencing. Our data revealed that L-Ag NPs induced a *triclosan-like* antibacterial effect against MDR *K. pneumoniae.* The inhibition of the type II fatty acid biosynthesis along with Ag^+ induced oxidative stress were responsible for the anti-*K. pneumoniae* effect. To the best of our knowledge, this is the first study that reports the triclosan-like antimicrobial effect of silver NPs and a full transcriptional analysis of their antibacterial action against *K. pneumoniae*. Our results provide molecular insights into how bacteria might deploy antibacterial strategies to counteract the toxic effects of Ag NPs. This allowed us to model how *K. pneumoniae* might develop resistance against Ag NPs (Chopra, 2007).

MATERIALS AND METHODS

Bacteria and Media

Klebsiella pneumoniae MGH78578 (ATCC® 700721) is a clinical isolate chosen for its MDR phenotype (Ogawa et al., 2005; Anes et al., 2019) and the availability of its whole genome sequence (NC_009648.1). Bacteria were grown in Luria Bertani (LB) and modified LB (mLB) media constituted without NaCl (Chambers et al., 2013; Bhargava et al., 2018). Bacteria were recovered from long-term storage (at −80°C in glycerol stocks) in mLB medium (casein enzyme hydrolysate 10 g L^{-1} and yeast extract 5 g L^{-1}, pH 7.2 ± 0.2) for 12 h at 37°C with shaking (150 rpm). For the preparation of inoculum, an overnight grown bacterial culture was inoculated into freshly prepared mLB medium and grown until the mid-log phase ($OD_{600\,nm}$ 0.5–0.6). An overnight grown bacterial culture (approximately 10^7 CFU mL^{-1}) was inoculated separately in freshly prepared LB and mLB broth medium. Bacterial growth was determined by measuring the optical density (OD) at 600 nm at 2 h time intervals. Biological experiments were carried out in both technical and biological duplicates.

Synthesis of L-Ag NPs

L-Ag NPs were synthesized following a protocol adapted from Ashraf et al. (2014; see **Supplementary Material**). To determine the size, shape, crystallinity and surface capping, L-Ag NPs were characterized by Transmission Electron Microscopy (TEM), Energy Dispersive Spectroscopy (EDS) on a Quantax EDS (Bruker AXS, Coventry, United Kingdom), X-ray Diffraction (XRD) on a Rigaku MiniFlex Benchtop XRD System (Rigaku Company, United States), UV-vis spectroscopy on a V-630 UV-vis spectrophotometer (Jasco Corporation, Tokyo, Japan), and Fourier Transform Infrared spectroscopy (FTIR) on a Prestige-21 FTIR Spectrometer (Shimadzu, Nakagyo, Japan). The zeta potential of L-Ag NPs was measured with a Zetasizer Nano ZS (Malvern Instruments, United Kingdom). The acellular oxidative potential of L-Ag NPs was assessed by measuring the depletion in antioxidants (uric acid, ascorbic acid, reduced glutathione) by HPLC following incubation of L-Ag NPs in a simplified synthetic respiratory tract lining fluid for 4 h at 37°C (Crobeddu et al., 2017). The dissolution kinetics of L-Ag NPs in mLB was measured by inductively coupled plasma optical emission spectrometry (ICP-OES) (Avio 200, PerkinElmer, United States). All measurements were performed in duplicate. The detailed protocols are described in the **Supplementary Information file**. Freshly prepared L-Ag NPs were used for all the experiments.

Antibacterial Susceptibility Determinations

The minimum inhibitory concentration (MIC) was determined using the broth microdilution assay following CLSI guidelines. Bacterial cells were exposed to L-Ag NPs (ranging from 0.5–64 μg (Ag) mL^{-1}) and incubated at 37°C in the dark for 24 h. Bacterial growth was determined by measuring the OD_{600nm}. In addition, the free lysozyme was tested in parallel for any antibacterial activity. Bacterial cells exposed to L-Ag NPs were spread plated and incubated for 12 h at 37°C to determine the minimum bactericidal concentration (MBC). Media without L-Ag NPs and bacterial cells were used as positive- and negative-controls, respectively (Bhargava et al., 2018). All experiments were done in biological duplicates and the results are represented as mean ± standard deviation.

Mode of Action Studies-Measurement of Reactive Oxygen Species (ROS)

The generation of ROS inside the bacterial cell following exposure to L-Ag NPs was measured using a 2,7-dichlorodihydrofluorescein diacetate (DCFH-DA) assay (Wang and Joseph, 1999). DCFH-DA was added to the bacterial cell suspension at a final concentration of 10 μM and incubated for 1 h at 37°C in the dark. Free dye was then separated from the DCFH-DA loaded bacterial cells by centrifugation at 8,000 rpm for 15 min followed by washing with PBS. Bacterial cells were exposed to different (sub)-MIC concentrations of L-Ag NPs (i.e., MIC_{25}, MIC_{50}, MIC_{75}, and MIC_{100}) for 30 min at 37°C in fresh mLB medium with shaking (150 rpm). The fluorescence intensity of dichlorodihydrofluorescein (DCF) was detected using a VICTOR X Multilabel Plate Reader (PerkinElmer, United States) at an excitation and emission wavelength of 485 and 535 nm, respectively. The experiments were performed in duplicates and the results expressed as mean ± standard deviation.

The effect of L-Ag NPs on the bacterial cell envelope was examined by TEM. To prepare sample for TEM analysis, bacterial cells exposed to MIC_{75} L-Ag NPs were centrifuged at 8,000 rpm for 10 min. Subsequently, the supernatant was discarded, and the bacterial pellet was washed twice with PBS followed by fixation in 2.5% v/v electron microscopy grade glutaraldehyde in 0.05 M sodium cacodylate buffer pH 7.2 for 2 h at 4°C. TEM samples were prepared by drop-casting the bacterial cell suspension on to a carbon-coated copper grid that was later imaged on a Hitachi H-7650 TEM instrument (Hitachi High-Technologies Corporation, Tokyo, Japan) at an acceleration voltage of 100 kV. Bacterial cells that were not exposed to L-Ag NPs were used as the control. A minimum number of 50 bacterial cells were analyzed on different TEM images in each condition.

The membrane damage was analyzed using the MDA and anthrone assays. Bacterial cells were treated with different (sub)-MIC concentrations of L-Ag NPs, i.e., MIC_{25}, MIC_{50}, MIC_{75}, and MIC_{100}. The determination of MDA concentration was done as described previously (Buege and Aust, 1978). The anthrone assay was done as described previously (Bhargava et al., 2018). The experiments were performed in biological duplicates and the results expressed as mean ± standard deviation.

The intracellular concentration of Ag was measured by ICP-OES following exposure to MIC_{75} L-Ag NPs for 5, 30, and 60 min at 37°C. A freshly grown bacterial culture (approximately 10^7 CFU mL^{-1}) was exposed to MIC_{75} L-Ag NPs followed by incubation for 5, 30, and 60 min at 37°C in mLB. After incubation, bacterial cells were pelleted by centrifugation at 8,000 rpm for 10 min at 4°C then dried and digested in a 1 mL mixture of H_2O_2:HNO_3 (50:50) for 2 h. After acid digestion, the final volume was made up to 10 mL and filtered using 0.22 μm syringe filter. The silver concentration of the sample was measured by ICP-OES (Avio 200, PerkinElmer, United States) (McQuillan et al., 2012). Untreated bacterial cells were taken as a control for the respective time points. The experiments were performed in biological duplicates and the results expressed as mean ± standard deviation. Detailed protocols are described in SI.

RNA Sequencing

A freshly grown culture of *K. pneumoniae* MGH78578 from mid-log_{10} phase (approximately 10^7 CFU mL^{-1}) was exposed to MIC_{75} L-Ag NPs for 5 and 30 min at 37°C in mLB broth. Bacterial cells not exposed to L-Ag NPs were selected as a control for each time point. RNA was isolated using RNAeasy extraction kit (Qiagen) and treated with Turbo DNase kit (Ambion's). RNA integrity was assessed using a Bioanalyzer 2100 RNA 6000 nanochip (Agilent Technologies). RNA library sequencing was performed at the Centre for Genomic Research, University of Liverpool, United Kingdom. Ribosomal RNA was removed with a Ribo-Zero rRNA removal kit (Illumina). Libraries were prepared with NEBNext Directional RNA Library Prep Kit (BioLabs). Pooled libraries (**Supplementary Table 1**) were loaded on cBot (Illumina) and cluster generations was performed. Single-sequencing using 150 bp read length was performed on lane of the HiSeq 4000 sequencer (Illumina). Raw sequencing data was processed as described in **Supplementary Material**. The RNAseq data produced from the present work were deposited to the NCBI-GEO database and are available under the accession number GSE151953.

Comparative Gene Expression Analysis With *E. coli* MGH1655 Exposed to Individual Antibiotics

A comparison of our transcriptional data with the global transcriptome profiling of *E. coli* MGH1665 K12 strain exposed to 37 antibiotics was carried out. Only those genes that gave statistically significant differential expression patterns were selected from both datasets. Our gene expression dataset was compared to each of the 37 *E. coli* transcriptional profiles and genes that had similar expression patterns (both up-and down-regulation) were counted.

Validation of RNA-Seq Data by Quantitative RT-PCR Analysis

RNA isolated from the samples were converted to cDNA by using high-capacity RNA to cDNA kit (Thermo Fisher Scientific, Ireland). Primers based on the selected genes of interest were

designed with 6-FAM/ZEN/IBFQ double-quenched probes and synthesized commercially by Integrated DNA Technologies (IDT, Belgium) (**Supplementary Table 2**). The cDNA was used as a template and analysis was done by the addition of PrimeTime Gene Expression Master Mix. qRT-PCR was performed in an Eppendorf Mastercycler realplex ep gradient S (Eppendorf, United Kingdom). This analysis was carried out in two biological replicates each along with three technical replicates. The fold-change in the expression of the genes of interest was determined by the method of Livak and Schmittgen (2001), i.e., $2^{-\Delta\Delta Ct}$ method using *rho* as a housekeeping gene.

Statistical Analysis

The results for the biochemical assay were analyzed using unpaired Student *t*-test as appropriate for the dataset. The qRT-PCR measurements data were statistically analyzed using Prism software (v. 8.0 GraphPad Software) following the two-way analysis of variance. Boneferroni method was used to analyze the multiple comparisons. The symbol "ns" used in the graphs corresponds to statistically non-significant with $p > 0.05$. The asterisk symbols in the graphs correspond to $^{*}p \leq 0.05$, $^{**}p \leq 0.01$, and $^{***}p \leq 0.001$. All the data points represent the mean of two independent measurements. The uncertainties were represented as standard deviations. In RNAseq results, NSE represents non-significant expression.

RESULTS AND DISCUSSION

Synthesis and Characterization of L-Ag NPs

L-Ag NPs were synthesized by a co-reduction method wherein lysozyme functions both as a reducing and stabilizing agent using heat reflux action at 120°C (Eby et al., 2009; Ashraf et al., 2014). Lysozyme acts as a capping material devoid of enzymatic activity. We selected L-Ag NPs based on their bactericidal activity against MDR *K. pneumoniae* MGH78578. The synthesis of L-Ag NPs was associated with the appearance of the plasmon peak at 414 nm (**Figure 1A**) (Singh et al., 2018). The average diameter of L-Ag NPs measured by TEM was 5.2 ± 1.2 nm (**Figures 1B,C**). The X-ray diffraction pattern obtained corresponds to the face-centered cubic lattice structure of crystalline silver (JCPDS file 04-0783) (**Figure 1D** and **Supplementary Figure 1**) (Jain et al., 2011; Pareek et al., 2020). The surface charge of L-Ag NPs was estimated by measuring their zeta potential in water and modified LB (mLB) medium (devoid of NaCl) at 37°C. L-Ag NPs were found to be negatively charged in both conditions with $\zeta = -38.2 \pm 1.6$ mV in water and $\zeta = -24.2 \pm 0.9$ mV in mLB medium. The 1,632 cm^{-1} peak in the FTIR spectrum corresponds to the amide I vibration characteristic of the protein backbone, confirming the presence of lysozyme associated with Ag NPs (**Figure 1E**) (Baker et al., 2014).

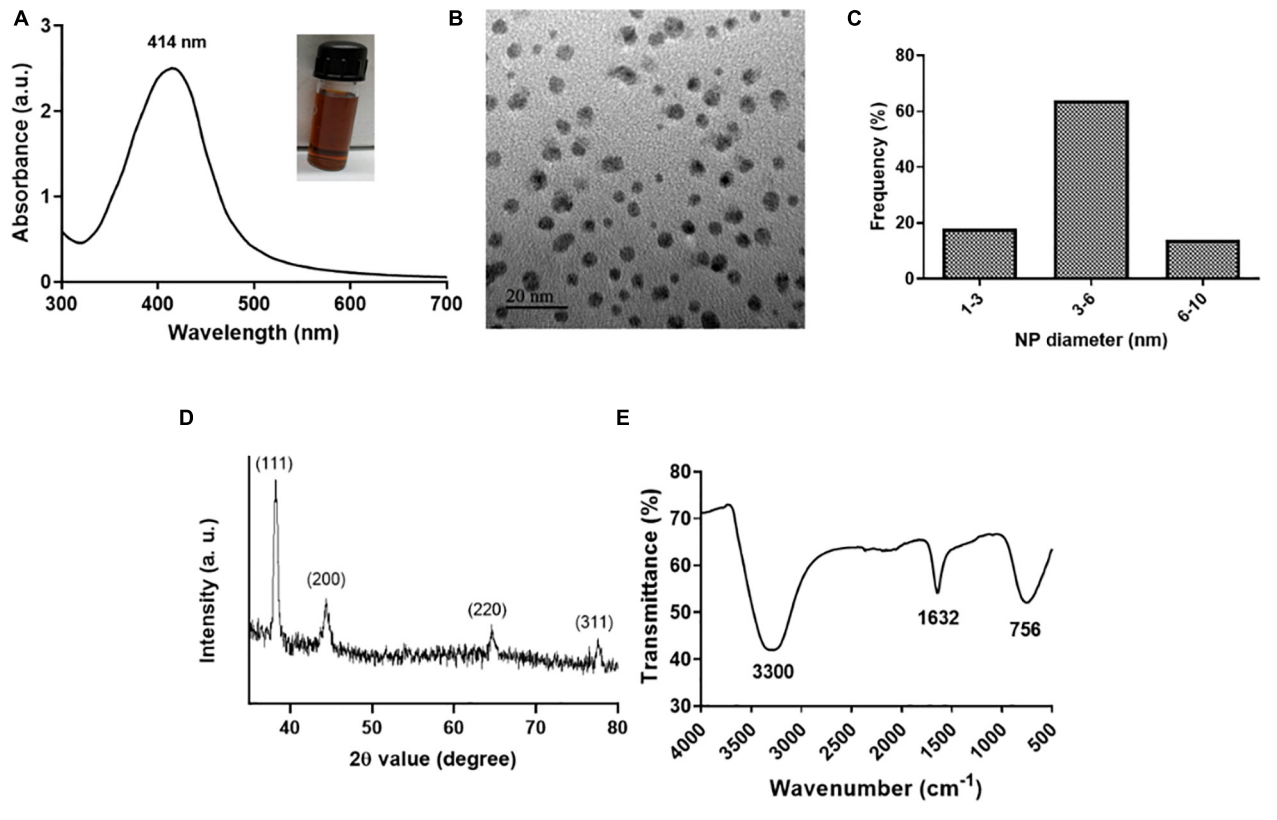

FIGURE 1 | Characterization of L-Ag NPs. **(A)** UV-visible spectrum (inset shows a picture of the L-Ag NP suspension after synthesis). **(B)** TEM image. **(C)** Distribution of L-Ag NP diameter determined from TEM analysis. **(D)** XRD diffraction spectrum. **(E)** FTIR spectrum.

L-Ag NPs Inhibit the Proliferation of *K. pneumoniae* MGH78578

In media with high salt content like chloride and phosphate, Ag NPs may aggregate and free Ag^+ can precipitate, potentially reducing their bactericidal activity (Lok et al., 2007; McQuillan et al., 2012; Chambers et al., 2013; Pareek et al., 2018). Hence, the bactericidal effect of L-Ag NPs against *K. pneumoniae* MGH78578 was assessed in mLB medium (LB medium devoid of NaCl) (Pelletier et al., 2010; Chatterjee et al., 2011). No significant difference between the growth of *K. pneumoniae* in mLB and LB media was observed (**Figure 2A**) confirming mLB had no phenotypic effect. Approximately 3×10^7 CFU mL^{-1} log_{10} phase bacterial cells were exposed to L-Ag NPs. The MIC of L-Ag NPs was 21 μg (Ag) mL^{-1} (**Figure 2B**). To determine the bactericidal efficiency of L-Ag NPs, *K. pneumoniae* MGH78578 exposed to L-Ag NPs were spread plated and incubated for 12 h at 37°C. The MBC of L-Ag NPs was 45 μg (Ag) mL^{-1} (**Supplementary Figure 2**). These results show that L-Ag NPs inhibit the proliferation of *K. pneumoniae* MGH78578 at low concentrations.

L-Ag NPs Generate ROS and Limited Membrane Damage in *K. pneumoniae* MGH78578

Reactive oxygen species (ROS) could be generated outside the bacterial cells by L-Ag NPs and released Ag^+ (Le Ouay and Stellacci, 2015). Limited dissolution of L-Ag NPs was observed in mLB media for 8 h at 37°C (**Figure 2C**). Extracellular ROS production was evaluated by measuring the oxidative potential of L-Ag NPs in a simplified synthetic respiratory tract lining fluid. The depletion of antioxidants (uric acid, acetic acid, and reduced glutathione GSH) was also noted when measured by HPLC after 4 h incubation at 37°C (**Figure 3A**) (Crobeddu et al., 2017). We observed a dose-dependent depletion in ascorbic acid and GSH (up to 100%), showing that, at low NP concentration, L-Ag NPs can generate ROS extracellularly.

Then, we measured the concentration of silver that enter *K. pneumoniae* MGH78578 by ICP-OES following treatment with L-Ag NPs for 5, 30, and 60 min. The uptake of silver, either in the form of L-Ag NPs or Ag^+, was proportional to the time duration of treatment (**Supplementary Figure 3**). To determine whether ROS were also produced inside the bacterial cells following exposure to L-Ag NPs, we used the DCFH-DA assay (Aranda et al., 2013). A dose-dependent increase in the intracellular ROS was observed, a reflection of the oxidative stress external to the bacterial cell (**Figure 3B**).

The severe oxidative stress induced by L-Ag NPs could lead to many downstream phenotypes in bacteria including compromised membrane integrity (Durán et al., 2016; Zheng et al., 2018; Zou et al., 2018; Kang et al., 2019). TEM analysis of *K. pneumoniae* did not show any change in the membrane integrity of the exposed bacterial cells (**Figures 3C,D**). To verify this observation, we explored the degree of bacterial membrane damage in the whole population using an MDA assay. A limited though significant concentration-dependent increase in the level of lipid peroxidation was observed (**Figure 3E**). Additionally, a concentration-dependent increase of carbohydrate release was observed following L-Ag NP exposure (**Figure 3F**). Overall, our results show that L-Ag NPs induced limited bacterial membrane damage, a phenotype that was not observed by TEM.

Transcriptomic Profiling of L-Ag NPs Exposed *K. pneumoniae* MGH78578 Using RNA-Seq

We used RNA-seq to understand how *K. pneumoniae* MGH78578 responded to L-Ag NP exposure following a previously standardized protocol investigating the transcriptome of *K. pneumoniae* MGH78578 exposed to sub-inhibitory concentrations of a chemosensitizer (Anes et al., 2019). Here, we exposed *K. pneumoniae* MGH78578 to a sub-inhibitory concentration of L-Ag NPs at MIC_{75} (15.8 μg (Ag) mL^{-1}) for a period of 5- and 30-min. The 5 min time point was used to identify the transcriptional signals associated with early exposure, whilst the 30 min time point demonstrated the adaptive responses of L-Ag NP exposed *K. pneumoniae* (replication time is 20 min). Approximately 336 million reads were obtained across all 8 libraries with an average of 42 million reads *per* library (**Supplementary Table 1**) sufficient for downstream transcriptomic analysis (Haas et al., 2012; Anes et al., 2019). The *VOOM* function in the *limma* package (Ritchie et al., 2015)

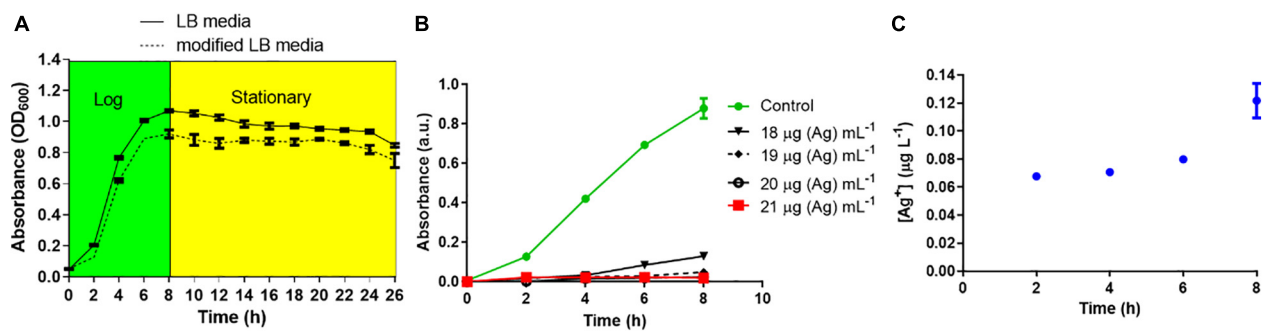

FIGURE 2 | (A) Bacterial growth curve analysis of *K. pneumoniae* MGH78578 in LB and mLB media. **(B)** Determination of *K. pneumoniae* L-Ag NP MIC in mLB medium. **(C)** Dissolution kinetics of L-Ag NPs in mLB medium at 37°C.

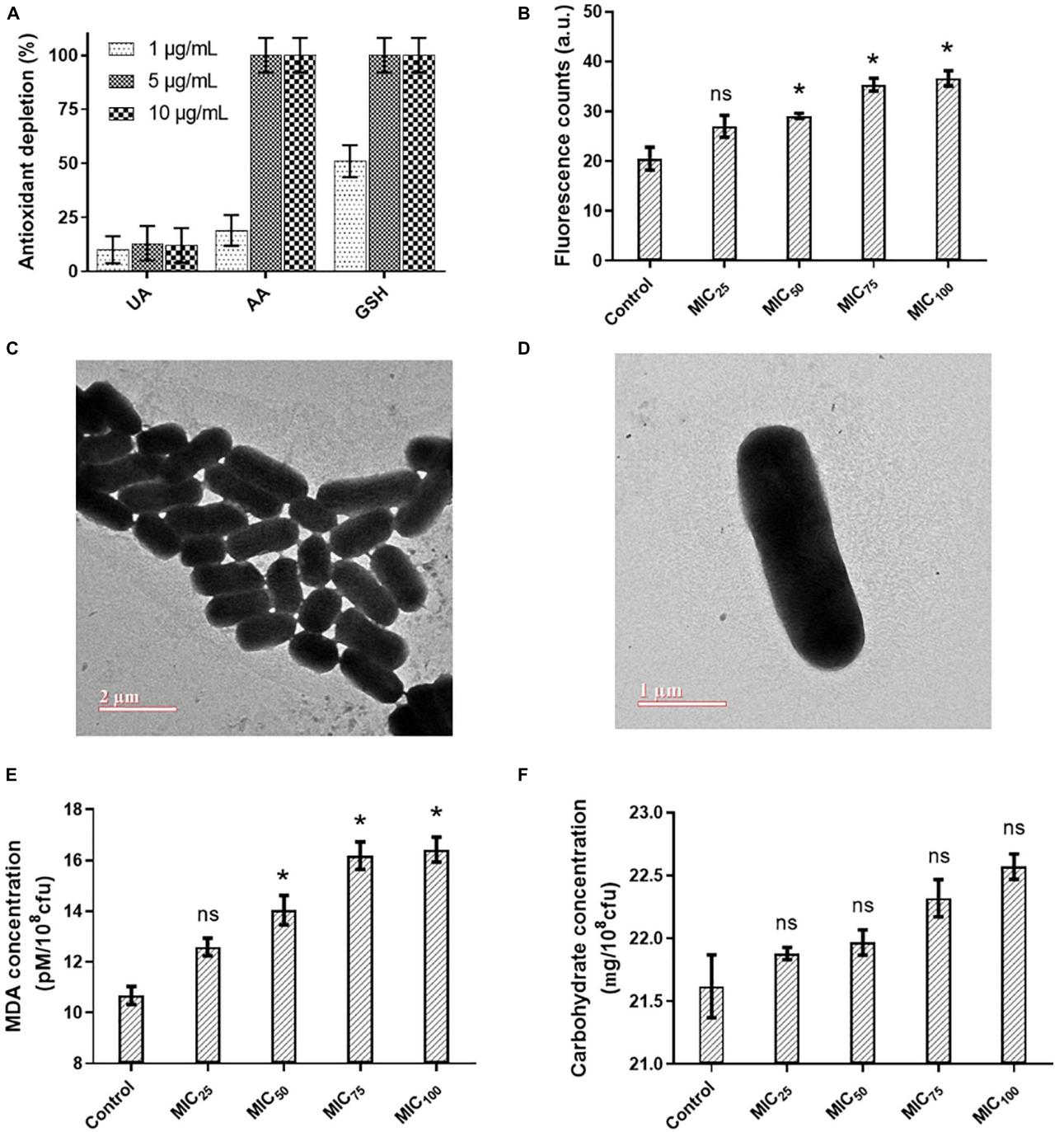

FIGURE 3 | (A) Acellular oxidative potential of L-Ag NPs measured by the depletion of antioxidants, uric acid (UA), ascorbic acid (AA), and reduced glutathione (GSH), in simplified synthetic lung lining fluid at 37°C. **(B)** Analysis of the intracellular ROS generation in *K. pneumoniae* MGH78578 following exposure to L-Ag NPs by the DCFH-DA assay. **(C,D)** Representative TEM images of untreated *K. pneumoniae* (control) **(C)** and *K. pneumoniae* exposed to MIC_{75} of L-Ag NPs **(D)**. **(E,F)** Membrane damage analysis of *K. pneumoniae* following exposure to L-Ag NPs. Analysis by MDA assay **(E)** and anthrone assay **(F)**. (*$p \leq 0.05$).

was used to identify differentially regulated genes. We obtained statistically significant data $p \leq 0.05$ for a total of 3,760 and 3,945 genes following 5 and 30 min exposure, respectively (**Figure 4A** and **Supplementary Dataset WS1**). Statistically significant genes with a $\log_2$ fold change expression of $\geq$1.0 and ≤ -1.0 (exposed *vs.* unexposed cells) were considered to be up- and down-regulated, respectively (Dash et al., 2018; Anes et al., 2019). For the post-5 min exposure, 1,008 genes were found to be upregulated and 1,063 genes were downregulated. At 30 min post exposure, 1,205 genes were found to be upregulated

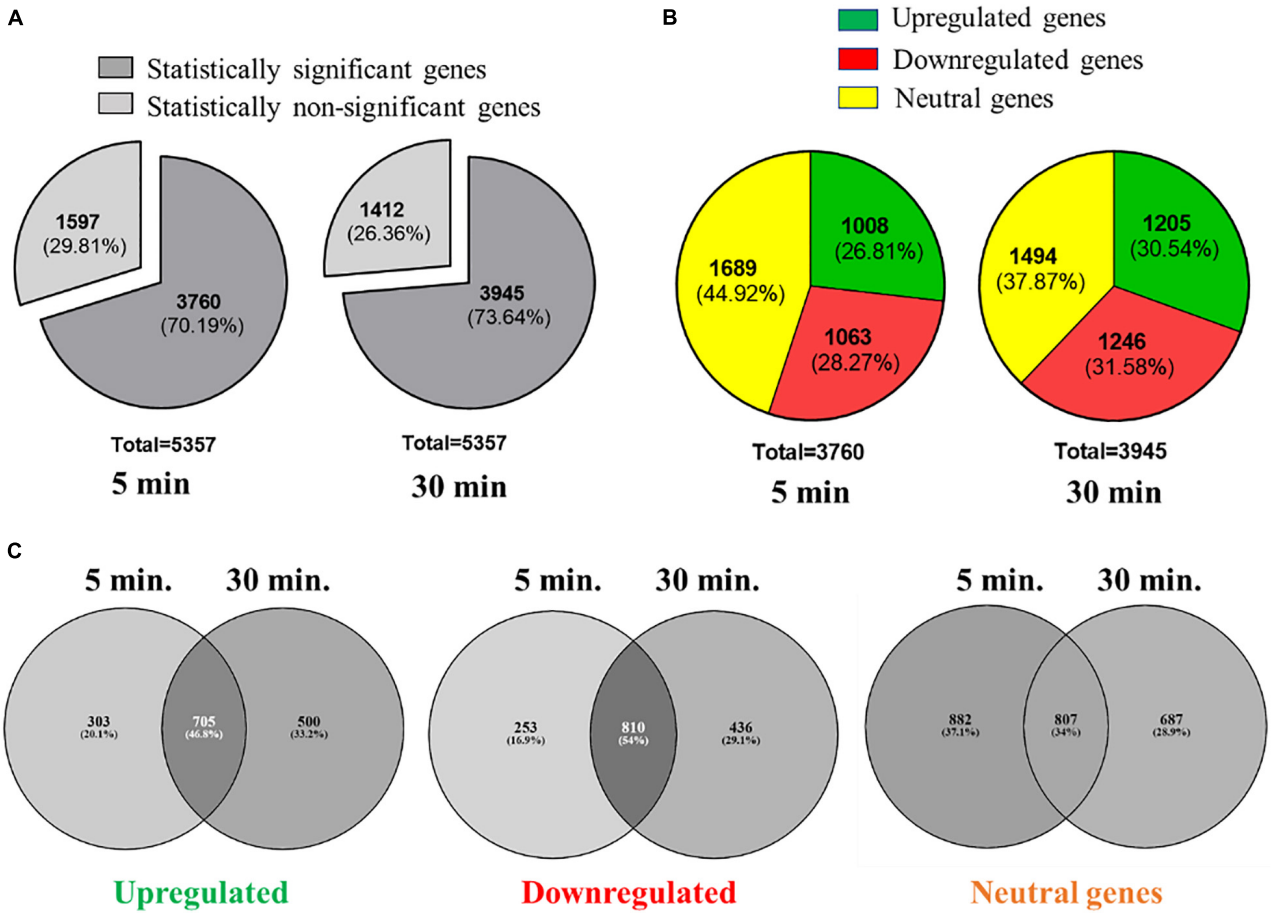

FIGURE 4 | Overview of the RNAseq analysis of *K. pneumoniae* MGH78578 following treatment with MIC_{75} L-Ag NPs. **(A)** Statistically significant and non-significant genes recorded at 5 and 30 min post-treatment. **(B)** Statistically significant upregulated, downregulated and neutral genes identified at 5 and 30 min post-treatment. **(C)** Comparison of the upregulated, downregulated, and neutral genes identified at 5 and 30 min post-treatment.

and 1,246 genes were downregulated (**Figure 4B**). Among all the upregulated genes at the 5- and 30-min, 705 genes were found to be commonly upregulated, whereas 303 and 500 genes were uniquely upregulated at 5 and 30 min, respectively. For downregulated genes, 810 genes were found to be commonly downregulated at both time points, whereas 253 and 436 genes were specifically downregulated at 5 and 30 min (**Figure 4C**).

We selected representative genes related to the bacterial defense system (*soxS*), transcriptional regulator (*ramA*), outer membrane porin proteins (*ompC*), and virulence (*rfaH*) to validate our transcriptomic data using qRT-PCR. Gene expression analysis reflected a similar pattern of results when compared to RNA-seq data (**Supplementary Figure 4**).

Bacterial Oxidative Stress Response Following Exposure to L-Ag NP

Our RNA-seq data shows that the oxidative stress response induced by ROS generation is choreographed by both *soxS* and *oxyR,* two major transcriptional factors that respond to oxidative stress in Enterobacteriaceae (Seo et al., 2015). The OxyR system functions as a global regulator of peroxide stress whilst the SoxRS system is involved in the control of superoxide stress (Zheng et al., 1998; Seo et al., 2015). Increased intracellular ROS levels induce the oxidation of OxyR protein, which in turn activates detoxifying processes including heme biosynthesis, thiol-disulfide isomerization, among others (Dubbs and Mongkolsuk, 2012). In the case of the SoxRS regulon, oxidative stress causes the oxidization of the SoxR protein, which activates the *soxS* transcriptional regulator, thereby triggering a bacterial defense mechanism involving various efflux pumps and redox counter measures (Seo et al., 2015). In L-Ag NP exposed *K. pneumoniae* MGH78578, *soxS* was highly upregulated (300- and 88-fold in 5 and 30 min) and in contrast *oxyR* was moderately upregulated (approximately 5-fold in both time points). This suggested that the oxidative stress regulon was active throughout the 30 min of L-Ag NP exposure time, particularly for the *soxS* regulon.

To confirm this, we compared our RNA-seq dataset to the *K. pneumoniae* MGH78578 **oxidative *soxS* regulon** generated earlier (Anes et al., 2020). We found that of the 254 genes belonging to the **oxidative *soxS* regulon**, 129 (51%) had similar

expression patterns in both datasets, confirming that the *soxS* regulon is activated in L-Ag NP exposed *K. pneumoniae* (**Supplementary Dataset WS2**). A typical example of *soxS* induction can be visualized in the expression of *fpr* (ferredoxin-NADP$^+$ reductase), which was induced at 22- and 9-fold at 5 and 30 min. In response to *soxS* activation, a redox neutralization process is triggered related to the overexpression of *fpr* by 4.5-fold at 5 min, that then reduced to 3.2-fold at 30 min post-treatment (Krapp et al., 2002).

Activation of Efflux Pumps Following Exposure to L-Ag NP

Bacteria activate various efflux pumps to expel the toxic Ag$^+$ (Randall et al., 2014; Gurbanov et al., 2018). Classic efflux pump-encoding genes such as *acrAB-tolC* (Hirakata et al., 2009; Baugh et al., 2013) and *marRAB* were found to be highly upregulated following treatment with L-Ag NPs, a feature that was sustained throughout the testing period of 30 min, possibly driven by the positive regulation *via* SoxS (Seo et al., 2015; Anes et al., 2020). Another efflux pump encoded by the *silCFBA* operon conferring a silver resistance phenotype was also upregulated (Randall et al., 2014; Elkrewi et al., 2017). Transcription of the *silCFBA* operon and *silP* are controlled by the *silRS*, which encodes a two-component system wherein SilR acts as a response regulator and SilS acts as a histidine kinase (Starodub and Trevors, 1989; Massani et al., 2018). SilP is a P-type ATPase efflux pump, which facilitates the passage of Ag$^+$ from cytoplasm to the periplasm. SilF acts as a chaperone and transfers Ag$^+$ from periplasm to the SilCBA complex, a three-protein dependent cation/proton antiporter system. Another protein from silver resistance system is SilE, present downstream to the *silRS* (**Figure 5**) (Starodub and Trevors, 1989; Massani et al., 2018). Upregulation of *silC/B/E/R/S/P* and KPN_pKPN3p05946 genes were noted in our RNA-seq data showing the activation of efflux pumps, encoding a possible silver resistance in response to L-Ag NP exposure.

The Type II Fatty Acid Biosynthesis Genes Were Down-Regulated in L-Ag NP Exposed *K. pneumoniae* MGH78578

Since *K. pneumoniae* MGH78578 expressed an MDR phenotype (Anes et al., 2017), L-Ag NP exposure dependent activation

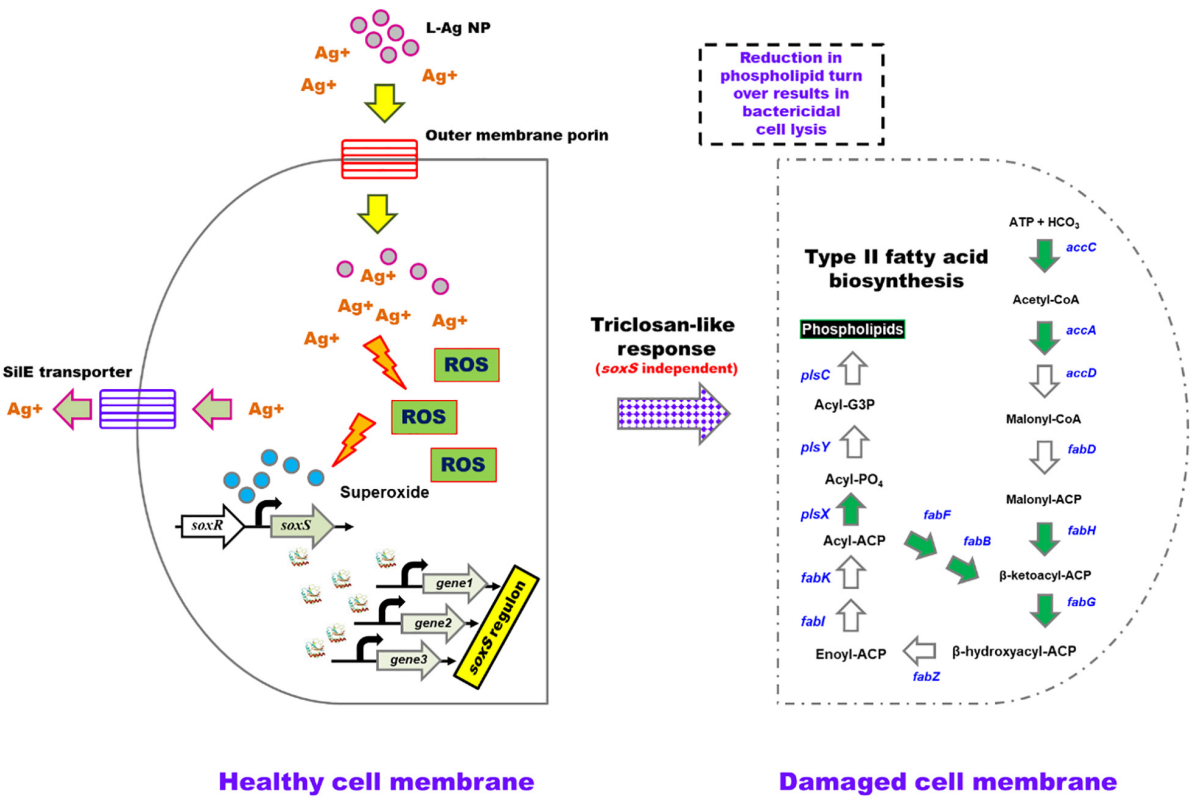

FIGURE 5 | A model depicting the bactericidal action of L-Ag NPs on *K. pneumoniae* MGH78578. L-Ag NPs and silver ions (Ag$^+$) enter the bacterial cell *via* outer membrane porins. Increasing cytoplasmic Ag$^+$ concentration elicits the production of reactive oxygen species (ROS) including superoxide radicals, which then activate the *soxS*-mediated oxidative stress response. The SilE efflux system functions to eliminate Ag$^+$ from the cytoplasm. RNA-seq data identified seven genes (denoted by the green arrowheads) associated with type II fatty acid biosynthesis that are down-regulated leading to reduced phospholipid biosynthesis. This reduction in phospholipid turnover will affect the membrane stability leading to cell lysis underpinning the bactericidal activity. Gray arrows represent genes that are activated. White arrows represent genes that are either not identified in the *K. pneumoniae* MGH78578 genome or not differentially regulated when the bacteria are exposed to L-Ag NPs.

of *acrAB-tolC, marRAB,* and *sil* genes should, in principle, confer silver resistance in *K. pneumoniae*. Additionally, the strong oxidative stress response should enable the bacterium to counter the oxidative stress induced by L-Ag NPs. Both of these mechanisms should render *K. pneumoniae* MGH78578 resistant against silver. However, *K. pneumoniae* MGH78578 was found to be susceptible to L-Ag NPs. We hypothesized that the bactericidal activity of L-Ag NPs could be due to a hitherto unknown mechanism, rather than the most commonly reported oxidative stress based bactericidal activity (Durán et al., 2016). To investigate, we compared our RNA-seq data to the transcriptional response of *E. coli* exposed to 37 antimicrobial compounds (O'Rourke et al., 2020). This global transcriptional profile of *E. coli* exposed to 37 antibiotics generated a list of 447 genes whose signature expression pattern characterized the mechanism of action associated with each antibiotic, leading the authors to hypothesize that the antibacterial action mechanism of any unknown/uncharacterized compounds can be deduced by comparing the transcriptional profile of a compound of interest with that of these 447 *E. coli* MG1665 K12 genes. We compared our exposed *K. pneumoniae* MGH78578 transcriptional data set with each individual dataset obtained from *E. coli* global transcriptional profile. Our comparative analysis showed that the highest number of similarly expressed gene pairs were obtained from the **triclosan exposure** dataset, suggesting that exposure to L-Ag NPs induced a *triclosan-like* exposure response in *K. pneumoniae* MGH78578. Some 76% of the gene pairs (73/96) at 5 min L-Ag NP exposure (**Supplementary Datasets WS3, WS4**) and 74% (87/117) at 30 min exposure (**Supplementary Datasets WS5, WS6**) had similar expression patterns compared with the *E. coli* triclosan dataset.

Triclosan is a broad-spectrum antimicrobial compound that acts by inhibiting FabI (a NADH-dependent enoylacyl carrier), a protein belonging to the type II fatty acid biosynthesis, part of a well-conserved pathway that is essential for bacterial survival. Inhibition of fatty acid biosynthesis compromises the bacterial cell membrane. During exposure to L-Ag NPs, some *K. pneumoniae* MGH78578 genes associated with type II fatty acid biosynthesis including *fabA/H/D/G/F/B* were significantly downregulated particularly during the adaptive response at 30 min. The downregulation of the different *fab* genes signals a compromised type II fatty acid biosynthesis underpinning the *triclosan-like* L-Ag NP bactericidal activity. Importantly, *fadL* and *fadD* were downregulated. FadL is a porin that transports extracellular fatty acids across the outer membrane to the inner membrane where they are activated by acyl CoA synthetase FadD. Downregulation of both *fadL* and *fadD* shows that extracellular fatty acids are not transported leading to subsequent suppression of type II fatty acid biosynthesis pathway. We, however, did not observe any differential expression in the *fabI* gene, possibly because the triclosan affects FabI post-translationally.

Recently, the TraDIS-Xpress approach involving a transposon mutant library and massively parallel sequencing of transposon chromosome junctions was used to identify *E. coli* genes that respond to triclosan exposure (Yasir et al., 2020). In comparison with these data, we identified genes that were both enriched in the *E. coli* TraDIS-Xpress dataset and that were found to be differentially expressed in our *K. pneumoniae* MGH78578 dataset. Common genes like *purL, purH, waeL, wzx* were downregulated at either one or both time points while *metB* was upregulated. Similarly, *K. pneumoniae* MGH78578 genes like *trkA, pcnB, infB,* and *ubiB/F* were downregulated at least in one or both time points, while *lonH* was upregulated (**Supplementary Dataset WS1**). TraDIS-Xpress selected *rbs* in their triclosan exposure screen. In *E. coli*, RbsABC forms the ABC-type high-affinity D-ribose transporter, while RbsD/K phosphorylates D-ribose to D-ribose 5-phosphate (Shimada et al., 2013). Though we did not observe a statistically significant differential expression for *rbsB,* down-regulation was observed for *rbsD* and *rbsC,* showing similarly compromised D-ribose uptake. These common observations across different datasets gave confidence to our earlier observation that L-Ag NP exposure elicits a *triclosan-like* bactericidal effect in *K. pneumoniae* inhibiting type II fatty acid biosynthesis.

The L-Ag NP Based Antibacterial Action Is Cumulative of Oxidative Stress and Fatty Acid Biosynthesis Inhibition

We investigated whether the L-Ag NP based antibacterial effect was primarily due to type II fatty acid biosynthesis inhibition or as a cumulative effect of both oxidative stress and fatty acid biosynthesis inhibition. We exposed the isogenic *K. pneumoniae MGH78578*Δ*soxS* mutant, which has a compromised oxidative stress response mechanism (Anes et al., 2020) to L-Ag NPs. The MIC of L-Ag NPs reduced to 15 μg mL^{-1} from 21 μg mL^{-1} showing that oxidative stress did contribute to a significant antibacterial effect. The antibacterial effect of L-Ag NPs is, therefore, a cumulative effect of both type II fatty acid biosynthesis inhibition and oxidative stress responses.

Concluding Observations

L-Ag NPs were very efficient in killing MDR *K. pneumoniae* MGH78578, triggering oxidative stress and a *triclosan-like* mechanism to exert their anti-*Klebsiella* effect. With toxicity studies in appropriate cell models, L-Ag NPs may be a future candidate as an antimicrobial agent. We hypothesized that our RNA-seq data could provide clues as to how *K. pneumoniae* might develop resistance against L-Ag NPs. Genes including *rbsD/C*, *trkA*, *pcnB*, and *infB* were downregulated during the adaptive response at 30 min. Transposon insertional mutants in *E. coli* genes *trkA*, *pcnB*, and *infB* exhibit better survival in the presence of triclosan (Yasir et al., 2020). Further, transposon insertion in *rbsB,* inhibiting the periplasmic ribose-binding domain of the RbsABC ribose importer, gave a selective survival advantage in the presence of triclosan. We hypothesize that by downregulating these genes during the adaptive response, *K. pneumoniae* MGH78578 could elicit strategies to combat the effects of exposure whilst resistance against L-Ag NPs. Exposure to sub-inhibitory concentrations of antimicrobial compounds is one of the main drivers in the evolution of AMR. By continuous exposure to sub-inhibitory concentrations of silver and the subsequent downregulation of these genes, *K. pneumoniae* might offer a transient resistance to L-Ag NPs. This hysteresis

effect might be the prelude to developing a fully expressed antimicrobial resistance mechanism against silver. However, the triclosan-like antibacterial action mechanism could be a *Klebsiella* specific effect. The reproduction of this effect in other bacterial pathogens needs to be experimentally evaluated.

DATA AVAILABILITY STATEMENT

The RNAseq data produced from the present work were deposited to the NCBI-GEO database and are available under the accession number GSE151953.

AUTHOR CONTRIBUTIONS

SD, SS, SF, VP, and JP designed the study. VP, AB, and SD characterized the silver NPs. VP and SS carried out the RNA-seq experiments. SKS generated the bioinformatics based gene expression dataset. SS, SD, VP, and SF carried out the detailed RNA-seq dataset analysis that led to the triclosan observation. All authors read and approved the manuscript.

FUNDING

VP acknowledges CSIR-SRF [09/719(0090)/2018-EMR-l] and EMBO Short Term Fellowship (ESTF 7654) for the financial support. This project was supported, in part, by the Ulysses PHC Scheme (CNRS).

ACKNOWLEDGMENTS

We are thankful to BITS Pilani, University College Dublin, and Université de Paris for providing lab facilities. We acknowledge Justine Renault, Linh-Chi Bui, and the Bioprofiler Facility (BFA) for the HPLC analysis.

SUPPLEMENTARY MATERIAL

The Supplementary Material for this article can be found online at: https://www.frontiersin.org/articles/10.3389/fmicb.2021.638640/full#supplementary-material

REFERENCES

Adamo, R., and Margarit, I. (2018). Fighting antibiotic-resistant *Klebsiella pneumoniae* with "sweet". immune targets. *mBio* 9:e00874-18.

Alexander, J. W. (2009). History of the medical use of silver. *Surg. Infect. (Larchmt.)* 10, 289–292. doi: 10.1089/sur.2008.9941

Anes, J., Dever, K., Eshwar, A., Nguyen, S., Cao, Y., Sivasankaran, S. K., et al. (2020). Analysis of the oxidative stress regulon identifies soxS as a genetic target for resistance reversal in multi-drug resistant *Klebsiella pneumoniae*. *bioRxiv* [preprint] doi: 10.1101/2020.08.21.262022

Anes, J., Hurley, D., Martins, M., and Fanning, S. (2017). Exploring the genome and phenotype of multi-drug resistant *Klebsiella Pneumoniae* Of clinical origin. *Front. Microbiol.* 8:1913. doi: 10.3389/fmicb.2017.01913

Anes, J., Sivasankaran, S. K., Muthappa, D. M., Fanning, S., and Srikumar, S. (2019). Exposure to sub-inhibitory concentrations of the chemosensitizer 1-(1-naphthylmethyl)-piperazine creates membrane destabilization in multi-drug resistant *Klebsiella pneumoniae*. *Front. Microbiol.* 10:92. doi: 10.3389/fmicb.2019.00092

Antoniadou, A., Kontopidou, F., Poulakou, G., Koratzanis, E., Galani, I., Papadomichelakis, E., et al. (2007). Colistin-resistant isolates of *Klebsiella pneumoniae* emerging in intensive care unit patients: first report of a multiclonal cluster. *J. Antimicrob. Chemother.* 59, 786–790. doi: 10.1093/jac/dkl562

Aranda, A., Sequedo, L., Tolosa, L., Quintas, G., Burello, E., Castell, J. V., et al. (2013). Dichloro-dihydro-fluorescein diacetate (DCFH-DA) assay: a quantitative method for oxidative stress assessment of nanoparticle-treated cells. *Toxicol. Vitr.* 27, 954–963. doi: 10.1016/j.tiv.2013.01.016

Ashraf, S., Chatha, M. A., Ejaz, W., Janjua, H. A., and Hussain, I. (2014). Lysozyme-coated silver nanoparticles for differentiating bacterial strains on the basis of antibacterial activity. *Nanoscale Res. Lett.* 9, 1–10.

Baker, M. J., Trevisan, J., Bassan, P., Bhargava, R., Butler, H. J., Dorling, K. M., et al. (2014). Using Fourier transform IR spectroscopy to analyze biological materials. *Nat. Protoc.* 9:1771.

Baugh, S., Phillips, C. R., Ekanayaka, A. S., Piddock, L. J. V., and Webber, M. A. (2013). Inhibition of multidrug efflux as a strategy to prevent biofilm formation. *J. Antimicrob. Chemother.* 69, 673–681. doi: 10.1093/jac/dkt420

Bhargava, A., Pareek, V., Roy Choudhury, S., Panwar, J., and Karmakar, S. (2018). Superior bactericidal efficacy of fucose-functionalized silver nanoparticles against *Pseudomonas aeruginosa* PAO1 and prevention of its colonization on urinary catheters. *ACS Appl. Mater. Interfaces* 10, 29325–29337. doi: 10.1021/acsami.8b09475

Buege, J. A., and Aust, S. D. (1978). "[30] Microsomal lipid peroxidation," in *Methods in Enzymology*, Vol. 52, eds S. Fleischer and L. Packer (Amsterdam: Elsevier), 302–310. doi: 10.1016/s0076-6879(78)52032-6

Cassini, A., Högberg, L. D., Plachouras, D., Quattrocchi, A., Hoxha, A., Simonsen, G. S., et al. (2019). Attributable deaths and disability-adjusted life-years caused by infections with antibiotic-resistant bacteria in the EU and the European Economic Area in 2015: a population-level modelling analysis. *Lancet Infect. Dis.* 19, 56–66. doi: 10.1016/S1473-3099(18)30605-4

Chambers, B. A., Afrooz, A. R. M. N., Bae, S., Aich, N., Katz, L., Saleh, N. B., et al. (2013). Effects of chloride and ionic strength on physical morphology, dissolution, and bacterial toxicity of silver nanoparticles. *Environ. Sci. Technol.* 48, 761–769. doi: 10.1021/es403969x

Chatterjee, S., Bandyopadhyay, A., and Sarkar, K. (2011). Effect of iron oxide and gold nanoparticles on bacterial growth leading towards biological application. *J. Nanobiotechnology* 9:34. doi: 10.1186/1477-3155-9-34

Chernousova, S., and Epple, M. (2013). Silver as antibacterial agent: ion, nanoparticle, and metal. *Angew. Chemie Int. Ed Engl.* 52, 1636–1653. doi: 10.1002/anie.201205923

Chopra, I. (2007). The increasing use of silver-based products as antimicrobial agents: a useful development or a cause for concern? *J. Antimicrob. Chemother.* 59, 587–590. doi: 10.1093/jac/dkm006

Chowdhury, S., Basu, A., and Kundu, S. (2014). Green synthesis of protein capped silver nanoparticles from phytopathogenic fungus *Macrophomina phaseolina* (Tassi) Goid with antimicrobial properties against multidrug-resistant bacteria. *Nanoscale Res. Lett.* 9:365. doi: 10.1186/1556-276X-9-365

Crobeddu, B., Aragao-Santiago, L., Bui, L. C., Boland, S., and Baeza Squiban, A. (2017). Oxidative potential of particulate matter 2.5 as predictive indicator of cellular stress. *Environ. Pollut.* 230, 125–133. doi: 10.1016/j.envpol.2017.06.051

Dash, S., Sarashetti, P. M., Rajashekar, B., Chowdhury, R., and Mukherjee, S. (2018). TGF-β2-induced EMT is dampened by inhibition of autophagy and TNF-α treatment. *Oncotarget* 9:6433. doi: 10.18632/oncotarget.23942

Dubbs, J. M., and Mongkolsuk, S. (2012). Peroxide-sensing transcriptional regulators in bacteria. *J. Bacteriol.* 194, 5495–5503. doi: 10.1128/jb.00304-12

Durán, N., Durán, M., de Jesus, M. B., Seabra, A. B., Fávaro, W. J., and Nakazato, G. (2016). Silver nanoparticles: a new view on mechanistic aspects on antimicrobial activity. *Nanomedicine* 12, 789–799. doi: 10.1016/j.nano.2015.11.016

Eby, D. M., Schaeublin, N. M., Farrington, K. E., Hussain, S. M., and Johnson, G. R. (2009). Lysozyme catalyzes the formation of antimicrobial silver nanoparticles. *ACS Nano* 3, 984–994. doi: 10.1021/nn900079e

Elkrewi, E., Randall, C. P., Ooi, N., Cottell, J. L., and O'Neill, A. J. (2017). Cryptic silver resistance is prevalent and readily activated in certain Gram-negative pathogens. *J. Antimicrob. Chemother.* 72, 3043–3046. doi: 10.1093/jac/dkx258

Gupta, A., Mumtaz, S., Li, C. H., Hussain, I., and Rotello, V. M. (2019). Combatting antibiotic-resistant bacteria using nanomaterials. *Chem. Soc. Rev.* 48, 415–427. doi: 10.1039/c7cs00748e

Gurbanov, R. S., Ozek, N., Tunçer, S., Severcan, F., and Gozen, A. G. (2018). Aspects of silver tolerance in bacteria: infrared spectral changes and epigenetic clues. *J. Biophotonics* 11:e201700252. doi: 10.1002/jbio.201700252

Haas, B. J., Chin, M., Nusbaum, C., Birren, B. W., and Livny, J. (2012). How deep is deep enough for RNA-Seq profiling of bacterial transcriptomes? *BMC Genomics* 13:734. doi: 10.1186/1471-2164-13-734

Han, J. H., Goldstein, E. J. C., Wise, J., Bilker, W. B., Tolomeo, P., and Lautenbach, E. (2016). Epidemiology of carbapenem-resistant *Klebsiella pneumoniae* in a network of long-term acute care hospitals. *Clin. Infect. Dis.* 64, 839–844.

Hirakata, Y., Kondo, A., Hoshino, K., Yano, H., Arai, K., Hirotani, A., et al. (2009). Efflux pump inhibitors reduce the invasiveness of *Pseudomonas aeruginosa*. *Int. J. Antimicrob. Agents* 34, 343–346. doi: 10.1016/j.ijantimicag.2009.06.007

Hu, Y., Anes, J., Devineau, S., and Fanning, S. (2020). *Klebsiella pneumoniae*: prevalence, reservoirs, antimicrobial resistance, pathogenicity, and infection: a hitherto unrecognized zoonotic bacterium. *Foodborne Pathog. Dis.* 17. doi: 10.1089/fpd.2020.2847

Huh, A. J., and Kwon, Y. J. (2011). "Nanoantibiotics": a new paradigm for treating infectious diseases using nanomaterials in the antibiotics resistant era. *J. Control. Release* 156, 128–145. doi: 10.1016/j.jconrel.2011.07.002

Jagnow, J., and Clegg, S. (2003). *Klebsiella pneumoniae* MrkD-mediated biofilm formation on extracellular matrix-and collagen-coated surfaces. *Microbiology* 149, 2397–2405. doi: 10.1099/mic.0.26434-0

Jain, N., Bhargava, A., Majumdar, S., Tarafdar, J. C., and Panwar, J. (2011). Extracellular biosynthesis and characterization of silver nanoparticles using *Aspergillus flavus* NJP08: a mechanism perspective. *Nanoscale* 3, 635–641. doi: 10.1039/c0nr00656d

Kalia, V. C., Patel, S. K. S., Kang, Y. C., and Lee, J. K. (2019). Quorum sensing inhibitors as antipathogens: biotechnological applications. *Biotechnol. Adv.* 37, 68–90. doi: 10.1016/j.biotechadv.2018.11.006

Kang, J., Dietz, M. J., Hughes, K., Xing, M., and Li, B. (2019). Silver nanoparticles present high intracellular and extracellular killing against *Staphylococcus aureus*. *J. Antimicrob. Chemother.* 74, 1578–1585. doi: 10.1093/jac/dkz053

Klemm, E. J., Wong, V. K., and Dougan, G. (2018). Emergence of dominant multidrug-resistant bacterial clades: lessons from history and whole-genome sequencing. *Proc. Natl. Acad. Sci.U.S.A.* 115, 12872–12877. doi: 10.1073/pnas.1717162115

Krapp, A. R., Rodriguez, R. E., Poli, H. O., Paladini, D. H., Palatnik, J. F., and Carrillo, N. (2002). The flavoenzyme ferredoxin (flavodoxin)-NADP (H) reductase modulates NADP (H) homeostasis during the soxRS response of *Escherichia coli*. *J. Bacteriol.* 184, 1474–1480. doi: 10.1128/jb.184.5.1474-1480.2002

Le Ouay, B., and Stellacci, F. (2015). Antibacterial activity of silver nanoparticles: a surface science insight. *Nano Today* 10, 339–354. doi: 10.1016/j.nantod.2015.04.002

Lee, G. C., and Burgess, D. S. (2012). Treatment of *Klebsiella pneumoniae* carbapenemase (KPC) infections: a review of published case series and case reports. *Ann. Clin. Microbiol. Antimicrob.* 11:32. doi: 10.1186/1476-0711-11-32

Li, B., Zhao, Y., Liu, C., Chen, Z., and Zhou, D. (2014). Molecular pathogenesis of *Klebsiella pneumoniae*. *Future Microbiol.* 9, 1071–1081.

Li, R., Chen, J., Cesario, T. C., Wang, X., Yuan, J. S., and Rentzepis, P. M. (2016). Synergistic reaction of silver nitrate, silver nanoparticles, and methylene blue against bacteria. *Proc. Natl. Acad. Sci. U.S.A.* 113, 13612–13617. doi: 10.1073/pnas.1611193113

Livak, K. J., and Schmittgen, T. D. (2001). Analysis of relative gene expression data using real-time quantitative PCR and the 2- ΔΔCT method. *Methods* 25, 402–408. doi: 10.1006/meth.2001.1262

Logan, L. K., and Weinstein, R. A. (2017). The epidemiology of Carbapenem-resistant *enterobacteriaceae*: the impact and evolution of a global menace. *J. Infect. Dis.* 215, S28–S36. doi: 10.1093/infdis/jiw282

Lok, C.-N., Ho, C.-M., Chen, R., He, Q.-Y., Yu, W.-Y., Sun, H., et al. (2007). Silver nanoparticles: partial oxidation and antibacterial activities. *JBIC J. Biol. Inorg. Chem.* 12, 527–534. doi: 10.1007/s00775-007-0208-z

Massani, M. B., Klumpp, J., Widmer, M., Speck, C., Nisple, M., Lehmann, R., et al. (2018). Chromosomal Sil system contributes to silver resistance in E. coli ATCC 8739. *BioMetals* 31, 1101–1114. doi: 10.1007/s10534-018-0143-1

McQuillan, J. S., Groenaga Infante, H., Stokes, E., and Shaw, A. M. (2012). Silver nanoparticle enhanced silver ion stress response in *Escherichia coli* K12. *Nanotoxicology* 6, 857–866. doi: 10.3109/17435390.2011.626532

Mijnendonckx, K., Leys, N., Mahillon, J., Silver, S., and Van Houdt, R. (2013). Antimicrobial silver: uses, toxicity and potential for resistance. *Biometals* 26, 609–621. doi: 10.1007/s10534-013-9645-z

Mulani, M. S., Kamble, E. E., Kumkar, S. N., Tawre, M. S., and Pardesi, K. R. (2019). Emerging strategies to combat ESKAPE pathogens in the era of antimicrobial resistance: a review. *Front. Microbiol.* 10:539. doi: 10.3389/fmicb.2019.00539

Neuner, E. A., Yeh, J.-Y., Hall, G. S., Sekeres, J., Endimiani, A., Bonomo, R. A., et al. (2011). Treatment and outcomes in carbapenem-resistant *Klebsiella pneumoniae* bloodstream infections. *Diagn. Microbiol. Infect. Dis.* 69, 357–362.

Ogawa, W., Li, D.-W., Yu, P., Begum, A., Mizushima, T., Kuroda, T., et al. (2005). Multidrug resistance in *Klebsiella pneumoniae* MGH78578 and cloning of genes responsible for the resistance. *Biol. Pharm. Bull.* 28, 1505–1508. doi: 10.1248/bpb.28.1505

O'Rourke, A., Beyhan, S., Choi, Y., Morales, P., Chan, A. P., Espinoza, J. L., et al. (2020). Mechanism-of-action classification of antibiotics by global transcriptome profiling. *Antimicrob. Agents Chemother.* 64:e01207-19.

Otari, S. V., Pawar, S. H., Patel, S. K. S., Singh, R. K., Kim, S. Y., Lee, J. H., et al. (2017). Canna edulis leaf extract-mediated preparation of stabilized silver nanoparticles: characterization, antimicrobial activity, and toxicity studies. *J. Microbiol. Biotechnol.* 27, 731–738. doi: 10.4014/jmb.1610.10019

Pareek, V., Bhargava, A., and Panwar, J. (2020). Biomimetic approach for multifarious synthesis of nanoparticles using metal tolerant fungi: a mechanistic perspective. *Mater. Sci. Eng. B* 262:114771. doi: 10.1016/j.mseb.2020.114771

Pareek, V., Gupta, R., and Panwar, J. (2018). Do physico-chemical properties of silver nanoparticles decide their interaction with biological media and bactericidal action? A review. *Mater. Sci. Eng. C* 90, 739–749. doi: 10.1016/j.msec.2018.04.093

Pelletier, D. A., Suresh, A. K., Holton, G. A., McKeown, C. K., Wang, W., Gu, B., et al. (2010). Effects of engineered cerium oxide nanoparticles on bacterial growth and viability. *Appl. Environ. Microbiol.* 76, 7981–7989. doi: 10.1128/aem.00650-10

Pendleton, J. N., Gorman, S. P., and Gilmore, B. F. (2013). Clinical relevance of the ESKAPE pathogens. *Expert Rev. Anti. Infect. Ther.* 11, 297–308. doi: 10.1586/eri.13.12

Podschun, R., and Ullmann, U. (1998). Klebsiella spp. as nosocomial pathogens: epidemiology, taxonomy, typing methods, and pathogenicity factors. *Clin. Microbiol. Rev.* 11, 589–603. doi: 10.1128/cmr.11.4.589

Rai, M. K., Deshmukh, S. D., Ingle, A. P., and Gade, A. K. (2012). Silver nanoparticles: the powerful nanoweapon against multidrug-resistant bacteria. *J. Appl. Microbiol.* 112, 841–852. doi: 10.1111/j.1365-2672.2012.05253.x

Randall, C. P., Gupta, A., Jackson, N., Busse, D., and O'Neill, A. J. (2014). Silver resistance in Gram-negative bacteria: a dissection of endogenous and exogenous mechanisms. *J. Antimicrob. Chemother.* 70, 1037–1046. doi: 10.1093/jac/dku523

Randall, C. P., Oyama, L. B., Bostock, J. M., Chopra, I., and O'Neill, A. J. (2012). The silver cation (Ag+): antistaphylococcal activity, mode of action and resistance studies. *J. Antimicrob. Chemother.* 68, 131–138. doi: 10.1093/jac/dks372

Ritchie, M. E., Phipson, B., Wu, D., Hu, Y., Law, C. W., Shi, W., et al. (2015). limma powers differential expression analyses for RNA-sequencing and microarray studies. *Nucleic Acids Res.* 43:e47. doi: 10.1093/nar/gkv007

Roe, D., Karandikar, B., Bonn-Savage, N., Gibbins, B., and baptiste, R. J. (2008). Antimicrobial surface functionalization of plastic catheters by silver nanoparticles. *J. Antimicrob. Chemother.* 61, 869–876. doi: 10.1093/jac/dkn034

Seo, S. W., Kim, D., Szubin, R., and Palsson, B. O. (2015). Genome-wide reconstruction of OxyR and SoxRS transcriptional regulatory networks under oxidative stress in *Escherichia coli* K-12 MG1655. *Cell Rep.* 12, 1289–1299. doi: 10.1016/j.celrep.2015.07.043

Sharma, V. K., Yngard, R. A., and Lin, Y. (2009). Silver nanoparticles: green synthesis and their antimicrobial activities. *Adv. Colloid Interface Sci.* 145, 83–96. doi: 10.1016/j.cis.2008.09.002

Shimada, T., Kori, A., and Ishihama, A. (2013). Involvement of the ribose operon repressor RbsR in regulation of purine nucleotide synthesis in *Escherichia coli*. *FEMS Microbiol. Lett.* 344, 159–165. doi: 10.1111/1574-6968.12172

Singh, D. K., Kumar, J., Sharma, V. K., Verma, S. K., Singh, A., Kumari, P., et al. (2018). Mycosynthesis of bactericidal silver and polymorphic gold nanoparticles: physicochemical variation effects and mechanism. *Nanomedicine* 13, 191–207. doi: 10.2217/nnm-2017-0235

Starodub, M. E., and Trevors, J. T. (1989). Silver resistance in *Escherichia coli* R1. *J. Med. Microbiol.* 29, 101–110. doi: 10.1099/00222615-29-2-101

Vimbela, G. V., Ngo, S. M., Fraze, C., Yang, L., and Stout, D. A. (2017). Antibacterial properties and toxicity from metallic nanomaterials. *Int. J. Nanomedicine* 12, 3941–3965. doi: 10.2147/IJN.S134526

Wang, H., and Joseph, J. A. (1999). Quantifying cellular oxidative stress by dichlorofluorescein assay using microplate reader. *Free Radic. Biol. Med.* 27, 612–616. doi: 10.1016/s0891-5849(99)00107-0

World Health Organization (2019). *No Time to Wait: Securing the Future From Drug-Resistant Infections.* Report to the Secretary-General of the United Nations. Geneva: World Health Organization.

Yasir, M., Turner, A. K., Bastkowski, S., Baker, D., Page, A. J., Telatin, A., et al. (2020). TraDIS-Xpress: a high-resolution whole-genome assay identifies novel mechanisms of triclosan action and resistance. *Genome Res.* 30, 239–249. doi: 10.1101/gr.254391.119

Zheng, K., Setyawati, M. I., Leong, D. T., and Xie, J. (2018). Antimicrobial silver nanomaterials. *Coord. Chem. Rev.* 357, 1–17. doi: 10.1016/j.ccr.2017.11.019

Zheng, M., Åslund, F., and Storz, G. (1998). Activation of the OxyR transcription factor by reversible disulfide bond formation. *Science* 279, 1718–1722. doi: 10.1126/science.279.5357.1718

Zou, L., Wang, J., Gao, Y., Ren, X., Rottenberg, M. E., Lu, J., et al. (2018). Synergistic antibacterial activity of silver with antibiotics correlating with the upregulation of the ROS production. *Sci. Rep.* 8:11131. doi: 10.1038/s41598-018-29313-w

Conflict of Interest: The authors declare that the research was conducted in the absence of any commercial or financial relationships that could be construed as a potential conflict of interest.

frontiers in Microbiology

ORIGINAL RESEARCH
published: 25 February 2021
doi: 10.3389/fmicb.2021.629429

Studying the Ability of Thymol to Improve Fungicidal Effects of Tebuconazole and Difenoconazole Against Some Plant Pathogenic Fungi in Seed or Foliar Treatments

Larisa Shcherbakova[1], Oleg Mikityuk[1], Lenara Arslanova[2], Alexander Stakheev[3], Denis Erokhin[2], Sergey Zavriev[3] and Vitaly Dzhavakhiya[2]**

[1] *Laboratory of Physiological Plant Pathology, All-Russian Research Institute of Phytopathology, Moscow, Russia,* [2] *Department of Molecular Biology, All-Russian Research Institute of Phytopathology, Moscow, Russia,* [3] *Laboratory of Molecular Diagnostics, Shemyakin-Ovchinnikov Institute of Bioorganic Chemistry, Moscow, Russia*

OPEN ACCESS

Edited by:
Jong H. Kim, United States Department of Agriculture, Agricultural Research Service, United States

Reviewed by:
Valeria Scala, Centro di Ricerca Difesa e Sperimentazione (CREA-DC), Italy
Claudio Altomare, National Research Council (CNR), Italy

***Correspondence:**
Larisa Shcherbakova
larisavniif@yahoo.com
Vitaly Dzhavakhiya
dzhavakhiya@yahoo.com

Specialty section:
This article was submitted to Antimicrobials, Resistance and Chemotherapy, a section of the journal Frontiers in Microbiology

Received: *14 November 2020*
Accepted: *03 February 2021*
Published: *25 February 2021*

Citation:
Shcherbakova L, Mikityuk O, Arslanova L, Stakheev A, Erokhin D, Zavriev S and Dzhavakhiya V (2021) Studying the Ability of Thymol to Improve Fungicidal Effects of Tebuconazole and Difenoconazole Against Some Plant Pathogenic Fungi in Seed or Foliar Treatments. Front. Microbiol. 12:629429. doi: 10.3389/fmicb.2021.629429

Thymol, a secondary plant metabolite possessing antifungal and chemosensitizing activities, disrupts cell wall or membrane integrity and interferes with ergosterol biosynthesis. Thymol also functions as a redox-active compound inducing generation of reactive oxygen species and lipid peroxidation in fungal cells. Previously, we showed thymol significantly enhanced the *in vitro* growth inhibitory effect of difenoconazole against *Bipolaris sorokiniana* and *Parastagonospora nodorum*. More recently, we demonstrated a possibility to use thymol to overcome the resistance of a *P. nodorum* strain able to grow on difenoconazole-containing media. However, potential for thymol to serve as a chemosensitizing agent in seed or plant treatments, to provide an effective suppression of the above-mentioned plant pathogens by triazole fungicides applied in lowered dosages, had yet to be tested. In the work presented here, we showed combined treatments of naturally infected barley seeds with thymol and difenoconazole (Dividend® 030 FS) synergistically exacerbated the protective effect against common root rot agent, *B. sorokiniana*, and other fungi (*Fusarium* spp. and *Alternaria* spp.). Similarly, co-applied treatment of wheat seeds, artificially inoculated with *Fusarium culmorum*, resulted in equivalent reduction of disease incidence on barley seedlings as application of Dividend®, alone, at a ten-fold higher dosage. In foliar treatments of wheat seedlings, thymol combined with Folicur® 250 EC (a.i. tebuconazole) enhanced sensitivity of *P. nodorum*, a glume/leaf blotch pathogen, to the fungicide and provided a significant mitigation of disease severity on treated seedlings, compared to controls, without increasing Folicur® dosages. Folicur® co-applied with thymol was also significantly more effective against a strain of *P. nodorum* tolerant to Folicur® alone. No additional deoxynivalenol or zearalenone production was found

when a toxigenic *F. culmorum* was cultured in a nutrient medium containing thymol at a concentration used for chemosensitization of root rot agents. Accordingly, *F. culmorum* exposure to thymol at the sensitizing concentration did not up-regulate key genes associated with the biosynthesis of trichothecene or polyketide mycotoxins in this pathogen. Further studies using field trials are necessary to determine if thymol-triazole co-applications result in sensitization of seed- and foliar-associated plant pathogenic fungi, and if thymol affects production of fusarial toxins under field conditions.

Keywords: thymol, chemosensitization to agricultural fungicides, triazoles, *Fusarium* spp., *Bipolaris sorokiniana*, *Parastagonospora nodorum*

INTRODUCTION

Redox-active secondary metabolites of various plants attract continuing interest with regard to the diversity of their biological activity (Jacob, 2014; de Oliveira et al., 2018). Since many of these natural compounds, including thymol, possess antibacterial, antifungal, anti-insect, and other protective properties, they are used in medicine and agriculture or are continually studied for further usage in these areas (Marchese et al., 2016). For example, thymol and thymol-containing essential oils are applied as antimicrobials (Ahmad et al., 2011; Najafloo et al., 2020) and other medical preparations (Riella et al., 2012; El-Marasy et al., 2020) or are proposed as putative ecologically friendly plant-protecting fungicides (Navarro et al., 2011; González-Aguilar et al., 2013; Castillo et al., 2014) and insecticides (Park et al., 2017), as alternatives to chemical pesticides.

An important specific feature of a number of redox-active compounds rendering them as promising agents for control of various pathogenic microorganisms, including some plant pathogenic fungi, is their ability to induce oxidative stress in pathogens or impair fungal antioxidation systems (Kim et al., 2012; Teixeira et al., 2013; Zhang et al., 2015; Shen et al., 2016; Ait Dra et al., 2017; Ji et al., 2018; Ma et al., 2019). In addition, such compounds were shown to augment the effect of antibacterial (Ait Dra et al., 2017; Kissels et al., 2017; Veras et al., 2017; Porter and Monu, 2019; Aksoy et al., 2020) and antifungal (Kordali et al., 2008; Kim et al., 2014, 2015, 2019; Rosato et al., 2018; Schlemmer et al., 2019) agents and to considerably enhance the pathogen sensitivity to antibiotics and antimycotics. In agriculture, this ability of natural redox-active products to improve the efficacy of chemical plant protection (Kim et al., 2017; Shcherbakova et al., 2019) and combat fungal strains resistant to industrial fungicides without increasing dosages (Campbell et al., 2012; Kim et al., 2012) could have significant importance, economically and ecologically.

The damaging and regulatory effects of redox-active molecules are realized through their interaction with lipids, proteins and DNA. These molecules cause lipid peroxidation, oxidative injury of the cell plasma membrane, protein, and DNA oxidation, as well as nitrosylation and S-glutathionylation of proteins (Belozerskaya and Gessler, 2007; Oktyabrsky and Smirnova, 2007). Thymol (2-isopropyl-5-methylphenol), a monoterpene phenol, is the major component of essential oil of *Thymus vulgaris* found also in other *Thymus* and *Lamiaceae* species. Thymol attacks several cellular and metabolic targets in pathogenic fungi. It disrupts cell wall or membrane integrity and interferes with ergosterol biosynthesis (Ahmad et al., 2011; De Lira Mota et al., 2012). Thymol functions also as a redox-active compound, inducing generation of reactive oxygen species and lipid peroxidation in fungal cells (Gao et al., 2016; Shen et al., 2016). Earlier, we showed addition of thymol together with Dividend SC, 3% (a.i. difenoconazole) into nutrient media significantly enhanced the inhibitory effect of this triazole fungicide on the colony growth of *Bipolaris sorokiniana* and *Parastagonospora nodorum* (Dzhavakhiya et al., 2012). Recently, we also demonstrated a potential for using thymol to overcome fungicide resistance of a *P. nodorum* strain that was able to grow on difenoconazole-containing media (Kartashov et al., 2019). However, the possibility to employ thymol as a chemosensitizing agent in seed or plant treatments to provide an effective suppression of the aforementioned plant pathogens by triazole fungicides, applied in lowered dosages, to date, not been tested. At the same time, lowering of effective dosages of these common fungicides could counter expanding pollution of agricultural areas with xenobiotics. In addition, the sensitized resistant strains could be rendered more vulnerable to the fungicides. In this regard, we explored whether seed or foliar treatments with two triazole-based formulations combined with thymol resulted in lowering effective fungicidal dosages in parallel with providing sufficient plant protection and effective control of the aforementioned pathogens. To this end, we studied the protective effect of difenoconazole (Dividend® 030 FS) against *B. sorokiniana*, *F. culmorum* and also accompanying *Fusarium* and *Alternaria* species on seedlings grown from barley and wheat seeds treated with this fungicide in combination with thymol. In another experimental series, protection efficacy of wheat seedlings sprayed with thymol-combined tebuconazole (Folicur® 250 EC) against *P. nodorum* was assessed. We found significant synergistic augmentation of the protective effect of both difenoconazole and tebuconazole when co-applied with thymol. In addition, a possibility to control a tebuconazole-tolerant *P. nodorum* mutant strain by co-application of thymol with Folicur® was showed. We also analyzed deoxynivalenol (DON) and zearalenone (ZEN) production in a toxigenic *F. culmorum* exposed to thymol and profiled expression of key genes associated with the biosynthesis of trichothecene or polyketide mycotoxins in this pathogen. These experiments demonstrated thymol at sensitizing concentrations did not stimulate DON and ZEN biosynthesis. Collectively, our findings

confirm the promise of using chemosensitizing agents as an approach to controlling fungal pathogens in agriculture and possibly contributing to development of better environmentally friendly integrated crop protection systems.

MATERIALS AND METHODS

Fungi

Strains of *Fusarium culmorum* (OR-02-37) and *Parastagonospora nodorum* (B-9/47) pathogenic to wheat were provided by the State Collection of Plant Pathogenic Microorganisms at the All-Russian Research Institute of Phytopathology (ARRIP) and the ARRIP Department of Mycology, respectively. *F. culmorum* stock cultures of the fungi maintained on potato dextrose agar slants were resumed by culturing for 10–14 days in Petri plates on the same medium to obtain spore-producing colonies. Suspensions of fungal conidia for inoculations of wheat seeds with *F. culmorum* and detached wheat leaves with *P. nodorum* were prepared according to Shcherbakova et al. (2018) and Shagdarova et al. (2018), respectively.

Samples of barley grain naturally infected with *Bipolaris sorokiniana*, a common root rot agent, were collected from plants grown on the ARRIP experimental plots.

Thymol and Fungicides

Since thymol (CAS 89-83-8) is slightly soluble in water, solutions of 99% commercial thymol (>99%; REARUS, Russia) in dimethyl sulfoxide, (CAS 67-68-5) 99.9% (Panreac, Spain) were used for seed and leaf treatments. Commercial fungicides tested included Dividend® 030 FS (a.i. difenoconazole, 3%) and Folicur® 250 EC (a.i. tebuconazole, 25%), which are commonly applied for seed and foliar treatments of various crops, including cereals.

Seed Treatments and Root Rot Development Assay

To select non-phytotoxic dimethyl sulfoxide (DMSO) and thymol concentrations, spring wheat (cv. Zlata) and barley (cv. Zazersky 85) seeds (200 seeds per each treatment) were soaked overnight in aqueous 0.5, 1.0, or 10% DMSO or in thymol dissolved in the DMSO solutions to final concentrations 10, 100, or 1000 ppm. After such treatments seeds were placed on paper towels (filter paper strips of 10 cm × 50 cm, 50 seeds per strip), which were rolled-up and put into beakers with distillated water. Plants were grown at 22°C (day) and 16°C (night), 60% relative humidity and 16-h light period for 7 days. Seeds treated with distillated water were used as controls. The number of germinated seeds, number of seedlings and their length were recorded after 7 days of plant growth.

Prior to conducting sensitization experiments, 50-g samples of non-disinfected barley seeds naturally infected by *B. sorokiniana* and wheat seeds artificially inoculated with *F. culmorum* were treated by a 3-h agitation in a minimal volume of aqueous Dividend® 030 FS allowing complete seed wetting. This was followed by 16–18 h incubation with the fungicide formulation at room temperature, without agitation. Prior to treatment with the fungicide, wheat seeds were disinfected (Shcherbakova et al., 2018), inoculated with *F. culmorum* using 1-h soaking in a conidial suspension (10^5 conidia/ml) at slow stirring, and then slightly dried. The highest difenoconazole concentration (500 ppm) used for fungicidal treatments of barley and wheat grain samples corresponded to Dividend® 030 FS dose rate recommended for agricultural practice (State Catalogue of Pesticides and Agrochemicals, 2018) for pre-sowing treatments of wheat and barley seeds (2.5 L/1000 kg of grain). To select sub-fungicidal dosages, several lower concentrations of Dividend® ranging from 5.0 to 250 ppm (i.e., from 0.15 to 7.5 ppm based on difenoconazole) were tested. After these treatments, the Dividend-exposed and water-exposed (control) seeds were assayed using rolled-towel test, as described above. After 12–14 days post-inoculation, the number of diseased seedling were counted to evaluate root rot incidence, and disease symptoms on were roots and root necks were visually estimated according to a five-score rating scale (Shcherbakova et al., 2018) to determine the average disease index.

Following the determination of sub-fungicidal Dividend® dosages and non-phytotoxic concentrations of DMSO-dissolved thymol, the respective fungicide and sensitizer dosages were used for combined treatments of barley seeds, naturally infected with *B. sorokiniana*, and wheat seeds, artificially inoculated with *F. culmorum*, as described above. Incidence and disease severity (R%) of common root rot and Fusarium root rot, on barley and wheat seedlings, respectively, were assayed using the rolled-towel test in parallel with the treatments with the fungicide alone. The incidence of *Fusarium* spp. and *Alternaria* spp. accompanying the predominant *B. sorokiniana* infection of barley seeds was also evaluated.

Evaluation of Folicur® Effect Against *Parastagonospora nodorum*

Detached Leaf Assay

In order to determine thymol concentrations, which did not injure wheat leaves but produced a minor disease-suppression effect (**Table 1**), detached wheat leaves were treated as described previously (Shagdarova et al., 2018). Briefly, *P. nodorum* spores were suspended to a final concentration of 10^6 conidia/ml in 1% aqueous DMSO or thymol (from 10 to 5000 ppm) dissolved in 1% DMSO. Control conidial suspensions (10^6 per ml) were prepared in sterile distilled water (SDW). Eight centimeter long leaf fragments were cut from central parts of detached wheat leaves and placed in Petri plates atop of 1% water agar supplemented with benzimidazole (40 μg/ml). Aliquots (10 μl) of the conidial suspensions in DMSO or thymol solutions were dropped on upper (distal) parts of 8-cm leaf fragments. Drops (10-μl) of conidial suspensions (10^6 conidia/ml) in SDW (control for DMSO-treated detached leaves) or 1% DMSO solutions (control for thymol-treated leaves) were applied to lower (basal) parts of the same 8-cm leaf fragments. *In situ* disease development was recorded on 10 leaf sections per each treatment. An additional plate, in which both distal and basal locations on each of 10 leaf fragment were inoculated with pathogenic conidia in SDW, was prepared to confirm that they was able to cause the

TABLE 1 | Effect of treatments of detached wheat leaves with Folicur® 250 EC or thymol solutions in DMSO on the severity of blotch symptoms caused by *Parastagonospora nodorum*.

Leaf treatments	Average score*	Disease suppression, % of control**
H_2O	2.97[a]	–
1% DMSO	2.95[a]	0.6
Thymol in 1% DMSO, ppm		
5000	0.55[b]	81.3
500	1.90[c]	35.6
100	2.60[d]	10.5
50	2.80[a]	5.2
10	2.98[a]	0.0
Folicur® in H_2O, ppm		
0.5	0.40[b]	86.5
0.25	1.63[e]	45.0
0.1	2.13[f]	28.3
0.05	2.85[a]	4.0

The mean of three replicated assays, 10 detached leaf fragments per treatment in each assay. Mean values indicated with different superscript letters are significant ($p \leq 0.05$: t-test for independent variables, STATISTICA 6.0). Percent suppression calculated relative to scores in corresponding control treatments of leaf fragments: water or 1% DMSO for fungicide or thymol, respectively (see section "Materials and Methods," "Detached Leaf Assay"). A five score rating scale (1 – small dark lesions; 2 – dark-brown clearly bordered spots, leaf tissue remains green; 3 – light-brown or brown growing spots edged with chlorosis; 4 – light-brown or brown, pycnid formation) was used (Shagdarova et al., 2018).*

disease. Disease symptoms were scored at 5 days post-inoculation according to a five-score rating. Sub-fungicidal dosages of Folicur® 250 EC, tested at concentrations ranging from 0.05 to 0.5 ppm (based on tebuconazole) were determined using the same assay (**Table 1**). This assay was also used to assess efficacy of Folicur® combined with thymol against a tebuconazole-resistant *P. nodorum* mutant.

Foliar Treatment of Wheat Seedlings Under Controlled Conditions

Spring wheat seedlings (cv. Khakasskaya) were grown in pots (25–30 seedlings per pot, four pots per treatment) to the two-three leaf stage under controlled conditions (at 21°C during 16-h photoperiod and 18°C during dark, respectively, and 60% relative humidity). Young seedlings were sprayed with *P. nodorum* spore suspensions (10^6 conidia/ml, 30 ml per each treatment) supplemented with Folicur® alone or DMSO-dissolved thymol alone, each taken at two sub-fungicidal (0.1 and 0.25 ppm of tebuconazole) or two marginally fungitoxic (50 and 100 ppm of thymol) dosages. In parallel, another seedling series was sprayed with fungal conidia suspended in solutions of the fungicide at a concentration of 0.1 ppm combined with thymol at 50 or 100 ppm. To promote infection, pots with treated and inoculated seedlings were maintained in an inocubation chamber at 80–85% relative humidity and 18°C for 24 h. Thereafter plant growing was continued under above-mentioned controlled conditions for 2 weeks. The disease development was scored according to the commonly approved international James'scale (James, 1971) at 14–15 days post-inoculation (the tillering stage Z25, Zadoks et al., 1974) as recommended for registration of early disease symptoms on spring wheat in Non-Chernozem zone of Russia (Sanin and Sanina, 2013).

Mycotoxin Production Assessment

To estimate production of deoxynivalenol (DON) and zearalenone (ZEN), a toxigenic *F. culmorum* strains, Fc-M-01-55/3, was grown in submerged culture for 7–9 days at 25°Ñ and 220 rpm (New Brunswick™ Excella E25/25R incubation shaker, New Brunswick Scientific, United States) in 250-ml shaker flasks with toxigenesis-promoting liquid Myro medium (Greenhalgh et al., 1988) supplemented with thymol to a final concentration of 50 ppm. Fungal biomass obtained by the submerged culturing was used to assess expression of toxigenesis-associated genes. To prepare other series of samples of fungal mycelia for expression analyses, Fc-M-01-55/3 colonies were also grown in the presence of the same thymol concentration on the same medium with 1.5% agar in 90-mm Petri plates at 25°C for 5–7 days. Thymol was dissolved in 1.0% aqueous DMSO sterilized by filtration through 0.22 μm Millipore membrane filters (MilliporeSigma, United States) and added in the liquid medium or the melted agar medium prior to inoculation. The media were inoculated by addition of a pathogen spore suspension (10^6 conidia/ml) or by placing a piece of fungal mycelium grown on PDA into the center of the plates. Fungal cultures grown in/on thymol-free media supplemented with corresponding aliquots of 1.0% DMSO under the same conditions served as controls.

Mycotoxin Quantification in Submerged *F. culmorum* Cultures

Upon completion of the cultivation, DON and ZEN were quantified by reverse phase HPLC using a Waters 1525 Breeze HPLC system equipped with a Waters 2487 UV detector, applying isolation procedures slightly modified from those described previously (Shcherbakova et al., 2018; Stakheev et al., 2018). Briefly, the submerged culture of each experimental or control flask was extracted twice with an equal volume of ethyl acetate or dichloromethane (to isolate ZEN or DON, respectively) for 1-h on an incubator shaker at 220 rpm and 25°C. Mycelia were separated by centrifugation and dried at 102°C up to a constant weight. Organic phases of supernatants were passed through a layer of anhydrous Na_2SO_4 and evaporated on a rotary evaporator at 40°C. Dry residues were dissolved in a mixture of acetonitrile, methanol and water (1:1:0.75) or (1:1:4.0) used as mobile phases in RP-HPLC analyses of ZEN or DON, respectively. Aliquots (10 μL) of the prepared solutions were applied on a temperature-controlled Symmetry C18 (5 μm, 4.6 mm × 150 mm) column followed by toxin elution, using the above-mentioned mobile phases, and detected at 254 nm. Mycotoxin concentrations (μg/mg) were calculated using a calibration curve based on commercial DON and ZEN preparations (Sigma-Aldrich Corp., United States), which were also added in extracts obtained from control fungal cultures as external standards. All samples were analyzed twice. The limits of detection were 0.5 (DON) and 0.2 (ZEN) ng/mg; the recovery levels averaged 81% and 77% for DON and ZEN, respectively.

RNA Extraction and Reverse Transcription

Total RNA was extracted from fungal mycelium using RNeasy® Plant Mini Kit (QIAGEN, Germany) according to manufacturer's protocol. Ten microgram of total RNA were used for cDNA synthesis carried out by the MMLV RT kit (Evrogen JSC, Russia).

Quantitative PCR

Expression levels of the following four genes responsible for different steps of trichothecene and polyketide biosynthesis were quantified by qPCR: *TRI5* (trichodiene synthase), *TRI6* (transcription factor), *PKS4* and *PKS13* (polyketide synthesis) were analyzed by qPCR. The translation elongation factor 1 alpha gene (*TEF1α*) served as a control as the most suitable housekeeping gene according to Kim and Yun (2011). The sequences of primers and probes are presented in **Table 2**. The ClustalX algorithm and Oligo 6.71 program were used for designing gene-specific primers and estimation of their physical properties, respectively. qPCR analyses were performed in a DT-96 thermal cycler (DNA-technology, Russia) according to the following conditions: 94°C for 1 min followed by 45 cycles at 94°C for 10 s, 64°C for 15 s, 72°C for 10 s, and finally 72°C for 3 min. The PCR mix composition was described earlier (Stakheev et al., 2016). Threshold method was used for quantification cycle calculation and analysis of results. qPCR amplification efficiency was calculated using the C_q slope method. QGene96 software was used for analyzing the qPCR results.

Data Analysis and Statistics

Data obtained in the experiments involving seed treatments and spraying of wheat seedlings were analyzed using a STATISTICA 6.1 software (StatSoft Inc.). Mean values, standard deviations and standard errors were calculated. Significant difference between treatments and controls were determined using a *t*-test for independent variables at $p \leq 0.05$. Experiments involving spraying of wheat seedlings (100–120 ones for each treatment) or assessment of *Alternaria* incidence on barley seeds were replicated four times. Other experiments were run in triplicate. Each independent experiment with barley or wheat gain included 200 seeds per treatment.

Protection efficacy (PE) was calculated using formula PE% = Dc – Dt/Dc × 100, where Dc is the average incidence or disease severity in controls, while Dt represents these parameters for treated seeds or seedlings.

To reveal a putative synergy between thymol and tebuconazole or difenoconazole in co-applications on seeds or seedlings, the Limpel criterion, Er ≥ Ee (at $p \leq 0.05$), was determined (Richer, 1987). In this inequality, Er represented PE% obtained when Dividend® or Folicur® was combined with thymol. Ee is an expected additive effect, i.e., the estimated PE% that could result from summing the protective efficacy of each of components alone calculated using the formula Ee = (X% + Y%) – X% × Y%/100, where X% and Y% are PE% of thymol or the fungicide.

RESULTS

Improved Protective Efficacy of Triazoles Combed With Thymol

Enhancing the Fungicidal Effect of Dividend® Against Root Rot Agents

The testing phytotoxic effects of DMSO and thymol, which preceded the experiments on individual and thymol-combined fungicidal treatments, showed there was no inhibition of wheat seed germination and seedling formation after seed soaking in 0.5% or 1.0% DMSO. Application of 10% DMSO on barley seeds strongly suppressed germination (**Table 3**). The highest concentration of thymol (1000 ppm) in 10% DMSO was phytotoxic for wheat and barley based on roll-towel assay. However, thymol at a concentration of 100 ppm dissolved in 1% DMSO was not phytotoxic to seeds of wheat, but was toxic to barley seeds, but did not impede the development of barley seedlings when applied at lower concentrations (**Table 3**). Based on the results of these initial phytotoxicity assays, thymol at a final concentration of 50 ppm dissolved in 1% DMSO was selected for further chemosensitization experiments on barley and wheat seeds, naturally or artificially infected with fungal root rot agents, respectively.

The highest concentration of difenoconazole in our experiments reflected the commercial fungicidal dosage recommended for grain treatments with Dividend® to protect wheat and barley plants against Fusarium and common

TABLE 2 | Gene-specific primers and hydrolysis probes used.

Gene	Function	Primers	Probe	Efficiency
Tri5	Trichodiene synthase	F: TGGGCACTYGTCAACG R: ATCCARCATCCCTCR4AAAAAG	BHQ1-CCATAGTGCTACGGA(FAMdT)AAGGTTCAATGAGCAG	1.86
Tri6	Transcription factor	F: ACTATGAATCACCAACWTTCGAA R: TTGTGTATCCGCCTATAGTGATC	BHQ1-CAAGGGCACCGCAC(FAMdT)GTTGGTTTGTG	1.90
PKS4	Polyketide synthase	F: CACATCTCCATCCAAGTTCTG R: GGATCCTGCTTCAAAAAGTGT	BHQ1-GATGGTAGAAGGC(FAMdT)TGTGCATTGTACCGATC	1.91
PKS13	Polyketide synthase	F: TGGATGCGACGCCTACAC R: TGCCCGTGTCGGACAATAC	BHQ1-GGCCCAACCTAC(FAMdT)CACTCGACTCGGC	1.95
TEF1α	Translation elongation factor 1 alpha	F: GTTGGTCTCATTTTCCTCGATC R: GAGYGGCGGGGTATGAGC	BHQ1-CGACTCGATACGCGCC(FAMdT)GTTACCCCG	1.88

TABLE 3 | Influence of wheat and barley seed treatments with dimethyl sulfoxide (DMSO) and thymol dissolved in DMSO on seedling formation.

Plant	Treatments	Seedlings number, % ***
Wheat*	Control, water	96[a]
	10% DMSO	54[b]
	Thymol (1000 ppm) in 10% DMSO	36[c]
	1% DMSO	94[a]
	Thymol (100 ppm) in 1.0% DMSO	92[a]
	Thymol (50 ppm) in 1.0% DMSO	89[a]
	0.5% DMSO	95[a]
	Thymol (10 ppm) in 0.5% DMSO	90[a]
Barley**	Control, water	57[b]
	10% DMSO	9[d]
	Thymol (1000 ppm) in 10% DMSO	0
	1% DMSO	55[c]
	Thymol (100 ppm) in 1.0% DMSO	39[c]
	Thymol (50 ppm) in 1.0% DMSO	55[b]
	Thymol (10 ppm) in 0.5% DMSO	61[b]

**Seeds were surface-disinfect before treatments as described earlier (Shcherbakova et al., 2018). **Non-disinfect seeds naturally infected by fungal root rot agents. ***Percent relative to total seed number. Difference between means (200 seeds per treatment in each of three experiments) indicated with the same letters are insignificant at $p \leq 0.05$ (t-test for independent variables, STATISTICA 6.0).*

TABLE 4 | Development of *B. sorokiniana* on barley seedlings grown from naturally infected seeds treated with Dividend® 030 FS.

Treatments	Seed germination, %	Common root rot (*B. sorokiniana*)*	
		Diseased seedlings, %	Average disease index
Control (no fungicide)	87.0[a]	49.4[a]	2.8[a]
Dividend/1	75.0[b]	8.7[b]	0.3[b]
Dividend/05	65.0[b]	20.0[c]	0.8[c]
Dividend/01	87.0[a]	30.5[d]	2.0[d]
Dividend/001	85.0[a]	49.4[a]	2.8[a]

**The means of three experiments (n = 200 per treatment in each). Dividend® 030 FS dosage recommended for grain treatments against Fusarium and common root is indicated as Dividend/1; Dividend/05, /01, and /001 represent twofold-, tenfold-, and hundredfold-diminished dosages, respectively. Means within each column indicated with different superscript letters are significantly different ($p \leq 0.05$; t-test for independent variables, STATISTICA 6.0). A five-score rating scale (0 – no disease symptoms; 1– weak symptoms: brown streaks or spots on roots and above; 2 – medium-manifested symptoms; 3 – strong extensive symptoms, 4 – crown and root decaying or plant death) was used (Shcherbakova et al., 2018).*

TABLE 5 | Development of *Fusarium culmorum* on wheat seedlings grown from artificially infected seeds treated with different dosages of Dividend® 030 FS.

Treatments	Seed germination, %	Fusarium root rot (*F. culmorum*)*	
		Diseased seedlings, %	Average disease index
Control (no fungicide)	95.0	84.3[a]	3.6[a]
Dividend/1	95.0	54.5[b]	1.9[b]
Dividend/05	94.0	80.3[a]	2.3[b]
Dividend/01	95.0	71.4[c]	3.1[a]
Dividend/001	96.0	79.2[a]	3.5[a]

Numbers in the columns represent the means of three experiments (n = 200 per treatment in each). Means indicated with different letters are significant at $p \leq 0.05$. For additional explanations, see captions to **Tables 3, **4**.*

root rots. For three other treatments, this fungicide was used at dosages half, 10 and a 100 times lower than the highest concentration (i.e., at 7.5, 1.5, and 0.15 ppm based on difenoconazole). These four dosages are indicated below as Dividend/1 (the highest), Dividend/05, Dividend/01, and Dividend/001, respectively. Results of roll-towel assays showed Dividend/1 and Dividend/05 were effective against common root rot infection on barley seedling, while Dividend/01 was the lowest dosage still inhibiting development of *B. sorokiniana*, a predominant seed pathogen, and did not affect seed germination (**Table 4**). As with naturally infected barley grain, Dividend/01 was the lowest sub-fungicidal dosage when using artificial inoculations of wheat seeds with *F. culmorum* (**Table 5**). Based on these results, Dividend/01, i.e., the dosage tenfold lower than recommended in agricultural practice, was selected for subsequent chemosensitization experiments.

Studying the thymol ability to potentiate fungicidal effect of Dividend® toward *B. sorokiniana* showed this redox-active compound was able to sensitize the pathogen to difenoconazole in combined treatments of naturally infected barley seeds. Significantly higher disease suppression was found on seedlings grown from seeds treated with the fungicide combined with thymol, compared to seedlings germinated from seeds treated with Dividend/01 alone (**Figure 1**). After co-application on seeds, an almost fivefold decrease in pathogen incidence was observed on barley seedlings, and disease severity (R%) was six times lower than that on seedlings grown from seeds, which were soaked in Dividend/01 alone. Moreover, in our experiments, combining the fungicide with thymol provided an almost equal antifungal effect as the tenfold higher dosage, Dividend/1, recommended for agricultural practice. The real antifungal effect of the combined treatments (Er) significantly exceeded not only the impact of Dividend/01, taken alone, but also the calculated additive effect (Ee) expected if there was no synergy (**Figure 1**). Hence, the elevated protective efficacy of the co-applications resulted from a synergy (Richer, 1987) between thymol and difenoconazole.

In addition to the predominant root rot pathogen, *B. sorokiniana*, we found in preliminary mycological analyses that the barley seeds used were naturally infected with *Fusarium* spp. and *Alternaria* spp. as minor infections with the incidence 10.5% and 7% in DMSO-treated control, respectively. Therefore, we examined the effect of the fungicide-and-thymol treatments against these causative agents, as well. Twofold reduction of *Alternaria* incidence was noticed on the seedlings if Dividend/01 was applied on the seeds conjointly with thymol in two of four performed assays (to 2.7 and 3.5%), but no effect was found in two other ones. Compared to controls, the average incidence of Fusarium rot agents on seedlings decreased to 6.4% or 3.2% after seed treatments with Dividend/01, alone, or Dividend/01 + thymol at 50 ppm, respectively.

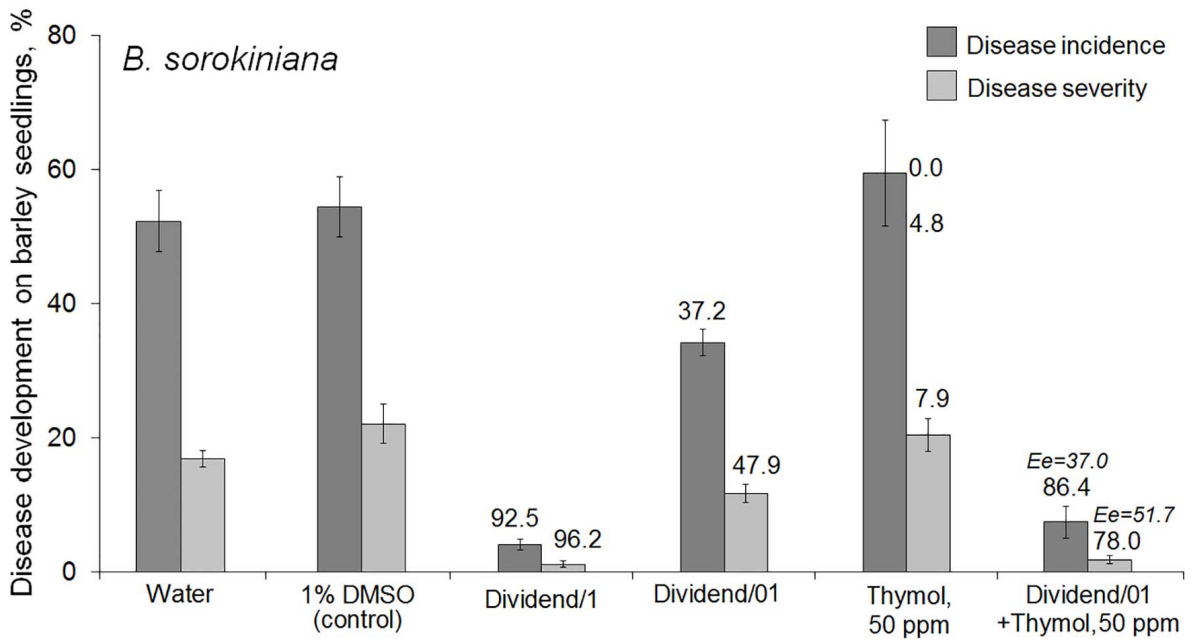

FIGURE 1 | Effect of seed treatments with Dividend® alone, thymol alone or their combination on the development of a root rot agent, *Bipolaris sorokiniana*, on spring barley seedlings (cv. Zazersky 85). Dividend/1, the fungicide dosage recommended for industrial seed treatments. Dividend/01, the fungicide dosage ten times lower than recommended. In treatments involving thymol, it was used as a solution in 1% dimethyl sulfoxide (DMSO). Numbers in regular font above the columns show percent disease suppression observed in experiments (Er). Percent suppression calculated for expected additive effect (Ee) is indicated with italic numbers (see section "Materials and Methods," "Data Analysis and Statistics"). Disease incidence was determined as the average percent of rotted seedlings compared to DMSO-treated controls. Disease severity was calculated by formula: $R\% = \Sigma (n \times d)/4N \times 100$, where n – the number of seedlings with the same disease index; d – the disease index according to a score rating scale (from 0 to 4); N – the number of seedlings per treatment; 4 – the maximal score in the scale (Shcherbakova et al., 2018). Results are expressed as the means of three independent roll-towel assays, 200 seeds per treatment in each assay. Y-bars show SE with a 95% confidence interval ($p \leq 0.05$, *t*-test for independent variables; STATISTICA v. 6.1, StatSoft Inc.).

Co-application of thymol and Dividend® on artificially inoculated wheat seeds also resulted in augmentation of the suppressive activity of this triazole fungicide against *F. culmorum* (**Figure 2**). After co-applications of Dividend/01 combined with thymol, both incidence and severity of the disease on wheat seedlings were almost twice as low compared to application of Dividend/01 only. Comparisons of Er with Ee values suggested the augmented fungicidal effect obtained in experiments involving artificial seed inoculation was most likely a result of both sensitizing and fungitoxic activity of thymol. Thus, reduction of *F. culmorum* incidence on wheat seedlings after the fungicide-thymol co-application significantly exceeded the estimated additive effect. However, mitigation of disease severity by these combined applications was induced to a certain degree by an additive interaction of the fungicide and thymol rather than by chemosensitization (**Figure 2**). Nevertheless, joint influence of Dividend/01 and thymol on the Fusarium root rot agent had total fungicidal effect equal to the effect of a tenfold higher dosage of the fungicide, alone.

Enhancing the Fungicidal Effect of Folicur® Against *Parastagonospora nodorum*

Thymol was found to augment protective action of Folicur® EC 250 against *P. nodorum* in foliar treatments of wheat seedlings grown under controlled conditions. Spraying of wheat seedlings with thymol at 50 ppm or with the fungicide at 0.1 ppm did not sufficiently suppress disease development. In contrast, the combined treatment with the same doses of tebuconazole and thymol increased the antifungal effect. The co-applications resulted in disease suppression at a level exceeding the effect of the higher dosage of the fungicide (0.25 ppm) after application of fungicide, alone (**Figure 3**). Calculation of Limpel's criterion (Richer, 1987) pointed to existence of synergy between thymol and tebuconazole in both combinations used. Er values (58.8 and 67.2%) exceeded Ee values (35.7 and 43.0%) at $p = 0.02$ and 0.03, respectively (**Figure 3**). Thus, joint treatments of wheat seedlings with fungicide and sensitizer produced an enhanced protective effect without increasing fungicide dosage.

Thymol-Folicur® combinations were used against a *P. nodorum* mutant strain manifesting tolerance to this fungicide. This mutant was able to grow on PDA supplemented with tebuconazole concentrations up to 1.25 ppm (i.e., up to 5 ppm based on the formulation) that was lethal to a sensitive wild strain (**Figure 4A**). Both thymol and tebuconazole at dosages of 50 ppm and 0.05 ppm, respectively, did not show a protective effect against the tolerant pathogen when applied separately. In contrast, the combined treatment at these dosages

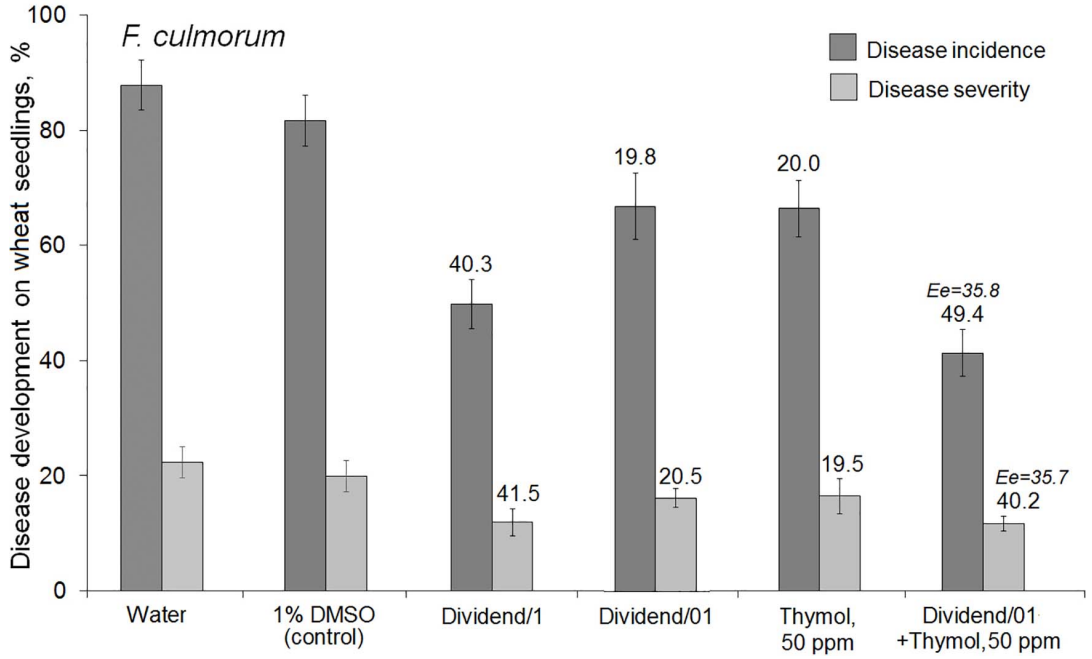

FIGURE 2 | Influence of seed treatments with Dividend® alone, thymol alone or their combination on the development of Fusarium root on spring wheat seedlings (cv. Zlata) from seeds artificially inoculated with *F. culmorum*. Dividend/1 and Dividend/01, the fungicide dosage recommended for industrial seed treatments and tenfold-lower dosage, respectively. Numbers above columns show Er values, while an expected additive effect (Ee) is indicated with italic numbers. The means of three independent roll-towel assays (n = 200 seeds per treatment in each assay). Y-bars show SE ($p \leq 0.05$). For additional explanations, see caption to **Figure 1** and section "Materials and Methods," "Data Analysis and Statistics."

resulted in an observable mitigation of lesions on detached leaves inoculated with either the wild or with the tolerant strain (**Figure 4B**).

Mycotoxin Production by Toxigenic *Fusarium culmorum* Exposed to Thymol

To ensure thymol did not induce production of sesquiterpenoid or polyketide fusariotoxins, DON and ZEN content was analyzed by HPLC after culturing a toxin-producing *F. culmorum* strain in media supplemented with thymol at 50 ppm, the concentration used to sensitize the pathogen to Dividend®. In addition, expression levels of selected genes associated with mycotoxin production by *Fusarium* fungi (Lysøe et al., 2006; Kimura et al., 2007; Villafana et al., 2019) were explored.

No statistically significant increase of DON and ZEN concentrations compared to control was determined using HPLC (**Table 6**). Expression levels of key mycotoxin biosynthetic genes of *F. culmorum* were analyzed by qPCR for four genes, two (*TRI5* and *TRI6*) localized in the trichothecene biosynthetic cluster and two (*PKS4* and *PKS13*) belonging to the polyketide biosynthetic cluster. Gene expression was analyzed 2 days before the maximal accumulation of DON or ZEN in thymol-containing culture media inoculated with the pathogen. Levels of *TRI5*, *TRI6*, *PKS4*, and *PKS13* expression were compared to those in control fungal cultures grown without thymol under the same conditions. Expression of the control gene (*TEF1α*) was stable in all the samples tested. Expression levels of four target genes in thymol-exposed samples were the same or slightly lower those of the control, in both submerged and agar cultures (**Figure 5**).

DISCUSSION

Thymol appears to be a promising chemosensitizing agent for various pathogenic and opportunistic fungi, based on several *in vitro* studies. For instance, Kim et al. (2015) found thymol synergistically interacted with another redox-active molecule, 2-hydroxy-4-methoxybenzaldehyde (2H4M), augmenting the efficacy of cell wall disruption by these compounds and enhancing their effect against *Aspergillus fumigatus* and *Aspergillus parasiticus*. Thymol and 2H4M co-applications resulted also in a lowering of fungicidal concentrations and an elevated antifungal activity of these compounds for *Aspergillus flavus*, *Saccharomyces cerevisiae*, and *Penicillium* strains, despite fractional inhibitory concentration indices (FICIs) pointing to the absence of a calculated synergism (Kim et al., 2015). Accordingly, Guarda et al. (2011) demonstrated the synergistic effect between thymol and its isomer, caracole, toward *Aspergillus niger* growth inhibition. A partial synergism was revealed when thymol was tested in combinations with monoterpene- and phenol-containing citronella and garlic essential oils used to inhibit *Penicillium corylophilum* causing a spoilage of dried meat foods (Ji et al., 2019). Thymol displayed also *in vitro* synergistic interaction with

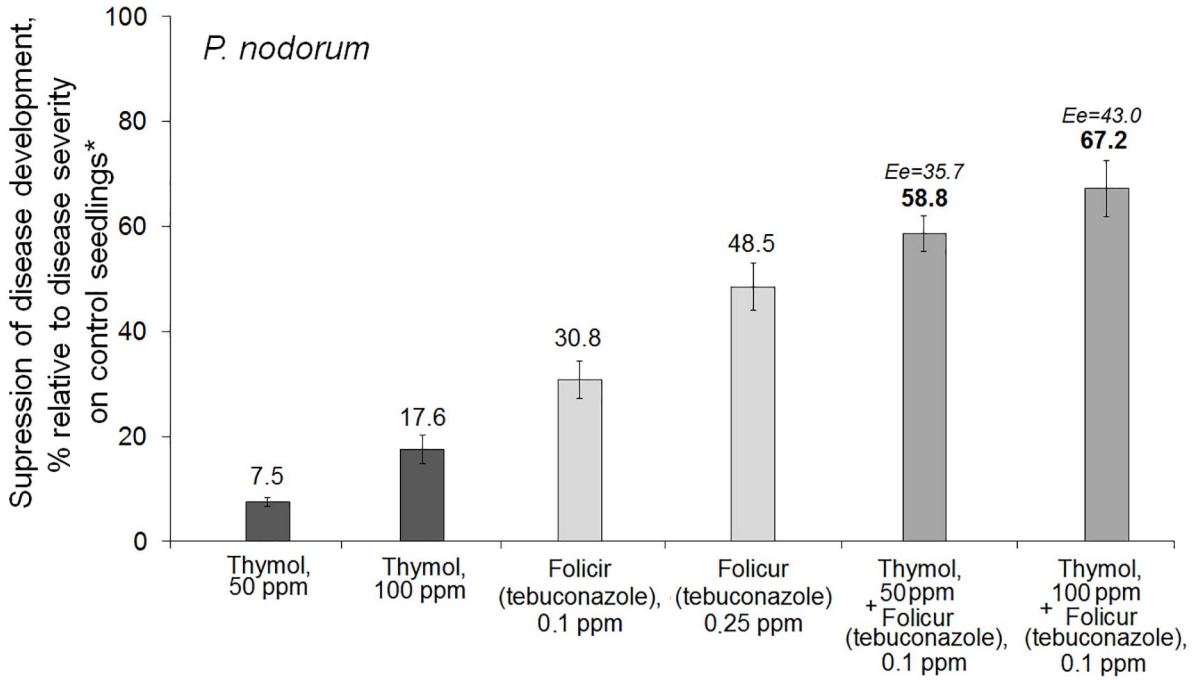

FIGURE 3 | Histograms showing the inhibitory effect of Folicur® EC 250 on development of *Parastagonospora nodorum*, a glume/leaf blotch agent, on wheat seedlings treated with thymol alone and the fungicide either alone or in two combinations with thymol. *The average percentage of disease development (100–120 seedlings per treatment); control plants were sprayed with *P. nodorum* conidia in water. The means of four experiments; Y-bars indicate SE (see section "Materials and Methods," "Data Analysis and Statistics" and caption to **Figure 1** for additional explanations).

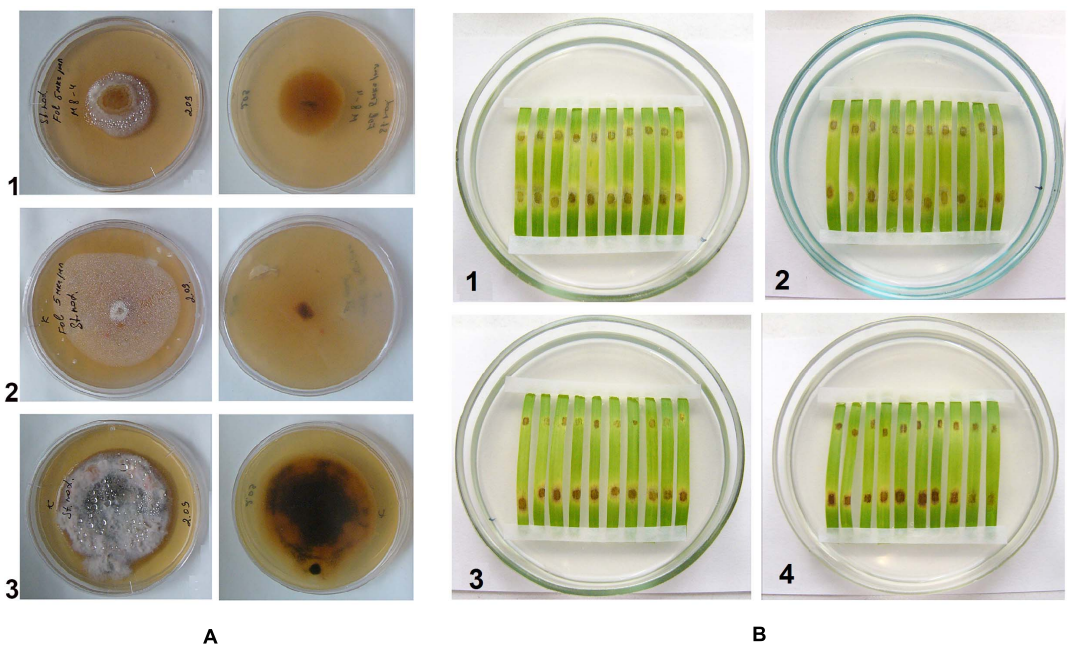

FIGURE 4 | (A) Colonies of tebuconazole-tolerant mutant **(1)** and wild **(2, 3)** strains of *Parastagonospora nodorum*, grown on potato-dextrose agar containing Folicur® **(1** and **2)** or not containing Folicur® **(3)** Photos in the right column show fungal colonies on reverse side of the plates. **(B)** *P. nodorum* blotch lesions on leaf fragments cut from detached wheat leaves. **(1, 2, 4)**, tebuconazole-tolerant mutant; **(3)**, wild strain. Upper (distal) portions of leaf fragments are inoculated with a suspension of conidia (10^6/ml) supplemented with Folicur® alone **(1)**, thymol alone **(2)** or their mixture **(3** and **4)** containing the same dosages as used for **(1, 2)**. Lower (basal) portions of leaf fragments are inoculated with conidia suspended in water to the same final concentration of 10^6 per ml.

TABLE 6 | Deoxynivalenol (DON) and zearalenone (ZEN) production by a toxigenic *F. culmorum* strain cultured in thymol-containing Myro medium.

Thymol, ppm	Mycotoxins, μg/mg of dried mycelium weight*			
	DON	*p***	ZEN	*p*
0.0	0.16 ± 0.04	0.067	0.98 ± 0.19	0.085
50.0	0.12 ± 0.02		1.08 ± 0.17	

**Mean ± SD of three independent cultivation experiments, three replications per treatment in each. **The differences of treatments from the control (Thymol, 0.0 ppm) are insignificant ($p > 0.05$).*

nystatin (FICI = 0.17) used against a zoophilic yeast *Malassezia pachydermatis* (Schlemmer et al., 2019).

Previously, we found thymol synergistically augmented *in vitro* ability of three fungicidal formulations to inhibit the growth of fungal colonies (Dzhavakhiya et al., 2012). In this research, enhanced antifungal activity was shown for Dividend® toward *B. sorokiniana and P. nodorum*, Folicur® against *Alternaria alternata*, and a strobilurin fungicide, Quadris®, against *B. sorokiniana*, *Phoma glomerata*, and *P. nodorum*. The current work, reported here, represents a next stage of our investigations involving seed and foliar treatments of barley and wheat with Dividend® or Folicur® combined with thymol to improve suppression of *B. sorokiniana* and *F. culmorum*, or *P. nodorum*, commonly controlled by difenoconazole and/or tebuconazole containing fungicides (State Catalogue of Pesticides and Agrochemicals, 2018). These fungi belong to the most destructive seed-born and leaf-associated pathogens of cereals (Bhathal et al., 2003; Shcherbakova et al., 2018) and cause a number of economically significant diseases, such as wheat and barley common root (*B. sorokiniana*) and Fusarium crown-foot-root rot, head blight (*F. culmorum*), and glume/leaf blotch of wheat (*P. nodorum*).

At certain concentrations, thymol is known to be phytotoxic and was reported to inhibit seed germination and growth of some weed plants (Kordali et al., 2008; Araniti et al., 2020). However, in our study we preliminarily determined DMSO-dissolved thymol concentrations for use in chemosensitization which did not negatively affect seed germination, or cause lesions on wheat leaves, and only marginally prevented pathogen development (**Tables 1**, **3**). In parallel, fungicide dosages of Dividend® and Folicur®, selected for our experiments to show sensitization by thymol, were at levels that did not protect seedlings or only provided a minor protective effect, and were far lower than dosages recommended for agricultural use (**Tables 1**, **4**, **5**). Results obtained using co-applications of thymol with Dividend® on naturally infected barley grain and artificially inoculated wheat seeds, as well as results of foliar treatments of wheat seedlings with Folicur® combined with thymol, showed this redox-active plant metabolite significantly improved the protective effects of difenoconazole and tebuconazole. In all cases, the combined treatments resulted in significantly more effective suppression of plant diseases than the application of the fungicide alone (**Figures 1**, **3**). Moreover, compositions of tested fungicides and the sensitizer provided the same effective protection as Dividend®, alone, or Folicur®, alone, if these fungicides were applied at 10 or 2.5 times higher dosages, respectively (**Figures 1**, **3**). The fact that Er values significantly exceeded Ee values showed this efficacy was synergistically enhanced by chemosensitization of the pathogens to both triazoles. The one exception was reduction of disease severity as an additive effect of difenoconazole and thymol against *F. culmorum*. Although in two of four performed assays, co-application of thymol and Dividend® on barley seeds did not enhance the protective effect against Alternaria root rot, a high efficacy of thymol-combined Dividend/01 toward the predominant *B. sorokiniana* provided the same reduction of incidence of common root rot as the fungicide alone at its highest dosage (Dividend/1) in all experiments.

Currently, a general concept explaining augmentation of pathogen sensitivity to antifungal agents co-applied with a sensitizing compound is based on the sensitizing compound and fungicide attacking different pathways of fungal metabolism or different stages of the same metabolic pathway. This concept seems to be quite reasonable to explain a possible mechanism underlying enhanced fungicidal effects demonstrated in our experiments. Indeed, for various natural sensitizers, destabilizing structural integrity of cellular and vacuolar membranes, induction of oxidative stress *via* ROS generation with the added provocation of osmotic stress, are main mechanisms augmenting sensitivity of fungi to triazoles and other antimycotics (Campbell et al., 2012). Although all potential mechanisms of thymol activity against plant pathogenic fungi are, so far, poorly understood, its antimicrobial effect has been reported to be mainly associated with extensive damage of fungal membranes. This effect is due to the thymol hydroxyl group binding to spore and hypha membranes and lipid peroxidation impairing ergosterol biosynthesis in fungal cells (Ahmad et al., 2011; De Lira Mota et al., 2012; Gao et al., 2016). Like other redox-active compounds with sensitizing activity, thymol causes oxidative and osmotic stress responses. For instance, it induces ROS, and then NO generation in *A. flavus* resulting in lysis and death of fungal spores (Shen et al., 2016). It is also hypothesized that, in some plant pathogens, MAPK signaling associated with reactions to the above-mentioned stresses (Campbell et al., 2012) can be modulated by thymol (Gao et al., 2016). Simultaneously, thymol and triazoles affect different targets. In contrast to thymol, difenoconazole and tebuconazole inhibit 14α-demethylase (CYP51) required for cytochrome P450-dependent oxidative demethylation of 24-methylene-24,25-dihydrolanosterol, a precursor of ergosterol (FRAC, 2020). Such multiple targeting of fungal metabolism can significantly weaken plant pathogens, enhancing their sensitivity to thymol and fungicidal doses ineffective alone, and thus elevate the suppressive effect of triazoles.

It is possible that mitigation of disease symptoms on detached wheat leaves inoculated with a tebuconazole-tolerant *P. nodorum* mutant was provided by synergy between the fungicide and thymol. Results obtained using detached leaf assays showed thymol can be co-applied with Folicur® to suppress development of a resistant pathogen in plant tissues at the same fungicidal dose inhibiting a sensitive wild strain. These findings warrant further investigations on sensitization of sensitive and resistant

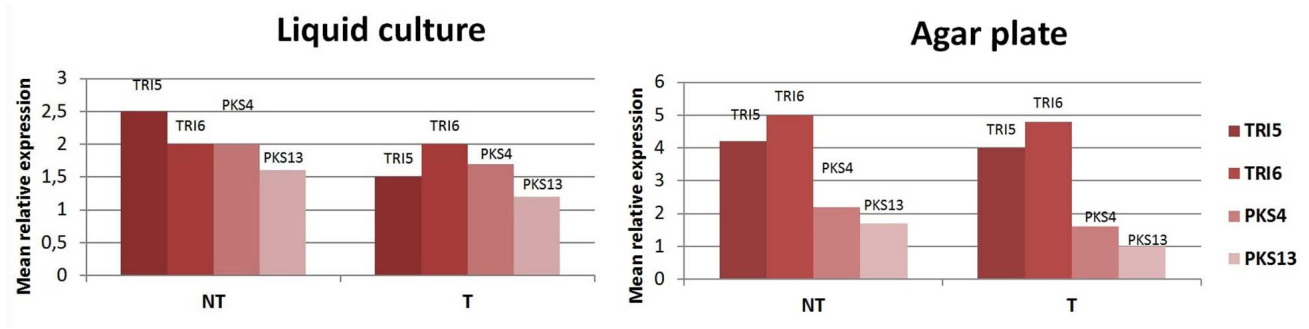

FIGURE 5 | Mean relative expression levels of *TRI5*, *TRI6*, *PKS4*, and *PKS13* after culturing *Fusarium culmorum* in submerged cultures and on agar plates. **T**, *F. culmorum* cultures exposed to thymol at a sensitizing concentration of 50 ppm; **NT**, non-exposed cultures.

P. nodorum strains under expanded assay conditions, such as greenhouse or field experiments.

Interestingly, in this study, thymol concentration enhancing the sensitivity of both *B. sorokiniana* and *P. nodorum* in seed and seedling treatments, respectively, exceeded *in vitro* sensitizing dose selected in prior experiments (Dzhavakhiya et al., 2012) using dilutions based on checkerboard assays (Odds, 2003). Hence, vegetation experiments are necessary as the first step in validating if sensitization discovered *in vitro* reflects augmentation of antifungal effects on plants in the field.

Some redox-active compounds including thymol, which induce oxidative stress, were reported to activate the biosynthesis of polyketide mycotoxins in *Aspergillus* spp. (Kim et al., 2015; Roze et al., 2015; Dzhavakhiya et al., 2016) and trichothecene production in some *Fusarium* species (Gardiner et al., 2010). Taking this into account, we cultured a DON- and ZEA-producing *F. culmorum* strain in the presence of thymol at 50 ppm, the same concentration used for seed treatments to improve the effect of lowered Dividend dosages. In these experiments, we evaluated production levels of both mycotoxins in the cultural liquor and expression of genes participating in mycotoxigenesis. Results showed that treatment of fungal cultures by thymol did not boost DON- and ZEA production, and did not up-regulate key toxin biosynthetic genes (**Table 6** and **Figure 5**). In the case of gene TRI5, encoding trichodiene synthase, and genes *PKS4* and *PKS13*, encoding polyketide synthases, the expression levels were slightly lower after thymol treatment. Expression levels of *TRI6*, a gene encoding a global transcription regulator, were the same in both treated and non-treated cultures. These results suggest thymol, at the sensitizing concentration, does not potentiate expression of genes associated with the biosynthesis of the test fusarial toxins and their subsequent production.

In conclusion, this research showed promise for applying thymol to improve fungicidal efficacy of difenoconazole and tebuconazole against cereal root rot and glume/leaf blotch agents, including fungicide-resistant mutants. Importantly, the same concentration of this sensitizer may be used in both seed and foliar treatments against different cereal pathogens. However, further research is necessary to confirm if the thymol-triazole co-applications will result in sensitization of seed- and leaf-associated plant pathogenic fungi or regulation of mycotoxin production under field conditions. Additional investigations are also needed to determine if thymol affects expression of other toxigenesis-related genes in other Fusarium root rot agents.

DATA AVAILABILITY STATEMENT

The primers and fluorogenic probes were designed based on the alignment of the following sequences retrieved from GenBank (https://www.ncbi.nlm.nih.gov/nucleotide/): U22464, AY130290, MN313473-313507 (TRI5); MH514940-514957, MH001614-MH001648 (TRI5 and TRI6); AY429625, XM009259983 (PKS4), AY495638, JF966273 (PKS13); DQ019316 (PKS4 and PKS13); KY205745-205748, DQ382164-382166 (TEF1a).

AUTHOR CONTRIBUTIONS

LS and VD conceived the concept of the research and designed the experiments. OM, LA, and DE performed the main experiments, prepared the reagents, materials, and analysis tools. AS performed the experiments on expression of genes associated with mycotoxigenesis. LS and AS wrote the original draft and prepared the figures and tables. LS, VD, and SZ reviewed and edited the drafts of the manuscript. All authors reviewed and approved the manuscript.

FUNDING

This study was supported by the Russian Science Foundation (project 18-16-00084).

ACKNOWLEDGMENTS

We acknowledge Tatyana M. Voinova, Senior Researcher of ARRIP Laboratory of Molecular Biology for kind provision of a tebuconazole-tolerant *P. nodorum* strain used in this research. We thank Bruce Campbell, USDA ARS Western Regional Research Center (retired), for kind assistance with the manuscript proofreading and additional editing.

REFERENCES

Ahmad, A., Khan, A., Akhtar, F., Yousuf, S., Xess, I., Khan, L. A., et al. (2011). Fungicidal activity of thymol and carvacrol by disrupting ergosterol biosynthesis and membrane integrity against *Candida*. *Eur. J. Clin. Microbiol. Infect. Dis.* 30, 41–50. doi: 10.1007/s10096-010-1050-8

Ait Dra, L., Brahim, M., Boualy, B., Aghraz, A., Barakate, M., Oubaassine, S., et al. (2017). Chemical composition, antioxidant and evidence antimicrobial synergistic effects of *Periploca laevigata* essential oil with conventional antibiotics. *Ind. Crops Prod.* 109, 746–752. doi: 10.1016/j.indcrop.2017.09.028

Aksoy, C. S., Avci, F. G., Ugurel, O. M., Atas, B., Sayar, N. A., and Akbulut, B. S. (2020). Potentiating the activity of berberine for *Staphylococcus aureus* in a combinatorial treatment with thymol. *Microb. Pathog.* 149:104542. doi: 10.1016/j.micpath.2020.104542

Araniti, F., Miras-Moreno, B., Lucini, L., Landi, M., and Abenavoli, M. R. (2020). Metabolomic, proteomic and physiological insights into the potential mode of action of thymol, a phytotoxic natural monoterpenoid phenol. *Plant Physiol. Biochem.* 153, 141–153. doi: 10.1016/j.plaphy.2020.05.008

Belozerskaya, T. A., and Gessler, N. N. (2007). Reactive oxygen species and the strategy of antioxidant defense in fungi: a review. *Appl. Biochem. Microbiol.* 43, 506–515. doi: 10.1134/S0003683807050031

Bhathal, J., Loughman, R., and Speijers, J. (2003). Yield reduction in wheat in relation to leaf disease from yellow (tan) spot and Septoria nodorum blotch. *Eur. J. Plant Pathol.* 109, 435–443. doi: 10.1023/A:1024277420773

Campbell, B. C., Chan, K. L., and Kim, J. H. (2012). Chemosensitization as a means to augment commercial antifungal agents. *Front. Microbiol.* 3:79. doi: 10.3389/fmicb.2012.00079

Castillo, S., Pérez-Alfonso, C. O., Martínez-Romero, D., Guillén, F., Serrano, M., and Valero, D. (2014). The essential oils thymol and carvacrol applied in the packing lines avoid lemon spoilage and maintain quality during storage. *Food Control* 35, 132–136. doi: 10.1016/j.foodcont.2013.06.052

De Lira Mota, K. S., de Oliveira Pereira, F., de Oliveira, W. A., Lima, I. O., and de Oliveira Lima, E. (2012). Antifungal activity of *Thymus vulgaris* L. essential oil and its constituent phytochemicals against *Rhizopus oryzae*: interaction with ergosterol. *Molecules* 17, 14418–14433. doi: 10.3390/molecules171214418

de Oliveira, M. S., Almeida, M. M., Salazar, M., de, L. A. R., Pires, F. C. S., Bezerra, F. W. F., et al. (2018). "Potential of medicinal use of essential oils from aromatic plants," in *Potential of Essential Oils*, ed. H. El-Shemy (London: InTech), 1–21.

Dzhavakhiya, V., Shcherbakova, L., Semina, Y., Zhemchuzhina, N., and Campbell, B. (2012). Chemosensitization of plant pathogenic fungi to agricultural fungicides. *Front. Microbiol.* 3:87. doi: 10.3389/fmicb.2012.00087

Dzhavakhiya, V. G., Voinova, T. M., Popletaeva, S. B., Statsyuk, N. V., Limantseva, L. A., and Shcherbakova, L. A. (2016). Effect of various compounds blocking the colony pigmentation on the aflatoxin B1 production by *Aspergillus flavus*. *Toxins* 8:11. doi: 10.1006/EXCR.2002.5662

El-Marasy, S. A., El Awdan, S. A., Hassan, A., and Abdallah, H. M. I. (2020). Cardioprotective effect of thymol against adrenaline-induced myocardial injury in rats. *Heliyon* 6:e04431. doi: 10.1016/j.heliyon.2020.e04431

FRAC (2020). *FRAC Code List ©*. Available online at: https://www.frac.info/docs/default-source/publications/frac-code-list/frac-code-list-2020-finalb16c2b2c512362eb9a1eff00004acf5d.pdf?sfvrsn=54f499a_2 (accessed January 17, 2021).

Gao, T., Zhou, H., Zhou, W., Hu, L., Chen, J., and Shi, Z. (2016). The fungicidal activity of thymol against *Fusarium graminearum* via inducing lipid peroxidation and disrupting ergosterol biosynthesis. *Molecules* 21:770. doi: 10.3390/molecules21060770

Gardiner, D. M., Kazan, K., Praud, S., Torney, F. J., Rusu, A., and Manners, J. M. (2010). Early activation of wheat polyamine biosynthesis during Fusarium head blight implicates putrescine as an inducer of trichothecene mycotoxin production. *BMC Plant Biol.* 10:298–302. doi: 10.1186/1471-2229-10-289

González-Aguilar, G., Ansorena, M., Viacava, G., Roura, S., and Ayala-Zavala, J. (2013). "Plant essential oils as antifungal treatments on the postharvest of fruit and vegetables," in *Antifungal Metabolites from Plants*, eds M. Razzaghi-Abyaneh and M. Rai (Berlin: Springer), 429–446.

Greenhalgh, R., Blackwell, B. A., Savard, M., Miller, J. D., and Taylor, A. (1988). Secondary metabolites produced by *Fusarium sporotrichioides* DAOM165006 in liquid culture. *Agric. Food Chem.* 36, 216–219. doi: 10.1021/jf00079a054

Guarda, A., Rubilar, J. F., Miltz, J., and Galotto, M. J. (2011). The antimicrobial activity of microencapsulated thymol and carvacrol. *Int. J. Food Microbiol.* 146, 144–150. doi: 10.1016/j.ijfoodmicro.2011.02.011

Jacob, C. (2014). Redox active natural products and their interaction with cellular signaling pathways. *Molecules* 19, 19588–19593. doi: 10.3390/molecules191219588

James, W. S. (1971). An illustrated series of assessment keys for plant diseases, their preparation and usage. *Canadian Plant Dis. Survey* 51, 36–65.

Ji, D., Chen, T., Ma, D., Liu, J., Xu, Y., and Tian, S. (2018). Inhibitory effects of methyl thujate on mycelial growth of *Botrytis cinerea* and possible mechanisms. *Postharvest Biol. Technol.* 142, 46–54. doi: 10.1016/j.postharvbio.2018.04.003

Ji, H., Kim, H., Beuchat, L. R., and Ryu, J. H. (2019). Synergistic antimicrobial activities of essential oil vapours against *Penicillium corylophilum* on a laboratory medium and beef jerky. *Int. J. Food Microbiol.* 291, 104–110. doi: 10.1016/j.ijfoodmicro.2018.11.023

Kartashov, M. I., Shcherbakova, L. A., Statsyuk, N. V., and Dzhavakhiya, V. G. (2019). Co-application of difenoconazole with thymol results in suppression of a *Parastagonospora nodorum* mutant strain resistant to this triazole. *KnE Life Sci.* 4, 1097–1106. doi: 10.18502/kls.v4i14.570

Kim, H. K., and Yun, S. H. (2011). Evaluation of potential reference genes for quantitative RT-PCR analysis in *Fusarium graminearum* under different culture conditions. *Plant Pathol. J.* 27, 301–309. doi: 10.5423/PPJ.2011.27.4.301

Kim, J., Chan, K. L., Cheng, L. W., Tell, L. A., Byrne, B. A., Clothier, K., et al. (2019). High efficiency drug repurposing design for new antifungal agents. *Methods Protoc.* 2:31. doi: 10.3390/mps2020031

Kim, J. H., Chan, K. L., Faria, N. G., and Campbell, B. C. (2012). Targeting the oxidative stress response system of fungi with safe, redox-potent chemosensitizing agents. *Front. Microbiol.* 3:88. doi: 10.3389/fmicb.2012.00088

Kim, J. H., Chan, K. L., and Mahoney, N. E. (2015). Augmenting the activity of monoterpenoid phenols against fungal pathogens using 2-hydroxy-4-methoxybenzaldehyde that target cell wall integrity. *Int. J. Mol. Sci.* 16, 26850–26870. doi: 10.3390/ijms161125988

Kim, J. H., Mahoney, N. E., Chan, K. L., Campbell, B. C., Haff, R. P., and Stanker, L. H. (2014). Use of benzoanologs to enhance antimycotic activity of kresoxim methyl for control of aflatoxigenic fungal pathogens. *Front. Microbiol.* 5:87. doi: 10.3389/fmicb.2014.00087

Kim, K., Lee, Y., Ha, A., Kim, J. I., Park, A. R., Yu, N. H., et al. (2017). Chemosensitization of *Fusarium graminearum* to chemical fungicides using cyclic lipopeptides produced by *Bacillus amyloliquefaciens* strain JCK-12. *Front Plant Sci.* 8:2010. doi: 10.3389/fpls.2017.02010

Kimura, M., Tokai, T., Takahashi-Ando, N., Ohsato, S., and Fujimura, M. (2007). Molecular and genetic studies of *Fusarium* trichothecene biosynthesis: pathways, genes, and regulation. *Biosci. Biotechnol. Biochem.* 71, 2105–2123. doi: 10.1271/bbb.70183

Kissels, W., Wu, X., and Santos, R. R. (2017). Short communication: interaction of the isomers carvacrol and thymol with the antibiotics doxycycline and tilmicosin: in vitro effects against pathogenic bacteria commonly found in the respiratory tract of calves. *J. Dairy Sci.* 100, 970–974. doi: 10.3168/jds.2016-11536

Kordali, S., Cakir, A., Ozer, H., Cakmakci, R., Kesdek, M., and Mete, E. (2008). Antifungal, phytotoxic and insecticidal properties of essential oil isolated from Turkish *Origanum acutidens* and its three components, carvacrol, thymol and p-cymene. *Bioresour. Technol.* 99, 8788–8795. doi: 10.1016/j.biortech.2008.04.048

Lysøe, E., Klemsdal, S. S., Bone, K. R., Frandsen, R. J. N., Johansen, T., Thrane, U., et al. (2006). The PKS4 gene of *Fusarium graminearum* is essential for zearalenone production. *Appl. Environ. Microbiol.* 72, 3924-3932. doi: 10.1128/AEM.00963-05

Ma, D., Cui, X., Zhang, Z., Li, B., Xu, Y., Tian, S., et al. (2019). Honokiol suppresses mycelial growth and reduces virulence of *Botrytis cinerea* by inducing autophagic activities and apoptosis. *Food Microbiol.* 88:103411. doi: 10.1016/j.fm.2019.103411

Marchese, A., Orhan, I. E., Daglia, M., Barbieri, R., Di Lorenzo, A., Nabavi, S. F., et al. (2016). Antibacterial and antifungal activities of thymol: a brief review of the literature. *Food Chem.* 210, 402–414. doi: 10.1016/j.foodchem.2016.04.111

Najafloo, R., Behyari, M., Imani, R., and Nour, S. (2020). A mini-review of thymol incorporated materials: applications in antibacterial wound dressing. *J. Drug Deliv. Sci. Technol.* 60:101904. doi: 10.1016/j.jddst.2020.101904

Navarro, D., Diaz-Mula, H. M., Guillen, F., Zapata, P. J., Castillo, S., Serrano, M., et al. (2011). Reduction of nectarine decay caused by *Rhizopus stolonifer*, *Botrytis cinerea* and *Penicillium digitatum* with Aloe vera gel alone or with the addition of thymol. *Int. J. Food Microbiol.* 151, 241–246. doi: 10.1016/j.ijfoodmicro.2011.09.009

Odds, F. C. (2003). Synergy, antagonism, and what the chequerboard puts between them. *J. Antimicrob. Chemother.* 52:1. doi: 10.1093/jac/dkg301

Oktyabrsky, O. N., and Smirnova, G. V. (2007). Redox regulation of cellular functions. *Biochemistry (Moscow)* 72, 132–145. doi: 10.1134/S0006297907020022

Park, J.-H., Jeon, Y.-J., Lee, C.-H., Chung, N., and Lee, H.-S. (2017). Insecticidal toxicities of carvacrol and thymol derived from *Thymus vulgaris* Lin. against *Pochazia shantungensis* Chou & Lu., newly recorded pest. *Sci. Rep.* 7:40902.

Porter, J. A., and Monu, E. A. (2019). Evaluating the antimicrobial efficacy of white mustard essential oil alone and in combination with thymol and carvacrol against *Salmonella*. *J. Food Prot.* 82, 2038–2043. doi: 10.4315/0362-028X.JFP-19-029

Richer, D. L. (1987). Synergism: a patent view. *Pest Manag. Sci.* 19, 309–315. doi: 10.1002/ps.2780190408

Riella, K. R., Marinho, R. R., Santos, J. S., Pereira-Filho, R. N., Cardoso, J. C., Albuquerque-Junior, R. L. C., et al. (2012). Anti-inflammatory and cicatrizing activities of thymol, a monoterpene of the essential oil from *Lippia gracilis*, in rodents. *J. Ethnopharmacol.* 143, 656–663. doi: 10.1016/j.jep.2012.07.028

Rosato, A., Carocci, A., Catalano, A., Clodoveo, M. L., Franchini, C., Corbo, F., et al. (2018). Elucidation of the synergistic action of *Mentha piperita* essential oil with common antimicrobials. *PLoS One*. 13:e0200902. doi: 10.1371/journal.pone.0200902

Roze, L. V., Laivenieks, M., Hong, S. Y., Wee, J., Wong, S. S., Vanos, B., et al. (2015). Aflatoxin biosynthesis is a novel source of reactive oxygen species – a potential redox signal to initiate resistance to oxidative stress? *Toxins.* 7, 1411–1430. doi: 10.3390/toxins7051411

Sanin, S. S., and Sanina, A. A. (2013). *Septoria Leaf Blotch and Stagonospora Leaf/Glume Blotch of Wheat: Diagnostics, Phytosanitary Observations, and Plant Protection Managing*. Moscow: AMA Press.

Schlemmer, K., Jesus, F. P., Tondolo, J. S., Weiblen, C., Azevedo, M., Machado, V., et al. (2019). In vitro activity of carvacrol, cinnamaldehyde and thymol combined with antifungals against *Malassezia pachydermatis*. *J. Mycol. Med.* 29, 375–377. doi: 10.1016/j.mycmed.2019.08.003

Shagdarova, B. T., Ilyina, A. V., Lopatin, S. A., Varlamov, V. P., Kartashov, M. I., and Arslanova, L. R. (2018). Study of the protective activity of chitosan hydrolyzate against Septoria leaf blotch of wheat and brown spot of tobacco. Appl. Biochem. Microbiol. 54, 71–75. doi: 10.1134/S0003683818010118

Shcherbakova, L. A., Nazarova, T. A., Mikityuk, O. D., Istomina, E. A., and Odintsova, T. I. (2018). An extract purified from the mycelium of a tomato wilt-controlling strain of *Fusarium sambucinum* can protect wheat against Fusarium and common root rots. *Pathogens* 7:61. doi: 10.3390/pathogens7030061

Shcherbakova, L. A., Syomina, Y. V., Arslanova, L. R., Nazarova, T. A., and Dzhavakhiya, V. G. (2019). Metabolites secreted by a nonpathogenic *Fusarium sambucinum* inhabiting wheat rhizosphere enhance fungicidal effect of some triazoles against *Parastagonospora nodorum*. *AIP Conf. Proc.* 2063:030018. doi: 10.1063/1.5087326

Shen, Q., Zhou, W., Li, H., Hu, L., and Mo, H. (2016). ROS involves the fungicidal actions of thymol against spores of *Aspergillus flavus* via the induction of nitric oxide. *PLoS One* 11:e0155647. doi: 10.1371/journal.pone.0155647

Stakheev, A. A., Khairulina, D. R., and Zavriev, S. K. (2016). Four-locus phylogeny of *Fusarium avenaceum* and related species and their species-specific identification based on partial phosphate permease gene sequences. *Int. J. Food Microbiol.* 225, 27–37. doi: 10.1016/j.ijfoodmicro.2016.02.012

Stakheev, A. A., Samokhvalova, L. V., Mikityuk, O. D., and Zavriev, S. K. (2018). Phylogenetic analysis and molecular typing of trichothecene-producing *Fusarium* fungi from Russian collections. *Acta Naturae* 10, 79–92.

State Catalogue of Pesticides and Agrochemicals (2018). *State Catalogue of Pesticides and Agrochemicals Approved For the Use in Russian Federation in 2020*. Moscow: Ministry of Agriculture of Russian Federation, 325.

Teixeira, B., Marques, A., Ramos, C., Neng, N. R., Nogueira, J. M. F., Saraiva, J. A., et al. (2013). Chemical composition and antibacterial and antioxidant properties of commercial essential oils. *Ind. Crops Prod.* 43, 587–595. doi: 10.1016/j.indcrop.2012.07.069

Veras, H. N. H., Rodrigues, F. F. G., Botelho, M. A., Menezes, I. R. A., Coutinho, H. D. M., and Costa, J. G. M. (2017). Enhancement of aminoglycosides and β-lactams antibiotic activity by essential oil of *Lippia sidoides* Cham. and the thymol. *Arab. J. Chem.* 10, S2790–S2795.

Villafana, R. T., Ramdass, A. C., and Rampersar, S. N. (2019). Selection of *Fusarium* trichothecene toxin genes for molecular detection depends on TRI gene cluster organization and gene function. *Toxins* 11:36. doi: 10.3390/toxins11010036

Zadoks, J. C., Chang, T. T., and Konzak, C. F. (1974). A decimal code for the growth of cereals. *Weed Res.* 14, 415–421. doi: 10.1111/j.1365-3180.1974.tb01084.x

Zhang, Z., Qin, G., Li, B., and Tian, S. (2015). Effect of cinnamic acid for controlling gray mold on table grape and its possible mechanisms of action. *Curr. Microbiol.* 71, 396–402. doi: 10.1007/s00284-015-0863-1

Conflict of Interest: The authors declare that the research was conducted in the absence of any commercial or financial relationships that could be construed as a potential conflict of interest.

frontiers in Microbiology

ORIGINAL RESEARCH
published: 15 April 2021
doi: 10.3389/fmicb.2021.617504

The Potent Trypanocidal Effect of LQB303, a Novel Redox-Active Phenyl-Tert-Butyl-Nitrone Derivate That Causes Mitochondrial Collapse in *Trypanosoma cruzi*

Carolina Machado Macedo[1], Francis Monique de Souza Saraiva[1], Jéssica Isis Oliveira Paula[1], Suelen de Brito Nascimento[1,2], Débora de Souza dos Santos Costa[3], Paulo Roberto Ribeiro Costa[4], Ayres Guimarães Dias[3], Marcia Cristina Paes[1,5] and Natália Pereira Nogueira[1,5]**

[1]Laboratório de Interação de Tripanossomatídeos e Vetores, Departamento de Bioquímica, IBRAG – Universidade do Estado do Rio de Janeiro, Rio de Janeiro, Brazil, [2]Laboratório de Hematologia, Departamento de Patologia, Faculdade de Medicina, Universidade Federal Fluminense, Rio de Janeiro, Brazil, [3]Departamento de Química Orgânica, Universidade do Estado do Rio de Janeiro, Rio de Janeiro, Brazil, [4]Laboratório de Química Bioorgânica, NPPN, Universidade Federal do Rio de Janeiro, Rio de Janeiro, Brazil, [5]Instituto Nacional de Ciência e Tecnologia - Entomologia Molecular (INCT-EM), Rio de Janeiro, Brazil

OPEN ACCESS

Edited by:
Kirkwood M. Land,
University of the Pacific,
United States

Reviewed by:
Gustavo Benaim,
Fundación Instituto de Estudios Avanzados (IDEA), Venezuela
Ana Claudia Torrecilhas,
Federal University of São Paulo, Brazil
Martin Craig Taylor,
University of London, United Kingdom

***Correspondence:**
Natália Pereira Nogueira
natty_nogueira@yahoo.com.br
Marcia Cristina Paes
marcia.paes.uerj@gmail.com

Specialty section:
This article was submitted to Antimicrobials, Resistance and Chemotherapy, a section of the journal Frontiers in Microbiology

Received: 14 October 2020
Accepted: 25 March 2021
Published: 15 April 2021

Citation:
Macedo CM, Saraiva FMdS, Paula JIO, Nascimento SdB, Costa DdSdS, Costa PRR, Dias AG, Paes MC and Nogueira NP (2021) The Potent Trypanocidal Effect of LQB303, a Novel Redox-Active Phenyl-Tert-Butyl-Nitrone Derivate That Causes Mitochondrial Collapse in Trypanosoma cruzi. Front. Microbiol. 12:617504. doi: 10.3389/fmicb.2021.617504

Chagas disease, which is caused by *Trypanosoma cruzi*, establishes lifelong infections in humans and other mammals that lead to severe cardiac and gastrointestinal complications despite the competent immune response of the hosts. Furthermore, it is a neglected disease that affects 8 million people worldwide. The scenario is even more frustrating since the main chemotherapy is based on benznidazole, a drug that presents severe side effects and low efficacy in the chronic phase of the disease. Thus, the search for new therapeutic alternatives is urgent. In the present study, we investigated the activity of a novel phenyl-tert-butyl-nitrone (PBN) derivate, LQB303, against *T. cruzi*. LQB303 presented trypanocidal effect against intracellular [IC_{50}/48 h = 2.6 μM] and extracellular amastigotes [IC_{50}/24 h = 3.3 μM] *in vitro*, leading to parasite lysis; however, it does not present any toxicity to host cells. Despite emerging evidence that mitochondrial metabolism is essential for amastigotes to grow inside mammalian cells, the mechanism of redox-active molecules that target *T. cruzi* mitochondrion is still poorly explored. Therefore, we investigated if LQB303 trypanocidal activity was related to the impairment of the mitochondrial function of amastigotes. The investigation showed there was a significant decrease compared to the baseline oxygen consumption rate (OCR) of LQB303-treated extracellular amastigotes of *T. cruzi*, as well as reduction of "proton leak" (the depletion of proton motive force by the inhibition of F1Fo ATP synthase) and "ETS" (maximal oxygen consumption after uncoupling) oxygen consumption rates. Interestingly, the residual respiration ("ROX") enhanced about three times in LQB303-treated amastigotes. The spare respiratory capacity ratio (SRC: cell ability to meet new energy demands) and the ATP-linked OCR were also impaired by LQB303 treatment, correlating the trypanocidal activity of LQB303 with the impairment of mitochondrial redox metabolism of amastigotes. Flow cytometric

analysis demonstrated a significant reduction of the $\Delta\Psi$m of treated amastigotes. LQB303 had no significant influence on the OCR of treated mammalian cells, evidencing its specificity against *T. cruzi* mitochondrial metabolism. Our results suggest a promising trypanocidal activity of LQB303, associated with parasite bioenergetic inefficiency, with no influence on the host energy metabolism, a fact that may point to an attractive alternative therapy for Chagas disease.

Keywords: *Trypanosoma cruzi*, chemotherapy, bioenergetics, high-resolution respirometry, mitochondrion, tropical neglected disease

INTRODUCTION

Chagas disease (CD), which is caused by the protozoan *Trypanosoma cruzi*, is the most important neglected tropical disease in the world, and it is a major social and public health problem in Latin America, according to the World Health Organization (WHO; Rassi et al., 2010; Pérez-Molina and Molina, 2018). It is estimated that 7 million people worldwide are infected with *T. cruzi* and due to globalization and migratory movements, it is estimated that around 75 million people are at risk of contracting the disease (WHO, 2020). Today, less than 10% of people with the disease are diagnosed and only 1% of them receive adequate treatment (Ribeiro et al., 2009). CD is defined by two phases, acute and chronic. The acute phase is characterized by high parasitemia and asymptomatic. About 30% of those infected develop the chronic phase of the disease and are characterized by indeterminate and asymptomatic clinical forms, cardiac, and digestive forms (Coura and Borges-Pereira, 2011; Echeverria and Morillo, 2019).

The *Trypanosoma cruzi* has a complex life cycle, alternating between the insect vector triatomine and the mammalian host. During its life cycle, *T. cruzi* presents four main stages: epimastigote and metacyclic trypomastigotes in the insect vector and the clinically relevant forms of the parasite, amastigotes, and bloodstream trypomastigotes in vertebrate hosts, which alternate through differentiation processes described as epimastigogenesis, metacyclogenesis, amastigogenesis, and trypomastigogenesis, respectively (Contreras et al., 2002; Hernández-Osorio et al., 2010; Kessler et al., 2017).

Among these processes, amastigogenesis is the differentiation from trypomastigotes into amastigotes that occurs inside vertebrate host cells after invasion and can be mimicked *in vitro* by low pH. Extracellular amastigotes (EAs) are believed to be generated not only by extracellular differentiation of trypomastigotes, but also by premature lysis of infected host cells. EAs are infective and able to invade a variety of mammalian cells (Ferreira et al., 2012). Dormant *T. cruzi* amastigotes occur spontaneously in the host tissues, but this condition does not seem to be a response to a lack of nutrients or the presence of stressors such as the host immune system. In addition, they resist being killed by various compounds that are highly active against replicating parasites (Sánchez-Valdéz et al., 2018; Barrett et al., 2019).

Although it was first described 112 years ago by the Brazilian researcher Carlos Chagas, the only treatments currently available for Chagas disease involve two nitroheterocyclic drugs (benznidazole and nifurtimox), which are unsatisfactory. This is due to their high toxicity and severe side effects, in addition to having low efficacy in the chronic phase of the disease and the natural resistance observed in some strains of the parasite (Urbina, 2010; Rassi et al., 2012; Bahia et al., 2014). Furthermore, several challenges remain to be overcome besides the development of new drugs. First of all, there is the need for proper access to diagnostics and the tools to assess parasitological cure. Then, there are the variety of unanswered questions regarding both the disease itself and parasite-host interactions, and finally, there is the optimization of the available antitrypanosomal drugs, which require long-term treatment, and even then, are unable to eliminate all parasites in some patients. There is, therefore, a clear need for new safe, effective, and accessible therapies for CD (Chatelain, 2015).

Unlike mammalian cells, *T. cruzi* displays a single mitochondrion with several unique features, such as a peculiar arrangement of the kinetoplast (mitochondrial DNA) and the presence of enzymes that participate in both the energy metabolism and antioxidant network. During the *T. cruzi* life cycle, the shape and functional plasticity of the single mitochondrion undergoes profound alterations, reflecting adaptations to different environments faced by the parasites (Paes et al., 2011). The mitochondrial metabolism of *T. cruzi* involves a variety of enzymes and proteins, connected to many metabolic processes. While the bioenergetic role of the mitochondrion is linked to the electron transport system and enzymes for oxidative phosphorylation, there are several important biosynthetic activities that take place in this organelle (Monzote and Gille, 2010). Furthermore, the mitochondrial differences between mammals and trypanosomatids make this organelle an excellent candidate for drug intervention.

Chemically, nitrones are organic molecules with activated carbon nitrogen double bond [$R^1R^2\mathbf{C}{=}\mathbf{N}^+$ ($\mathbf{O}^-$)R^3] and are able to trap and scavenge reactive oxygen/nitrogen species such as superoxide radical, hydrogen peroxide, nitric oxide, or peroxynitrite. Consequently, nitrones were initially used because they have extremely potent activity in biological systems, mainly due to their free radical "spin trap" capacity. Subsequent studies have shown that alpha-phenyl-*N*-*tert*-butylnitrone(PBN) nitrone, as well as its analogs demonstrated low toxicity and potent pharmacological activity against Parkinson's disease and Alzheimer's (Floyd et al., 2008, 2013) and ischemic stroke (Contelles, 2020).

In experimental research, epimastigotes, the replicative stage present in the insect vector are often used for the activity of new compounds, due to the availability and fast proliferation of their axenic cultures. However, epimastigotes are not directly involved in the pathology of the disease and the data obtained cannot always be extrapolated to other stages of development. Therefore, the use of clinically relevant forms of *T. cruzi* for human infection, such as amastigotes is necessary for the evaluation of new compounds (Romanha et al., 2010; Miranda et al., 2015).

The literature shows that the combination of PBN and benznidazole (BZ) decreased the level of mitochondrial reactive oxygen species (ROS) production and chronic heart failure in chagasic mice. However, mice treated with PBN alone did not show decreased parasite persistence (Wen et al., 2010). Modifications to the PBN molecule increases its trypanocidal effect, as seen with the PBN derivative, LQB123, which demonstrates trypanocidal effects on the proliferative and infective forms of *T. cruzi*, as well as low cytotoxicity to mammalian cells (Cupello et al., 2017).

In this present work, we evaluated the activity of the PBN derivative, LQB303, and its direct impact on the proliferative form of the mammalian host, amastigotes, as well as its mitochondrial physiology and bioenergetics.

MATERIALS AND METHODS

Compound

LQB303 was synthesized according to Costa (2020). Stock solutions of LQB303 were prepared in dimethyl sulfoxide (DMSO, MERCK, United States), and the final concentration of the solvent used in the experiment never exceeded 0.5%.

Mammalian Cell and Parasites

Vero cells (ATCC® CCL-81™) were cultured in complete RPMI supplemented with 10% FBS at 37°C in a 5% CO_2 humidified atmosphere. Tissue-derived trypomastigotes of *T. cruzi* (Y strain COLPROT 106) were obtained from the supernatant of infected Vero cells cultured with RPMI (Gibco – Thermo Fisher scientific, Waltham, MA, United States) supplemented with penicillin (100 units ml^{-1}) and streptomycin (70 mg ml^{-1}; Sigma-Aldrich, St. Louis, MO, United States), plus 10% heat-inactivated fetal bovine serum (FBS) at 37°C in a 5% CO_2 humidified atmosphere.

Effects of LQB303 on Intracellular Amastigotes

For infection assays, RAW264.7 macrophages (1.0×10^6 macrophages/well) were seeded and incubated at 37°C and 5% CO_2 for 24 h. Non-adherent cells were removed; the cultures were washed with phosphate-buffered saline (PBS, 100 mM phosphate buffer and 150 mM NaCl, pH 7.4) and then infected with trypomastigotes, Y strain (MOI 10: 1). After 3 h of interaction, the noninternalized parasites were removed by washing with PBS. The cells were then incubated with or without LQB303 in fresh complete DMEM (hgDMEM; Gibco – Thermo Fisher scientific, Waltham, MA, United States) supplemented with penicillin (100 units ml^{-1}) and streptomycin (100 mg ml^{-1}) (Sigma-Aldrich, St. Louis, MO, United States) and sodium bicarbonate (3.7 g/L) for 48 h. Benznidazole (50 μM) was used as the standard trypanocidal drug. The cells were stained by quick Romanowsky-type stain (Panotic LB) and examined under light microscopy. The percentage of infection and the number of intracellular amastigotes were quantified using light microscopy (not shown). The infection index was determined by the percentage of infected cells multiplied by the number of amastigotes per cell. The infection index was used to calculate the IC_{50}. The IC_{50} values were calculated by fitting the dose response curves with nonlinear regression analysis using the "(inhibitor) vs. normalized response" model of GraphPad Prism 5. All experiments were carried out in triplicate and repeated three times, and the results are presented as the average (±standard error).

As a control, uninfected macrophages (2.5×10^5 cells/well) were also treated with the LQB303 for 48 h, and their toxicity was evaluated by the alamarBlue (Thermo Fisher Scientific Waltham, MA, United States) assay (Roman et al., 2008). The reaction was analyzed at 570 nm $\lambda_{emission}$, using the 600 nm absorbance as the normalization value. The CC_{50} values were calculated by fitting the dose response curves with nonlinear regression analysis using the "(inhibitor) vs. normalized response" model of GraphPad Prism 5. All experiments were carried out in triplicate and repeated three times.

Amastigogenesis Assays

The differentiation process of trypomastigotes into amastigotes was induced by low pH according to the method described by Paula et al. (2020). Tissue culture-derived trypomastigotes were incubated at 5.0×10^6 cells ml^{-1} in hgDMEM at pH 5.0 and 37°C in a 5% CO_2 humidified atmosphere. After 24 h, almost 100% of the parasites showed amastigote morphology (rounded morphology).

LQB303 Activity on Extracellular Amastigotes

To access the trypanocidal effect of LQB303 on extracellular amastigotes, parasites were centrifuged at 3000 × *g* for 5 min, and the pellet was suspended in hgDMEM at pH 5.0 plus FBS 10%. The amastigote suspension was seeded into 96-well microplates at a density of 1.0×10^7 cells/well and treated with increasing concentrations of LQB303 for 24 h. After this time, cell viability was assessed by the MTT method (Mosmann, 1983). The IC_{50} value was calculated by fitting the dose response curves with nonlinear regression analysis using the "(inhibitor) vs. normalized response" model of GraphPad Prism 5. All experiments were carried out in duplicates and repeated three times, and the results are presented as the average (±standard error).

Flow Cytometry

Extracellular amastigotes were treated with 3 μM LQB303 for 24 h in hgDMEM pH 5.0 medium plus 10% FBS for proliferation. The mitochondrial membrane potential ($\Delta\Psi m$) was assessed

using tetramethylrhodamine methyl ester (TMRM, Invitrogen Corporation Carlsbad, California, United States), a cationic lipophilic fluorescent probe by flow cytometry on a Gallios apparatus with a 488-nm ion-argon laser. Parasites were incubated with 50 nM TMRM for 30 min, followed by the addition of carbonyl cyanide p-(trifluoromethoxy) phenylhydrazone (FCCP, Sigma-Aldrich, St. Louis, MO, United States) 5 μM for 5 min in order to measure the ΔΨm by flow cytometry. The F_{TMRM}/F_{FCCP} ratio was used to normalize the results from the triplicate experiments, where F_{TMRM} is the median fluorescence intensity of TMRM ($F_{maximal}$) and F_{FCCP} is the median fluorescence in the presence of FCCP ($F_{minimal}$; Carranza et al., 2009). All experiments were repeated two times, and the results are presented as the average (±standard error).

Oxygen Consumption Rates

In the respirometry assays, the extracellular amastigotes were treated with 3 μM LQB303 for 24 h in hgDMEM pH 5.0 media plus 10% FBS for proliferation. Oxygen consumption rates (OCR) of extracellular amastigote (5.0×10^7 parasites/chamber) were evaluated by high-resolution respirometry (Oxygraph-2 K; OROBOROS Instruments, Innsbruck, Austria) with a constant temperature of 37°C throughout the experiment under continuous stirring. Both the oxygen concentration and flux were recorded using DatLab software 5.1.1.9 (Oxygraph-2K-OROBOROS Instruments, Innsbruck, Austria). Subsequently, LEAK respiration was stimulated after the titration of the ATP synthase inhibitor oligomycin (Sigma-Aldrich, St. Louis, MO, United States). The noncoupled state of maximum respiration was induced by the addition of up to 3 μM FCCP, thus allowing the maximal capacity of the electron transfer system to be measured. Respiration was inhibited by the addition of 2 μg/ml Antimycin A, a complex III inhibitor (AA, Sigma-Aldrich, St. Louis, MO, United States) to determine residual oxygen consumption (ROX). The physiological OCR (Routine), the electron transport system maximal capacity (ETS) data were calculated by subtracting the ROX consumption values from the initial OCR and after the addition of FCCP, respectively. The proton leak was calculated after the addition of oligomycin, and the ATP-linked OCR was obtained by subtracting the routine respiration from the proton leak OCR. Finally, the spare respiratory capacity (SRC) was calculated by subtracting ETS from routine respiration (Gnaiger, 2014).

In order to access the non-infected cells respirometry, Vero cells were incubated in the presence or absence of 6 μM LQB303. Forty-eight hours later, 1.5×10^6 cells/chamber were evaluated by high resolution respirometry. Oligomycin (2 μg/ml) was added to achieve LEAK respiration, followed by the titration of up to 3 μM of FCCP to obtain the noncoupled respiration state and the maximum respiration of the electron system. Mitochondrial respiration was inhibited by the addiction of 0.5 μM Rotenone, a complex I inhibitor (Sigma-Aldrich, St. Louis, MO, United States) and 2 μg/ml AA, achieving ROX. Protein concentration was determined by the Lowry method (Lowry et al., 1951) using bovine serum albumin as the standard. All experiments were repeated at least three times, and the results are presented as the average (±standard error).

Statistical Analyses

All the data presented here were derived from 2–5 independent experiments. Statistical evaluation was performed using GraphPad Prism 5. One-way ANOVA and the Student's *t* test were used to analyze the statistical differences between the groups. Differences were considered as statistically significant at $p < 0.05$.

RESULTS

LQB303 Impairs the Proliferation of *Trypanosoma cruzi*

In order to determine the possible trypanocidal effect of LQB303 on amastigotes of *T. cruzi*, we verified the effect on the proliferation of extracellular and intracellular amastigote forms. The effect was evaluated at different concentrations, after 24 and 48 h of incubation, respectively, at 37°C. As shown in **Table 1**, LQB303 greatly impaired *T. cruzi* proliferation. The concentration corresponding to 50% of growth inhibition (IC_{50}) was calculated, with IC_{50}/24 h values of 3.3 ± 0.127 μM for the extracellular amastigotes and IC_{50}/48 h 2.6 ± 1.4 μM for intracellular amastigotes. We also calculated the CC_{50} for non-infected macrophages (770.12 μM), showing that this compound was only toxic to mammalian cells in concentrations 296.2 times (SI) greater than the intracellular amastigotes IC_{50}. These results indicate that LQB303 has relevant activity against the proliferative phase of the parasite even at low concentrations.

LQB303 Collapses the Mitochondrial Membrane of *Trypanosoma cruzi*

Once we determined the trypanocidal activity of LQB303, we then investigated if this derivative compound conserved the PBN activity in the mitochondria (Wen et al., 2010). Thus, we evaluated the mitochondrial membrane potential (ΔΨm) of amastigotes submitted to or not 3 μM of LQB303 and loaded with the fluorescent probe TMRM, which accumulates in the energized mitochondria. Flow cytometry data demonstrate that LQB303 induced a significant decrease in TMRM positive extracellular amastigotes (73%; **Figure 1A**). The uncoupler FCCP (5 μM) was used as the mitochondrial depolarization control. The F_{TMRM}/F_{FCCP} was plotted as ΔΨm and indicated that LQB303 significantly induced the depolarization of the

TABLE 1 | Trypanocidal activity of LQB303 on different forms of *Trypanosoma cruzi*.

Compound	IC_{50}/24 h [μM]	IC_{50}/48 h [μM]	CC_{50}[c]	SI[d]
	Extracellular amastigote	Intracellular amastigote[a,b]		
LQB303	3.3 ± 0.127	2.6 ± 1.4	770.12	296.2

[a]*Intracellular amastigotes in macrophages.*
[b]*IC_{50}/48 h of intracellular amastigotes was based on the infection index (percentage of infected host cells multiplied by the number of parasites per cell).*
[c]*CC_{50} (drug concentration which reduced 50% of macrophage viability).*
[d]*SI (selectivity index) = CC_{50}/48 h/IC_{50}/48 h for intracellular amastigotes; average ± standard deviation of at least three independent experiments.*

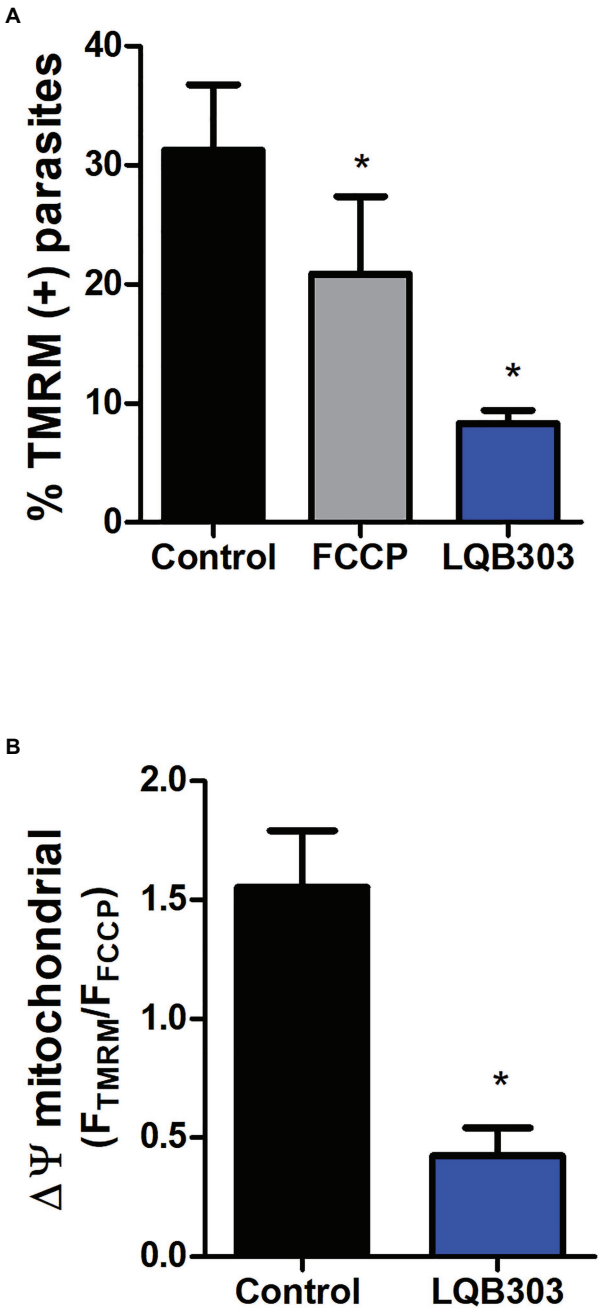

FIGURE 1 | Effect of LQB303 on extracellular amastigotes mitochondrial membrane potential ($\Delta\Psi$m). Extracellular amastigotes of *T. cruzi* were pre-incubated with LQB303 for 24 h. **(A)** Parasites were incubated with 50 nM TMRM for 30 min, following with the addition of FCCP 5 μM for 5 min to measure $\Delta\Psi$m by flow cytometry. Then the percentage of TMRM-labeled parasites was plotted in the presence or absence of 3 μM LQB303 and 5 μM FCCP. **(B)** The F_{TMRM}/F_{FCCP} ratio was used to estimate the $\Delta\Psi$m, where F_{TMRM} is the mean fluorescence intensity of TMRM (F_{max}) and F_{FCCP} is the mean fluorescence in the presence of the uncoupler FCCP (F_{min}). All experiments were expressed as median ± SD of four experiments. One hundred thousand cells were quantified in each experiment, $^*p < 0.05$ when compared to the control group by one-way ANOVA test (Tukey post-test).

$\Delta\Psi$m by about 72% compared to the control parasites, leading to a collapse of the mitochondria inner membrane potential (**Figure 1B**), confirming our hypothesis that LQB303 targets the mitochondria of the parasite.

LQB303 Decreases Oxygen Consumption Rates in Extracellular Amastigotes

Since LQB303 decreased the mitochondrial membrane potential, resulting in the collapse of the $\Delta\Psi$m, we continued to investigate the impact of LQB303 on the amastigotes mitochondrial physiology. Therefore, we incubated the parasites with 3 μM of LQB303 for 48 h and then submitted the amastigotes to high resolution respirometry. **Figure 2B** shows that the pre-incubation of the amastigotes with the compound for 48 h greatly impaired the cells routine oxygen consumption rate (OCR; 42.1 ± 12.3 pmols/s/mg protein) by about 83% compared to control parasites (252.4 ± 15.7 pmols/s/mg protein). Subsequently, we compared the proton leak (after the addition of oligomycin) of treated (59.8 ± 5.7 pmols/s/mg protein) and non-treated parasites (136.9 ± 12.6 pmols/s/mg protein) and observed a decreased of 56% in the treated amastigotes proton leak compared to control parasites (**Figures 2A,B**). This decrease in the proton leak led to a significant drop (60%) of the ATP-linked OCR of LQB303-treated parasites (54.2 ± 4.8 pmols/s/mg protein) compared to the non-treated amastigotes (135.1 ± 12.8 pmols/s/mg protein; **Figure 2C**).

Ruas et al. (2016) showed that the maximum oxygen consumption rate can be underestimated when the proton ionophore is added after the use of oligomycin. Therefore, we evaluated the maximum electron transfer capacity (ETS) by titration of the uncoupler FCCP in the absence of the ATP synthase inhibitor oligomycin (**Figure 2D**). The incubation of extracellular amastigotes with LQB303 for 48 h also led to significantly impair the maximum electron transfer capacity (18.1 ± 3.4 pmols/s/mg protein), compared to the non-treated parasites (261.9 ± 18.1 pmols/s/mg protein), reaching a 93% decrease of the ETS of LQB303-treated amastigotes compared to control (**Figures 2D,E**). **Figure 2F** shows that LQB303 also diminished the spare respiratory capacity (SRC) of treated amastigotes by about 77% (5.7 ± 1.6 pmols/s/mg protein) compared to the non-treated parasites (25.1 ± 6.3 pmols/s/mg protein). The residual oxygen consumption (non-related to the electron transport system) was achieved after the addition of AA, a classical inhibitor of Complex III. LQB303 treated amastigotes presented greater ROX (29.6 ± 2.3 pmols/s/mg protein), compared to control (11.6 ± 4.4 pmols/s/mg protein), by 2.6 times (**Figures 2D,E**). This demonstrated the severe impairment of the mitochondrial physiology of the amastigotes after exposure to LQB303 IC_{50}.

LQB303 Does Not Affect the Mitochondria of Mammalian Cells

Since amastigotes proliferate inside nucleated mammalian cells, we investigate if LQB303 could affect the mitochondrial physiology of non-infected mammalian cells using high-resolution respirometry. Therefore, VERO cells were submitted to two times the IC_{50} of extracellular amastigotes (6 μM) for 48 h. **Figure 3A** shows that non-treated VERO cells, treated with

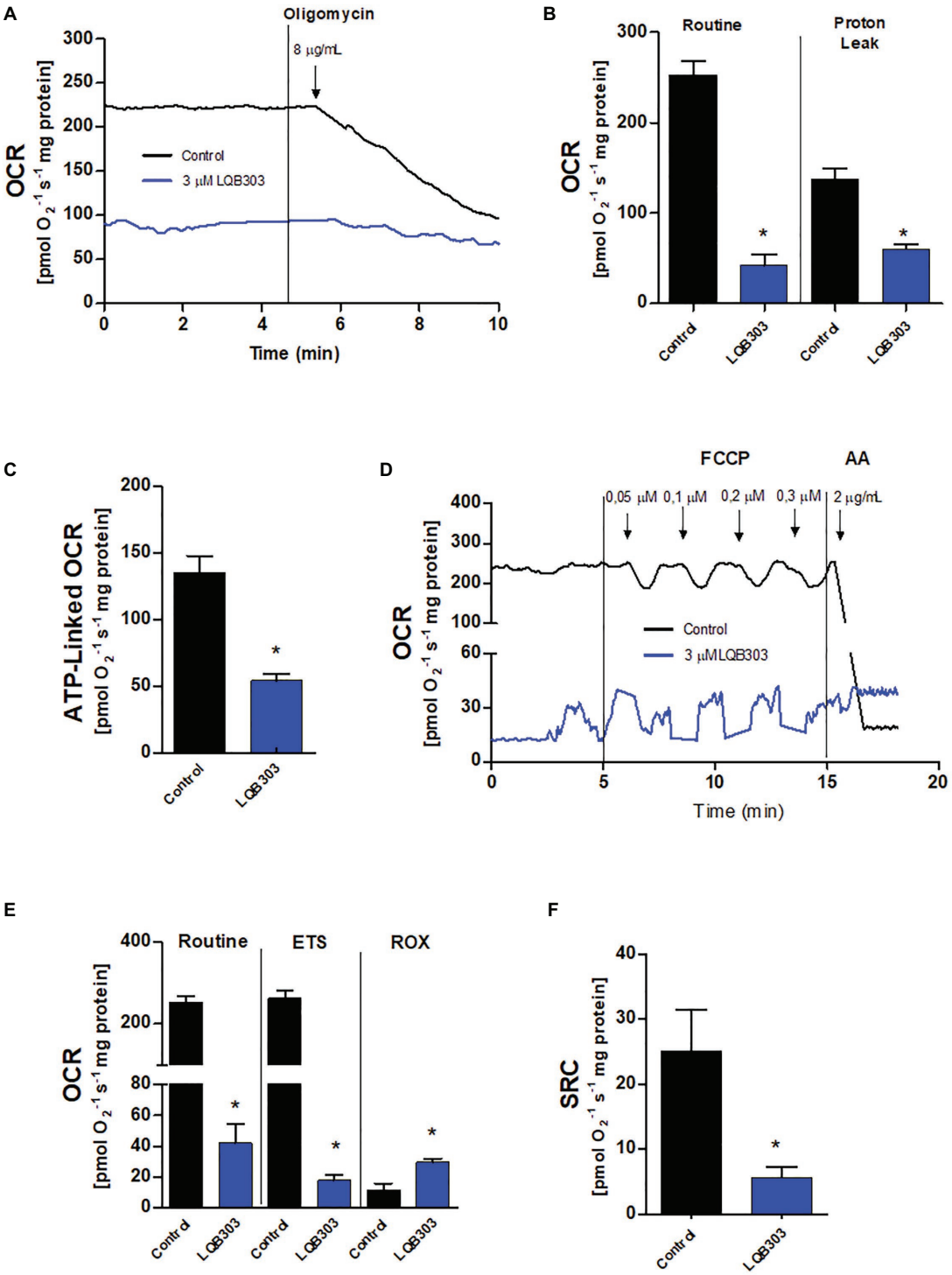

FIGURE 2 | Effect of LQB303 on the oxygen consumption rates of extracellular amastigotes. Extracellular amastigotes (5×10^7 cells/chamber) were incubated with LQB303 IC_{50}/48 h at 37°C and then submitted to high-resolution respirometry. **(A)** Representative oxygen consumption rate (OCR) traces of extracellular amastigotes. Where indicated 8 µg/ml oligomycin was added. **(B)** Routine OCR and Proton leak after the addition of 8 µg/ml oligomycin. **(C)** ATP linked OCR was calculated by subtracting basal oxygen consumption rates after adding oligomycin. **(D)** Representative OCR traces of extracellular amastigotes. Where indicated increasing concentrations of up to 0.3 µM FCCP were added. **(E)** Maximal oxygen consumption after ionophore FCCP titration. ROX = residual respiration after the addition of 2 µg/ml AA. **(F)** Spare respiratory capacity (SRC) was estimated as the difference between maximal and routine OCR. All data are presented as average ± SE of at least three independent experiments, performed in duplicate, $^*p < 0.05$ when compared to the control group by Student's *t* test.

twice the concentration that is enough to greatly impair amastigotes mitochondrial physiology, maintained comparable routine, and ETS and ROX oxygen consumption rates. LQB303-treated Vero cells also showed unaltered ATP-linked OCR and SCR (**Figures 3B,C**), showing the extreme specificity of LQB303 to *T. cruzi* mitochondrion.

DISCUSSION

Chagas disease was discovered in 1909, and in spite of that has limited clinical treatment. The two drugs available have serious side effects, variability in treatment and have low efficacy in the chronic phase of the disease, where parasitic persistence increases the risk of heart damage. Therefore, the elimination of the parasite must be done in the early stages of the disease (Wilkinson and Kelly, 2009; Aldasoro et al., 2018). The BENEFIT trial, a prospective and randomized study, showed the limitations of benznidazole in patients with established chronic infection, as there was no significant reduction in the progression of cardiomyopathy and mortality in the advanced cardiac stages (Morillo et al., 2015; Pecoul et al., 2016).

Therefore, there is an urgent need to discover new treatments for Chagas disease. LQB303 reduced the number of both the extracellular and intracellular amastigotes of *T. cruzi in vitro*, and this inhibitory effect on parasite growth was irreversible. Recently, another PBN derivative, LQB123 showed trypanocidal activity against the intracellular amastigotes and other clinically relevant forms of the parasite (Cupello et al., 2017). When comparing the IC_{50}/48 h for amastigotes incubated with LQB123 (188 μM) with parasites challenged with LQB303 (3 μM), we observed that LQB303 was 63 times more active than LQB123. Moreover, this result also shows that the new modification in the PBN molecule maintained the low toxicity to mammalian cells with a high selectivity index (>296.2; **Table 1**).

Unlike mammalian cells, the members of the order Trypanosomatida exhibit a single mitochondrion with peculiar functional and morphological characteristics, such as the presence of a dysfunctional complex I insensitive to rotenone, and the presence of a specific arrangement of mitochondrial DNA, named as kinetoplast. Due to its uniqueness, this organelle has become an attractive target in parasites for new drugs (Fidalgo and Gille, 2011; Menna-Barreto and de Castro, 2014).

Natural sources have been widely used to lead the discovery of new compounds for neglected diseases (Ioset and Chang, 2011; Ndjonka et al., 2013). Indeed, there are many natural bioactive molecules used to target the mitochondrial metabolism of these parasites. A substantial number of trypanocidal drugs, including compounds clinically used and others under investigation, have the mitochondrion as at least one of their targets. The mitochondrion as a target has been extensively explored in *Leishmania*, strongly correlating the organelle to the survival of the parasites. Apigenin is a good example of a well-studied naturally occurring molecule found in many plants with documented antiprotozoal activity (Singh et al., 2014). This bioactive flavone promoted mitochondrial dysfunction, ROS production, and parasite death in *Leishmania*

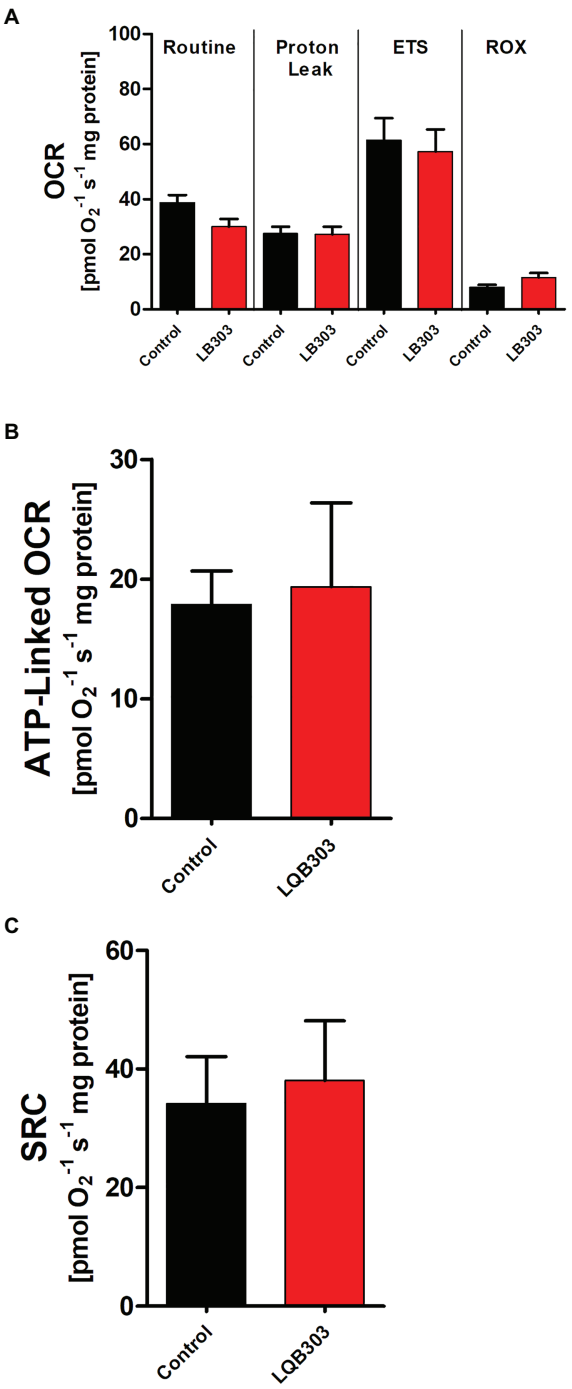

FIGURE 3 | Effect of LQB303 on oxygen consumption rates of non-infected Vero. **(A)** Non-infected VERO cells were cultured in RPMI medium supplemented with 10% FCS and were incubated in the presence or absence of 6 μM LQB303 for 48 h and were assessed by high resolution respirometry. The cells were subjected to 2 μg/ml oligomycin, increasing concentrations of FCCP up to 3 μM, 0.5 μM Rotenone, and 2 μg/ml AA. **(B)** ATP-linked OCR was calculated by subtracting routine oxygen consumption rates after adding oligomycin. **(C)** The spare respiratory capacity was calculated by subtracting the routine from the ETS. All data are presented as average ± SE of five independent experiments, performed in duplicate. There was no statistical difference when compared to the control group by Student's *t* test.

amazonensis in vitro (Fonseca-Silva et al., 2015) and *in vivo*, and it efficiently treated cutaneous leishmaniasis (Fonseca-Silva et al., 2016). Amphotericin B causes permeability of membranes with a rapid decrease of the mitochondrial membrane potential followed by a simultaneous induction of plasma membrane permeability (Lee et al., 2002). Naphthoimidazoles are another class of molecules that target the mitochondrion. β-lapachone derivatives directly impair *T. cruzi* electron transport system, resulting in increased ROS production and parasite death (Bombaça et al., 2019).

In fact, the analysis of the mitochondrial function of LQB303-treated extracellular amastigotes showed a loss of mitochondrial membrane potential (**Figure 1**). In addition, among the apoptotic phenotypes, mitochondrial membrane potential ($\Delta\Psi m$) loss and blebs in the plasma membrane are the most relevant (Menna-Barreto, 2019). We additionally studied the activity of LQB303 on the mitochondrial physiology of amastigotes and observed that the parasites treated with IC_{50}/24 h suffered an important decrease in oxygen consumption rates compared to the control parasites.

The mitochondrial flow of electrons through the electron transport system was reduced after the addition of oligomycin in non-treated amastigotes. FCCP interrupts ATP synthesis by transporting protons across the cell membrane, increasing the rate of oxygen consumption to the maximum (Lerchner et al., 2019). However, these effects were not observed in the LQB303-treated amastigotes, since the maximum electron transfer capacity did not exceed basal levels (**Figures 2B,E**). LQB303 induced mitochondrial dysfunction, which greatly impaired the ATP-linked OCR and the spare respiratory capacity of amastigotes (**Figures 2C,F**). This result, allied with increased ROX (**Figure 2E**) in treated parasites correlates with the loss of the mitochondrial membrane potential, strongly suggesting mitochondrial dysfunction, which could culminate with the decreased proliferation.

Another example of mitochondrial dysfunction resulting in parasite death is LQB-118-treated Leishmania. LQB-118 is a widely studied pterocarpanquinone that has demonstrated potent antileishmanial activity against *Leishmania amazonensis* (da Cunha-Júnior et al., 2011) as well as *L. braziliensis* inducing oxidative stress, mitochondrial dysfunction, ATP depletion, and DNA fragmentation, controlling the lesions of infected hamsters (Costa et al., 2014). The fact that LQB303 showed no interference in VERO cells viability or impaired the mitochondrial bioenergetics indicates the specificity of LQB303 for amastigotes mitochondria and is an encouragement to continue studies with this promising molecule.

In summary, our results suggest promising trypanocidal activity of LQB303, since it leads to specific inefficiency of amastigotes bioenergetics, but does not influence the host cell energy metabolism or growth, making this compound an attractive alternative for Chagas disease treatment. Further biochemical studies are needed to fully elucidate the mode of action of LQB303.

DATA AVAILABILITY STATEMENT

The raw data supporting the conclusions of this article will be made available by the authors, without undue reservation.

AUTHOR CONTRIBUTIONS

NN and CM: conceptualization. NN, MP, and FS: data curation. NN, MP, CM, FS, and JP: formal analysis. NN and MP: funding acquisition, project administration, and validation. NN, MP, FS, and AD: investigation. CM, FS, JP, SN, DC, PC, and AD: methodology. NN, MP, and AD: supervision.

FUNDING

This study was financed in part by the Fundação de Amparo à Pesquisa do Estado do Rio de Janeiro (FAPERJ) through a grant from Cientista do Nosso Estado (CNE) E-26/203.213/2015 (awarded to MP), the Conselho Nacional de Desenvolvimento Científico e Tecnológico (CNPq) through grant 421676/2016-7 (awarded to NN), and the master scholarship (awarded to CM). The funders had no role in the study design, data collection and analysis, decision to publish, or preparation of the manuscript.

REFERENCES

Aldasoro, E., Posada, E., Requena-Méndez, A., Calvo-Cano, A., Serret, N., Casellas, A., et al. (2018). What to expect and when: benznidazole toxicity in chronic Chagas' disease treatment. *J. Antimicrob. Chemother.* 73, 1060–1067. doi: 10.1093/jac/dkx516

Bahia, M. T., Diniz, L., and Mosqueira, V. C. (2014). Therapeutical approaches under investigation for treatment of Chagas disease. *Expert Opin. Investig. Drugs* 23, 1225–1237. doi: 10.1517/13543784.2014.922952

Barrett, M. P., Kyle, D. E., Sibley, L. D., Radke, J. B., and Tarleton, R. L. (2019). Protozoan persister-like cells and drug treatment failure. *Nat. Rev. Microbiol.* 17, 607–620. doi: 10.1038/s41579-019-0238-x

Bombaça, A., Viana, P. G., Santos, A., Silva, T. L., Rodrigues, A., Guimarães, A., et al. (2019). Mitochondrial disfunction and ROS production are essential for anti-*Trypanosoma cruzi* activity of β-lapachone-derived naphthoi midazoles. *Free Radic. Biol. Med.* 130, 408–418. doi: 10.1016/j.freeradbiomed.2018.11.012

Carranza, J. C., Kowaltowski, A. J., Mendonca, M. A., de Oliveira, T. C., Gadelha, F. R., and Zingales, B. (2009). Mitochondrial bioenergetics and redox state are unaltered in *Trypanosoma cruzi* isolates with compromised mitochondrial complex I subunit genes. *J. Bioenerg. Biomembr.* 41, 299–308. doi: 10.1007/s10863-009-9228-4

Chatelain, E. (2015). Chagas disease drug discovery: toward a new era. *J. Biomol. Screen.* 20, 22–35. doi: 10.1177/1087057114550585

Contelles, J. M. (2020). Recent advances on nitrones design for stroke treatment. *J. Med. Chem.* 63, 13413–13427. doi: 10.1021/acs.jmedchem.0c00976

Contreras, V. T., Navarro, M. C., De Lima, A. R., Arteaga, R., Duran, F., Askue, J., et al. (2002). Production of amastigotes from metacyclic trypomastigotes of *Trypanosoma cruzi*. *Mem. Inst. Oswaldo Cruz* 97, 1213–1220. doi: 10.1590/S0074-02762002000800025

Costa, D. S. S. (2020). Arylnitrones: Synthesis, evaluation of Neuroprotective and Antiparasitic activities and Evaluation of Pharmacokinetic Parameters. [thesis]. [Rio de Janeiro (RJ)]: Universidade Federal do Rio de Janeiro.

Costa, L., Pinheiro, R. O., Dutra, P. M., Santos, R. F., Cunha-Júnior, E. F., Torres-Santos, E. C., et al. (2014). Pterocarpanquinone LQB-118 induces apoptosis in *Leishmania (Viannia) braziliensis* and controls lesions in infected hamsters. *PLoS One* 9:e109672. doi: 10.1371/journal.pone.0109672

Coura, J. R., and Borges-Pereira, J. (2011). Chronic phase of Chagas disease: why should it be treated? A comprehensive review. *Mem. Inst. Oswaldo Cruz* 106, 641–645. doi: 10.1590/S0074-02762011000600001

Cupello, M. P., Saraiva, F. M., Ippolito, P., Fernandes, A. D., Menna-Barreto, R. F., Costa, D. S., et al. (2017). Mutagenic and cytotoxicity LQB 123 profile: safety and tripanocidal effect of a phenyl-t-butylnitrone derivative. *Biomed. Res. Int.* 2017, 1–8. doi: 10.1155/2017/2483652

da Cunha-Júnior, E. F., Pacienza-Lima, W., Ribeiro, G. A., Netto, C. D., do Canto-Cavalheiro, M. M., da Silva, A. J., et al. (2011). Effectiveness of the local or oral delivery of the novel naphthopterocarpanquinone LQB-118 against cutaneous leishmaniasis. *J. Antimicrob. Chemother.* 66, 1555–1559. doi: 10.1093/jac/dkr158

Echeverria, L. E., and Morillo, C. A. (2019). American trypanosomiasis (Chagas disease). *Infect. Dis. Clin. N. Am.* 33, 119–134. doi: 10.1016/j.idc.2018.10.015

Ferreira, É. R., Bonfim-Melo, A., Mortara, R. A., and Bahia, D. (2012). *Trypanosoma cruzi* extracellular amastigotes and host cell signaling: more pieces to the puzzle. *Front. Immunol.* 3:363. doi: 10.3389/fimmu.2012.00363

Fidalgo, L. M., and Gille, L. (2011). Mitochondria and trypanosomatids: targets and drugs. *Pharm. Res.* 28, 2758–2770. doi: 10.1007/s11095-011-0586-3

Floyd, R. A., Castro Faria Neto, H. C., Zimmerman, G. A., Hensley, K., and Towner, R. A. (2013). Nitrone-based therapeutics for neurodegenerative diseases: their use alone or in combination with lanthionines. *Free Radic. Biol. Med.* 62, 145–156. doi: 10.1016/j.freeradbiomed.2013.01.033

Floyd, R. A., Kopke, R. D., Choi, C. H., Foster, S. B., Doblas, S., and Towner, R. A. (2008). Nitrones as therapeutics. *Free Radic. Biol. Med.* 45, 1361–1374. doi: 10.1016/j.freeradbiomed.2008.08.017

Fonseca-Silva, F., Canto-Cavalheiro, M. M., Menna-Barreto, R., and Almeida-Amaral, E. E. (2015). Effect of Apigenin on *Leishmania amazonensis* is associated with reactive oxygen species production followed by mitochondrial dysfunction. *J. Nat. Prod.* 78, 880–884. doi: 10.1021/acs.jnatprod.5b00011

Fonseca-Silva, F., Inacio, J. D., Canto-Cavalheiro, M. M., Menna-Barreto, R. F., and Almeida-Amaral, E. E. (2016). Oral efficacy of Apigenin against cutaneous leishmaniasis: involvement of reactive oxygen species and autophagy as a mechanism of action. *PLoS Negl. Trop. Dis.* 10:e0004442. doi: 10.1371/journal.pntd.0004442

Gnaiger, E. (2014). *Mitochondrial Pathways and Respiration Control. An Introduction to OXPHOS Analysis. 4th Edn. Mitochondrial Physiology Network. 19.12.* Innsbruck: Oroboros MiPNet Publications, 80.

Hernández-Osorio, L. A., Márquez-Dueñas, C., Florencio-Martínez, L. E., Ballesteros-Rodea, G., Martínez-Calvillo, S., and Manning-Cela, R. G. (2010). Improved method for *in vitro* secondary amastigogenesis of *Trypanosoma cruzi*: morphometrical and molecular analysis of intermediate developmental forms. *J. Biomed. Biotechnol.* 2010, 1–10. doi: 10.1155/2010/283842

Ioset, J. R., and Chang, S. (2011). Drugs for neglected diseases initiative model of drug development for neglected diseases: current status and future challenges. *Future Med. Chem.* 3, 1361–1371. doi: 10.4155/fmc.11.102

Kessler, R. L., Contreras, V. T., Marliére, N. P., Aparecida Guarneri, A., Villamizar Silva, L. H., Mazzarotto, G., et al. (2017). Recently differentiated epimastigotes from *Trypanosoma cruzi* are infective to the mammalian host. *Mol. Microbiol.* 104, 712–736. doi: 10.1111/mmi.13653

Lee, N., Bertholet, S., Debrabant, A., Muller, J., Duncan, R., and Nakhasi, H. L. (2002). Programmed cell death in the unicellular protozoan parasite *Leishmania*. *Cell Death Differ.* 9, 53–64. doi: 10.1038/sj.cdd.4400952

Lerchner, J., Sartori, M. R., Volpe, P., Lander, N., Mertens, F., and Vercesi, A. E. (2019). Direct determination of anaerobe contributions to the energy metabolism of *Trypanosoma cruzi* by chip calorimetry. *Anal. Bioanal. Chem.* 411, 3763–3768. doi: 10.1007/s00216-019-01882-3

Lowry, O. H., Rosebrough, N. J., Farr, A. L., and Randall, R. J. (1951). Protein measurement with the Folin phenol reagent. *J. Biol. Chem.* 193, 265–275. doi: 10.1016/S0021-9258(19)52451-6

Menna-Barreto, R. F. S. (2019). Cell death pathways in pathogenic trypanosomatids: lessons of (over) kill. *Cell Death Dis.* 10, 1–11. doi: 10.1038/s41419-019-1370-2

Menna-Barreto, R. F., and de Castro, S. L. (2014). The double-edged sword in pathogenic trypanosomatids: the pivotal role of mitochondria in oxidative stress and bioenergetics. *Biomed. Res. Int.* 2014, 1–14. doi: 10.1155/2014/614014

Miranda, C. G., Solana, M. E., Curto, M., Lammel, E. M., Schijman, A. G., and Alba Soto, C. D. (2015). A flow cytometer-based method to simultaneously assess activity and selectivity of compounds against the intracellular forms of *Trypanosoma cruzi*. *Acta Trop.* 152, 8–16. doi: 10.1016/j.actatropica.2015.08.004

Monzote, L., and Gille, L. (2010). Mitochondria as a promising antiparasitic target. *Curr. Clin. Pharmacol.* 5, 55–60. doi: 10.2174/157488410790410605

Morillo, C. A., Marin-Neto, J. A., Avezum, A., Sosa-Estani, S., Rassi, A. Jr., Rosas, F., et al. (2015). Randomized trial of benznidazole for chronic Chagas' cardiomyopathy. *N. Engl. J. Med.* 373, 1295–1306. doi: 10.1056/NEJMoa1507574

Mosmann, T. (1983). Rapid colorimetric assay for cellular growth and survival: application to proliferation and cytotoxicity assays. *J. Immunol. Methods* 65, 55–63. doi: 10.1016/0022-1759(83)90303-4

Ndjonka, D., Rapado, L. N., Silber, A. M., Liebau, E., and Wrenger, C. (2013). Natural products as a source for treating neglected parasitic diseases. *Int. J. Mol. Sci.* 14, 3395–3439. doi: 10.3390/ijms14023395

Paes, L. S., Mantilla, B. S., Barison, M. J., Wrenger, C., and Silber, A. M. (2011). The uniqueness of the *Trypanosoma cruzi* mitochondrion: opportunities to target new drugs against chaga's disease. *Curr. Pharm. Des.* 17, 2074–2099. doi: 10.2174/138161211796904786

Paula, J. I. O., Pinto, J. S., Rossini, A., Nogueira, N. P., and Paes, M. C. (2020). New perspectives for hydrogen peroxide in the amastigogenesis of *Trypanosoma cruzi in vitro*. *BBA-Mol. Basis Dis.* 1866:165951. doi: 10.1016/j.bbadis.2020.165951

Pecoul, B., Batista, C., Stobbaerts, E., Ribeiro, I., Vilasanjuan, R., Gascon, J., et al. (2016). The BENEFIT trial: where do we go from here? *PLoS Negl. Trop. Dis.* 10:e0004343. doi: 10.1371/journal.pntd.0004343

Pérez-Molina, J. A., and Molina, I. (2018). Chagas disease. *Lancet* 391, 82–94. doi: 10.1016/S0140-6736(17)31612-4

Rassi, A. Jr., Rassi, A., and Marcondes de Rezende, J. (2012). American trypanosomiasis (Chagas disease). *Infect. Dis. Clin. N. Am.* 26, 275–291. doi: 10.1016/j.idc.2012.03.002

Rassi, A. Jr., Rassi, A., and Marin-Neto, J. A. (2010). Chagas disease. *Lancet* 375, 1388–1402. doi: 10.1016/S0140-6736(10)60061-X

Ribeiro, I., Sevcsik, A. M., Alves, F., Diap, G., Don, R., Harhay, M. O., et al. (2009). New, improved treatments for Chagas disease: from the R&D pipeline to the patients. *PLoS Negl. Trop. Dis.* 3:e484. doi: 10.1371/journal.pntd.0000484

Roman, A., Nawrat, D., and Nalepa, I. (2008). Chronic treatment with electroconvulsive shock may modulate the immune function of macrophages. *J. ECT* 24, 260–267. doi: 10.1097/YCT.0b013e31816726ae

Romanha, A. J., Castro, S. L., Soeiro, M., Lannes-Vieira, J., Ribeiro, I., Talvani, A., et al. (2010). *In vitro* and *in vivo* experimental models for drug screening and development for Chagas disease. *Mem. Inst. Oswaldo Cruz* 105, 233–238. doi: 10.1590/S0074-02762010000200022

Ruas, J. S., Siqueira-Santos, E. S., Amigo, I., Rodrigues-Silva, E., Kowaltowski, A. J., and Castilho, R. F. (2016). Underestimation of the maximal capacity of the mitochondrial electron transport system in oligomycin-treated cells. *PLoS One* 11:e0150967. doi: 10.1371/journal.pone.0150967

Sánchez-Valdéz, F. J., Padilla, A., Wang, W., Orr, D., and Tarleton, R. L. (2018). Spontaneous dormancy protects *Trypanosoma cruzi* during extended drug exposure. *eLife* 7:e34039. doi: 10.7554/eLife.34039

Singh, M., Kaur, M., and Silakari, O. (2014). Flavones: an important scaffold for medicinal chemistry. *Eur. J. Med. Chem.* 12, 206–239. doi: 10.1016/j.ejmech.2014.07.013

Urbina, J. A. (2010). Specific chemotherapy of Chagas disease: relevance, current limitations and new approaches. *Acta Trop.* 115, 55–68. doi: 10.1016/j.actatropica.2009.10.023

Wen, J. J., Gupta, S., Guan, Z., Dhiman, M., Condon, D., Lui, C., et al. (2010). Phenyl-alpha-tert-butyl-nitrone and benzonidazole treatment controlled the mitochondrial oxidative stress and evolution of cardiomyopathy in chronic chagasic rats. *J. Am. Coll. Cardiol.* 55, 2499–2508. doi: 10.1016/j.jacc.2010.02.030

WHO (2020). Chagas disease (American trypanosomiasis). Available at: https://www.who.int/health-topics/chagas-disease#tab=tab_1 (Accessed July 8, 2020).

Wilkinson, S. R., and Kelly, J. M. (2009). Trypanocidal drugs: mechanisms, resistance and new targets. *Expert Rev. Mol. Med.* 11:e31. doi: 10.1017/S1462399409001252

Conflict of Interest: The authors declare that the research was conducted in the absence of any commercial or financial relationships that could be construed as a potential conflict of interest.

frontiers in Microbiology

HYPOTHESIS AND THEORY
published: 16 April 2021
doi: 10.3389/fmicb.2021.663481

Thioredoxin Reductase Is a Valid Target for Antimicrobial Therapeutic Development Against Gram-Positive Bacteria

*LewisOscar Felix, Eleftherios Mylonakis and Beth Burgwyn Fuchs**

Division of Infectious Diseases, Rhode Island Hospital, Alpert Medical School and Brown University, Providence, RI, United States

There is a drought of new antibacterial compounds that exploit novel targets. Thioredoxin reductase (TrxR) from the Gram-positive bacterial antioxidant thioredoxin system has emerged from multiple screening efforts as a potential target for auranofin, ebselen, shikonin, and allicin. Auranofin serves as the most encouraging proof of concept drug, demonstrating TrxR inhibition can result in bactericidal effects and inhibit Gram-positive bacteria in both planktonic and biofilm states. Minimal inhibitory concentrations are on par or lower than gold standard medications, even among drug resistant isolates. Importantly, existing drug resistance mechanisms that challenge treatment of infections like *Staphylococcus aureus* do not confer resistance to TrxR targeting compounds. The observed inhibition by multiple compounds and inability to generate a bacterial genetic mutant demonstrate TrxR appears to play an essential role in Gram-positive bacteria. These findings suggest TrxR can be exploited further for drug development. Examining the interaction between TrxR and these proof of concept compounds illustrates that compounds representing a new antimicrobial class can be developed to directly interact and inhibit the validated target.

Keywords: allicin, antimicrobial, auranofin, drug resistance, ebselen, shikonin, thioredoxin system, thioredoxin reductase

OPEN ACCESS

Edited by:
Anjan Debnath, University of California, San Diego, United States

Reviewed by:
Kaushiki Mazudar, Kelly Government Solutions, United States
Marc Maresca, Aix-Marseille Université, France

***Correspondence:**
Beth Burgwyn Fuchs
helen_fuchs@brown.edu

Specialty section:
This article was submitted to Antimicrobials, Resistance and Chemotherapy, a section of the journal Frontiers in Microbiology

Received: *03 February 2021*
Accepted: *29 March 2021*
Published: *16 April 2021*

Citation:
Felix L, Mylonakis E and Fuchs BB (2021) Thioredoxin Reductase Is a Valid Target for Antimicrobial Therapeutic Development Against Gram-Positive Bacteria. Front. Microbiol. 12:663481. doi: 10.3389/fmicb.2021.663481

INTRODUCTION

Years of antibiotic misuse and over prescription has taken a toll on the current drug arsenal, resulting in the emergence and expansion of drug resistant microbes. Even with improved hygiene practices and the implementation of antibiotic stewardship, the pharmacopeia is insufficient to remedy the evolving problem. There is a definitive need to develop new antimicrobial agents and define novel bacterial targets. Measures have been taken to engage in high throughput screens to identify previously unrecognized antimicrobial compounds and their respective targets (Moy et al., 2006; Hu et al., 2014; Katzianer et al., 2014; Rajamuthiah et al., 2014; Kim et al., 2015; Bageshwar et al., 2016; Ollinger et al., 2019). Here we pose that thioredoxin reductase (TrxR), part of the antioxidant thioredoxin system (TS), can serve as a new antimicrobial target in Gram-positive and a limited number of Gram-negative bacteria. Cells are constantly bombarded by reactive oxygen species, coming from environmental niches, hostile hosts in the form of immune responses, or

even from the common task of metabolism and cellular respiration. Failure to maintain redox homeostasis leads to apoptosis.

Several compounds are recognized for inhibiting TrxR and provide proof of concept for validating this TrxR as an antimicrobial target. Within this review, we explore auranofin, shikonin, ebselen, and allicin as compounds that inhibit TrxR and remark on the antimicrobial activity profiles. The collective perspective is that TrxR can be targeted through new drug development with the aim of impacting predominately Gram-positive and glutathione independent bacteria.

THIOREDOXIN SYSTEM

The TS is present in all living cells, inclusive of bacteria and fungi. Foremost, it serves as an antioxidant system through the conversion of thiol and disulfide bonds (Arnér and Holmgren, 2000). The TS is comprised of two antioxidant oxidoreductase proteins: thioredoxin (Trx) and TrxR, and an electron donor in the form of NADPH (Karlenius and Tonissen, 2010; **Figure 1A**; **Table 1**).

Thioredoxin is a 10- to 12-kDa ubiquitous protein with a conserved catalytic site (Cys-Pro-Gly-Cys) (Lu and Holmgren, 2014). The primary role of Trx is to serve as a disulfide oxidoreductase and interact with a broad range of proteins involved in electron transport during substrate reduction or regulate the activity by controlling thiol-redox (Lu and Holmgren, 2014). Trx exerts influence of the overall redox system by reducing ribonucleotide reductase during DNA and protein repair and regulating transcription factors, suggesting significant involvement in cellular redox homeostasis (Lu and Holmgren, 2014). The ribbon structures of thioredoxin and TrxR from *Staphylococcus aureus* are given in **Figures 1B,C**.

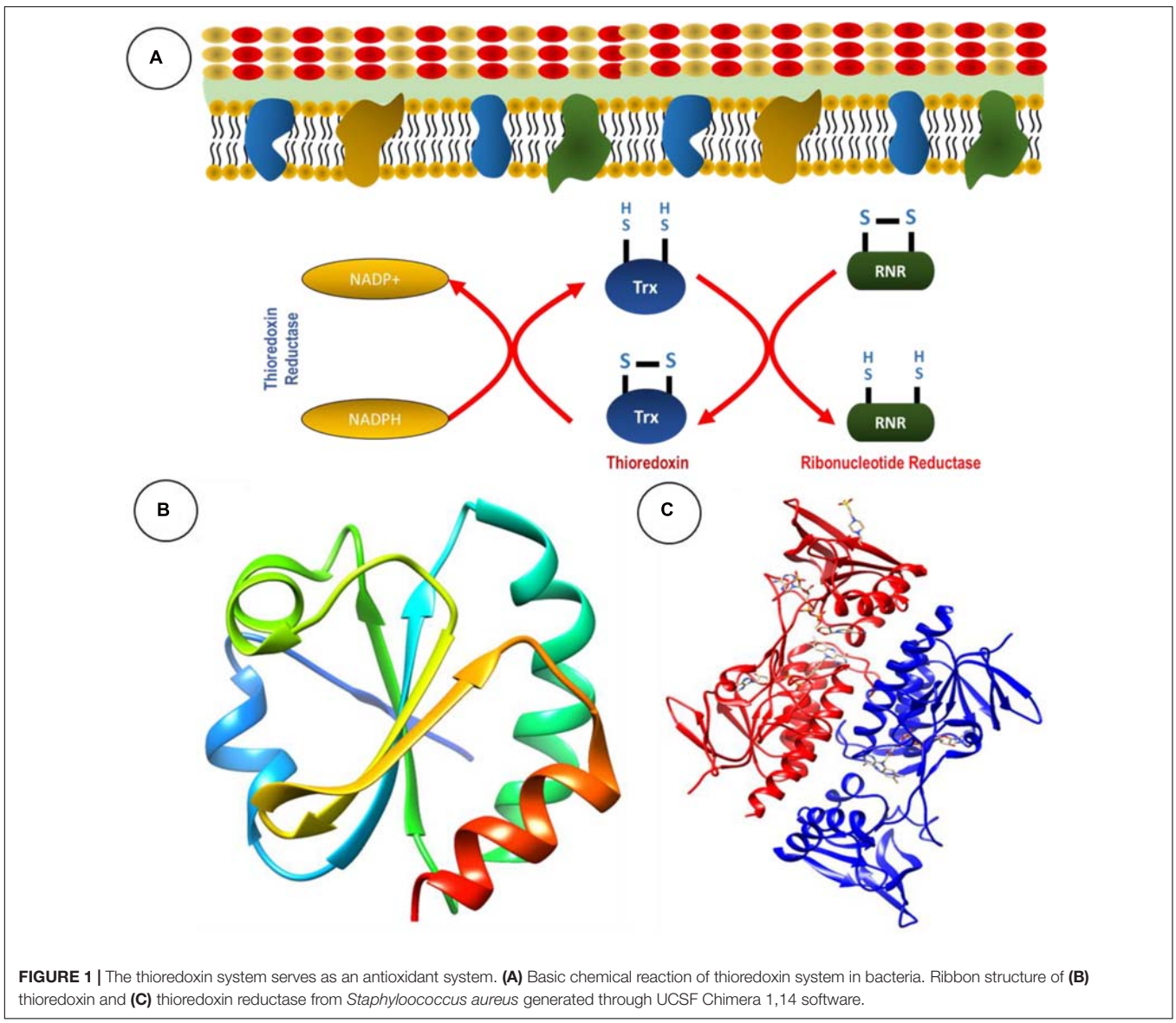

FIGURE 1 | The thioredoxin system serves as an antioxidant system. **(A)** Basic chemical reaction of thioredoxin system in bacteria. Ribbon structure of **(B)** thioredoxin and **(C)** thioredoxin reductase from *Staphyloococcus aureus* generated through UCSF Chimera 1,14 software.

TABLE 1 | Bacterial TS genes and their respective functions.

Bacteria	Trx Genes	TrxR Genes	Function	References
Staphylococcus aureus	*trxA*	*trxB*	Thioredoxin and thioredoxin reductase genes respond to oxygen and disulfide stress	Uziel et al., 2004
Helicobacter pylori	*trxA* and *trxC*	*trxR*	Required for colonization and survival	Baker et al., 2001
Mycobacterium tuberculosis	*trxA, trxB* and *trxC*	*trxR*	Needed for survival against reactive oxygen and nitrogen species produced by activated macrophages	Trivedi et al., 2012
Bacillus subtilis	*TrxA*	*trxA* and *trxB*	Needed for survival and virulence	Zheng et al., 2019
Escherichia coli	*trxA* and *trxC*	*trxB*	Used to prevent oxidative damage from reactive nitrogen intermediates	St. John et al., 2001; Potamitou et al., 2002

Thioredoxin reductase is part of the pyridine nucleotide-disulfide oxidoreductase family. The average subunit mass in bacteria, archaea, and lower eukaryotes is approximately 35 kDa (Williams et al., 2000). Some of the familiar examples are mercuric ion reductase, lipoamide dehydrogenase, glutathione reductase, and NADH oxidase (Lu and Holmgren, 2014). Prokaryotic TrxR have high substrate specificity (Becker et al., 2000; Gromer et al., 2004), while NADPH and FAD are the common binding sites present in TrxR of bacteria (Gromer et al., 2004). In the process of TrxR catalysis, NADPH reduces the FAD of TrxR, and then FAD reduces Trx by disulfide exchange. This mechanism provides reducing equivalents to other target proteins essential for maintaining cellular redox homeostasis (Becker et al., 2000).

Thioredoxin reductase contains the rare amino acid selenocysteine (Sec), making it a selenoprotein. Sec is a cysteine analog in which selenium replaces the sulfur present in the cysteine. It is a rare naturally occurring amino acid, known to be in 54 human proteins (Parsonage et al., 2016). The sequence UGA normally act as a stop codon; however, when the UGA codon is followed by an Sec insertion sequence (SecIS) in bacteria Sec is added through co-translational insertion (Parsonage et al., 2016).

Thioredoxin reductase importance in maintaining systemic redox homeostasis has been noted not only in Gram-positive bacteria but several parasites as well, where researchers have shown interruption of the enzyme presents a potential therapeutic target (Bonilla et al., 2008; Angelucci et al., 2009; Debnath et al., 2013; Andrade and Reed, 2015; Parsonage et al., 2016). Parsonage and colleagues examined TrxR structure from the parasite *Entamoeba histolytica* using crystallography and found auranofin interaction with Cys286 (Parsonage et al., 2016). However, a Cys286 TrxR mutant retained catalytic activity and auranofin susceptibility leading to the suggestion that it is a decoy site and binding is not fully dependent on this interaction. The authors also suggest that auranofin interaction alone with TrxR may not be sufficient to inhibit the *E. histolytica*, indicating the potential for additional targets. Angelucci et al. (2009) present alternative findings in the parasite *Schistosoma mansoni* where a glutaredoxin domain is fused with a TrxR domain to create thioredoxin-glutathione reductase. It is indicated by the data of this study, that auranofin interacts with thioredoxin-glutathione reductase through a selenocysteine mediated transfer of gold from auranofin to Cys sites and gold provides the inhibitory activity, essentially making auranofin the pro-drug for gold delivery (Angelucci et al., 2009). It is not yet be fully elucidated how auranofin interaction with TrxR in Gram-positive bacteria leads to inhibition but there is the potential that the CXXC motif could be a target. Another parasite, *Leishmania infantum*, offers insight into auranofin interference of the redox system by inhibiting trypanothione reductase, an enzyme that replaces many of the thioredoxin/TrxR and glutathione/glutathione reductase functions. Looking at the X-ray crystal structure of auranofin-trypanothione reductase-NADPH complex, gold was found bound to two cysteine residues (Cys52 and Cys57) while the sugar moiety bound to the docking site from another parasite, *L. infantum* (Ilari et al., 2012).

Where we have seen potential to target TrxR in Gram-positive bacteria and the functional orthologs in parasites, this opportunity is lacking for Gram-negative bacteria. In most Gram-negative bacteria, the TS is backed up by a glutathione-glutaredoxin (GSH) system that is also able to scavenge reactive oxygen and nitrogen species in order to maintain redox homeostasis (Couto et al., 2016). Therefore, TrxR lacks the essential nature in Gram-negative bacteria that it plays in Gram-positive bacteria. The GSH system is comprised of NADPH, glutathione reductase, glutathione, and glutaredoxin (Lu and Holmgren, 2014). The Gram-negative *Helicobacter pylori* proves to be an exception to the classification rule as a GSH-independent bacterium (Lu and Holmgren, 2014). Further, *Mycobacterium tuberculosis*, which does not fit within the Gram classification, is TrxR-dependent and GSH-independent (Lu and Holmgren, 2014). This suggests that compounds directly inhibiting the TS, especially through TrxR, hold the potential to inhibit medically important Gram-positive bacteria such as *Staphylococcus* spp., *Streptococcus* spp., *Enterococcus* spp., or the exceptional GSH independent bacteria *H. pylori* and *M. tuberculosis*.

RELIANCE ON Trx AND TrxR IN GSH-INDEPENDENT BACTERIA

Helicobacter pylori is an interesting organism for TS studies as one of the only Gram-negative bacteria to be GSH-independent. The important antioxidants TS system in this bacterium is comprised of one TrxR and two Trx (Trx1 and Trx2) proteins (**Table 1**; Windle et al., 2000). Though most bacteria fit within the Gram classification system, *M. tuberculosis* is another bacterium that does not, and also represents a GSH-independent bacterium utilizing the TS. It has three

Trx proteins, TrxA, TrxB, and TrxC, but only one TrxR (**Table 1**). However, *M. tuberculosis* TrxR does not transfer electrons to TrxA, making TrxB and TrxC the recipients and the active disulfide reductases (Trivedi et al., 2012). *M. tuberculosis* also has thiol peroxidase (Tpx) and alkyl hydroperoxide peroxidase (AhpC) that respond to oxidative and nitrosative stresses imposed by macrophages. Similarly, *H. pylori* also utilizes AhpC as an essential antioxidant for maintaining redox hemostasis (Baker et al., 2001). In *M. tuberculosis*, TrxB transfers electrons to Tpx, and TrxC can transfer to either Tpx or AhpC (Lu and Holmgren, 2014). As GSH-independent bacteria, *H. pylori* and *M. tuberculosis* are susceptible to TrxR targeting compounds, both demonstrating sensitivity to auranofin (Harbut et al., 2015; Owings et al., 2016). Thus, GSH designation as dependent or independent has thus far proven to influence bacterial susceptibility to TrxR targeting compounds and presents a new bacterial classification outside of the well-defined Gram system.

TrxR INHIBITORS AND THE IMPACT TO MICROBES

There are several drugs and molecules that target TrxR. Two naturally occurring compounds, shikonin and allicin (**Figure 2**), are produced by plant roots, presumptively to combat bacteria in the rhizosphere, an indication that nature has already identified TrxR as an antimicrobial target site. Screening efforts to explore the pharmacopeia for antimicrobial compounds also identified auranofin and ebselen for antimicrobial properties that appear to also target TrxR (**Figure 2**). By understanding and repurposing these molecules, we can define a path toward building a new class of antimicrobial compounds that specifically target bacterial TrxR.

Among the four molecules, auranofin has the lowest minimal inhibitory concentration (MIC) against most of the Gram-positive bacteria. Auranofin has shown efficacy toward *S. aureus* (0.0625–1 μg/mL), *Enteroccocus faecalis* (0.125–0.5 μg/mL), *Enterococcus faecium* (0.125–0.25 μg/mL), *Clostridium difficile* (0.25–4 μg/mL), *Bacillus subtilis* (0.3–0.05 μg/mL), *Streptococcus pneumoniae* (0.025–0.25 μg/mL), and *Streptococcus agalactiae* (0.0625–0.0015 μg/mL) (Harbut et al., 2015; Thangamani et al., 2016a; AbdelKhalek et al., 2019). The MIC of shikonin against Gram-positive bacteria including drug resistant methicillin-resistant *S. aureus* (MRSA) ranged between 6.5 and 31.2 μg/mL, thus showing a propensity to inhibit bacteria but not with the same impact as auranofin (Vegara et al., 2011; Lee et al., 2015).

Ebselen exhibited efficacy at inhibiting Gram-positive bacteria including: *B. subtilis*, *Bacillus cereus*, *S. aureus* [MRSA, Linezolid-resistant *S. aureus*, Mupirocin-resistant *S. aureus*, vancomycin resistant *S. aureus* (VRSA), and vancomycin intermediate *S. aureus* (VISA)] (MIC 0.125–0.64 μg/mL), *Staphylococcus epidermidis* (MIC 0.5 μg/mL), *E. faecium* (MIC 0.25–4 μg/mL), *E. faecalis* (MIC 0.125–2 μg/mL), *Streptococcus pyogenes* (MIC 0.5 μg/mL), and *S. agalactiae* (MIC 0.5 μg/mL) (Thangamani et al., 2015a,b; Gustafsson et al., 2016; AbdelKhalek et al., 2019). Allicin is the least potent among the group with activity against Gram-positive bacteria like *S. aureus* at an MIC of 32–64 μg/mL (Leng et al., 2011).

AURANOFIN

Auranofin is an FDA approved gold containing compound used to treatment rheumatoid arthritis. Since auranofin has

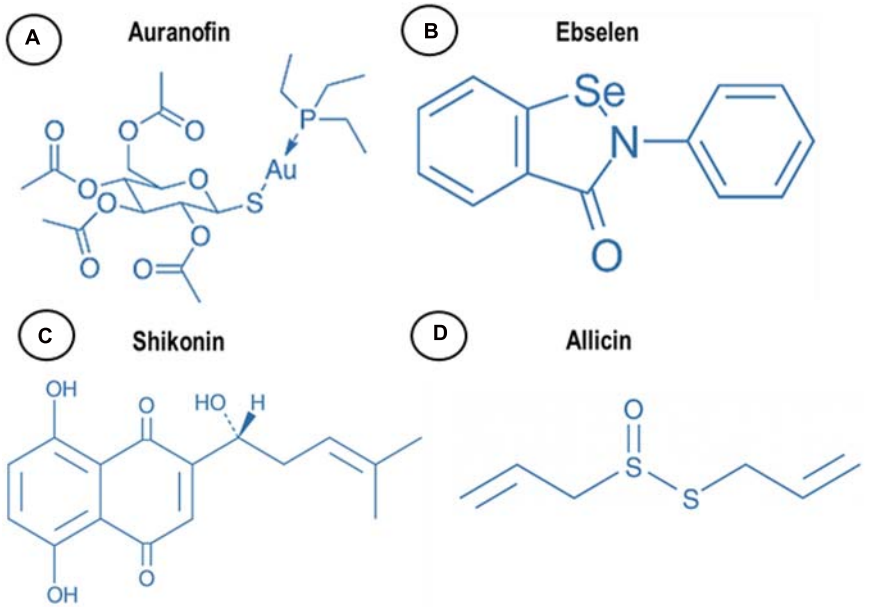

FIGURE 2 | Chemical structure of **(A)** auranofin, **(B)** ebselen, **(C)** shikonin, and **(D)** allicin.

been used since the mid 1980s and was even provided in studies to children ages 1–17, information is available related to drug safety at therapeutic dosages pertinent to arthritis (Kean et al., 1997). When provided orally at 6 mg/day, 25% of the administered compound is detected in the plasma bound to albumin with a half-life of 15–25 days. Approximately 55–80 days is required to fully eliminate the drug with excretion routes being urine and feces. Bioavailability is 40 and 60% protein binding (Finkelstein et al., 1976; Kean et al., 1997). The most common side effect encountered when using auranofin to treat arthritis was diarrhea and skin rash (Felson et al., 1990). Diarrhea was experienced by 40% of patients and rash occurred in 20% of patients (Kean et al., 1997). Proteinuria was also reported in 5% of treated patients and is hypothesized to be a result of gold or gold complexes from auranofin damaging the renal tubule. Auranofin manifest reduction in arthritis stiff joints, reduces the number of swollen joints, and improves grip strength through eliciting a reduction in blood IgG, decreasing α2-globulin, increasing albumin ratios, and decreasing rheumatoid factor titers (Finkelstein et al., 1976).

AURANOFIN BACTERIAL INHIBITORY MECHANISM

A high throughput screen identified auranofin for prolonging the survival of the invertebrate model *Caenorhabditis elegans* infected with *S. aureus*. The results demonstrated that auranofin could clear bacteria from the host at low concentrations (0.78 mg/mL), but the inhibitory impact was reduced by secondary oxidative scavenger glutathione (Fuchs et al., 2016). Indeed, auranofin has been identified by other screening efforts. In 2016, auranofin emerged as a hit when searching for compounds that disrupt preformed *S. aureus* biofilm (Torres et al., 2016).

The *S. aureus* target for auranofin was confirmed when it was shown to provide dose dependent inhibition of bacterial TrxR. Enzymatic activity was evaluated through a colorimetric assay where DTNB is reduced with NADPH to become TNB in an assay catalyzed by TrxR. The reaction produces a yellow color but the color is reduced by the presence of a TrxR inhibitor (Tharmalingam et al., 2019).

This was not the first implication that auranofin could inhibit TrxR. Using the colorimetric assay where DTNB is reduced with NADPH to become TNB in the presence of TrxR, Harbut and colleagues showed auranofin appears to directly reduce the enzymatic activity of *M. tuberculosis* and *S. aureus* TrxR in a dose-dependent manner (Harbut et al., 2015). Lin et al. (2016) used a conditional mutant to show TrxR targeting reduced bacterial burden in a mouse infection model, concluding that auranofin targets TrxB2 but acknowledge this may not be the only enzyme affected.

There are possibly other targets or influences asserted by auranofin. Thangamani et al. (2016a) suggested that auranofin has antibacterial activity against Gram-positive bacteria by inhibiting several biosynthesis mechanisms or pathways like protein, DNA, and cell wall synthesis. The authors observed suppressed protein synthesis in *S. aureus* leading to reduced MRSA toxin productivity.

AURANOFIN INHIBITS BACTERIAL PATHOGENS

Auranofin is able to inhibit a significant cache of bacteria and exhibited antibacterial activity against non-replicating and replicating strains of *M. tuberculosis* under nutrient deprivation. After 5 days, 1.3 and 3.7 log reductions in bacterial viability were recorded when treated with 100 nM and 1.0 μM of auranofin, respectively (Harbut et al., 2015). The MIC of auranofin against *M. tuberculosis* (Δ*panCD,*Δ*RD1*) and *M. tuberculosis* H37Ra was 0.5 μg/mL, while the MIC of *B. subtilis* was between 0.3 and 0.05 μg/mL (Harbut et al., 2015). Clinical isolates of *C. difficile* were inhibited up to 50% by 1 μg/mL of auranofin. At this concentration, the toxin productivity and spore formation of *C. difficile* were also inhibited. Clinical and reference strains of *C. difficile* exhibited an MIC between 0.25 and 4 μg/mL. Reference strains of *E. faecalis* and *E. faecium* had an MICs ranging between 0.125–1 and 0.25–4 μg/mL, respectively (Harbut et al., 2015; Thangamani et al., 2016a; AbdelKhalek et al., 2019).

Staphylococcus aureus has demonstrated susceptible to auranofin, inclusive of drug resistant isolates. Reference strains, clinical isolates, MRSA, VISA, VRSA, linezolid resistant *S. aureus*, and glycopeptide intermediate *S. aureus* exhibited MICs ranging between 0.0625 and 1 μg/mL (Harbut et al., 2015; Thangamani et al., 2016a; AbdelKhalek et al., 2019). In 2019, auranofin was tested to have an MIC ranging between 0.125 and 1 μg/mL against 503 clinical isolates of *S. aureus* (Tharmalingam et al., 2019). *S. agalactiae* also demonstrated susceptibility with MICs ranging between 0.0625 and 0.0015 μg/mL. Thus, showing susceptibility of Gram-positive bacteria and lack of resistance, even among drug resistant isolates.

ANTIMICROBIAL EFFICACY IN ANIMAL MODELS

Auranofin antimicrobial efficacy extends beyond *in vitro* data and was found to have an *in vivo* impact by prolonging survival of mice infected with Gram-positive bacteria in several reports (**Table 2**). Provision of auranofin in systemic, peritonitis, and topical infection mouse models inhibited MRSA, demonstrated through bacterial load reduction (Thangamani et al., 2016b).

Oral administration of auranofin (0.125 or 0.25 mg/kg) promoted survival in 80% of mice post MRSA infection in a lethal septicemic mouse model. Similar survival rates (80%) were observed in mice treated with linezolid (25 mg/kg) showing comparable results with a standard of care medication. Further, auranofin reduced mean bacterial load by 90% in the liver compared to a 70% reduction in animals treated with linezolid. Auranofin given to mice infected with a non-lethal dose of MRSA USA300 reduced the bacterial load up to 95% in the spleen (Thangamani et al., 2016b). In another infection model,

TABLE 2 | *In vivo* efficacy of auranofin in animal models.

Mouse models	Route of administration	Bacterial strains	Result of the experiment	References
Skin infection model	Topical (petroleum gel as vehicle)	*S. aureus* (MRSA USA300)	Reduction of MRSA CFU (3.64 ± 0.14 $\log_{10}$) Reduction in inflammatory cytokines tested (IL-6, IL-1β, TNFα and MCP-1)	Thangamani et al., 2016b
Murine systemic infection	Peritoneal	*S. aureus* (MRSA strain Sanger 252)	Survival of mice after for 7 d after treatment	Harbut et al., 2015
Peritonitis–sepsis infection model	Oral	*S. pneumoniae* serotype 23F strain; serotype 8 strain (strain 3498)	Reduced mortality and 50% of mice survived Reduction in bacterial load within 24h	Aguinagalde et al., 2015
Intramuscular infection	Subcutaneous	*S. aureus* (MRSA 132)	Reduction of bacterial load within 24h	Aguinagalde et al., 2015
Mesh associated biofilm infection	Intraperitoneal	*S. aureus* (MRSA 132)	Decrease in bacterial load attached to the mesh	Aguinagalde et al., 2015
C. difficile infection model	Intraperitoneal	*C. difficile*	Protected 100% of mice at lowest concentration of drug (0.25 mg/Kg) from *C. difficile* infection	Abutaleb and Seleem, 2020
Infected pressure ulcer wound model in obese mice	Topical	*S. aureus* MRSA	8-$\log_{10}$ reduction in MRSA	Mohammad et al., 2020

Harbut et al. (2015) tested auranofin in CD1 female mice using a MRSA peritonitis model. The animals were injected with 0.12 or 0.012 mg/kg of auranofin daily. After treatment, four out of eight mice (50%) experienced prolonged survival by day 7 when provided with 0.12 mg/kg auranofin compared to three out of eight mice (37.5%) survived to day 7 of the study when provided with 0.012 mg/kg (Harbut et al., 2015).

The *in vivo* efficacy of auranofin was also tested against the drug resistant strain *S. pneumoniae* 48 (serotype) in a mouse bacteremia model. After auranofin treatment at the concentrations of 1, 5, or 10 mg/kg mouse survival was observed at 50, 30, and 20%, respectively within a 96-h period. The same time interval results in 100% mortality of infected mice in the placebo group. Dosing with 1 mg/kg auranofin was determined to significantly prolong survival and no trace of bacteria was reported in tail vein collected blood samples 24 h after of infection (Aguinagalde et al., 2015). The greater efficacy at lower doses of 1 and 5 mg/kg suggested in this study by Aguinagalde et al. (2015) implicate potential influence by the paradoxical Eagle effect as seen with other antibiotics, a phenomenon where a decrease in net cell death occurs when drug concentrations exceed optimal bactericidal levels (Eagle, 1948; Prasetyoputro et al., 2019).

The same study interrogated MRSA strain 132 susceptibility to auranofin in an intramuscular infection model. At 24 h post infection, bacteria were enumerated revealing a significant reduction when provided with 5 mg/kg auranofin compared to untreated mice (Aguinagalde et al., 2015). Using the same 5 mg/kg auranofin concentration, it was also reported to reduce MRSA biofilm seeded onto mesh implanted intraperitoneally. After 6 days, auranofin daily therapy significant reduced the number of *S. aureus* CFUs recovered from the recovered mesh compared to untreated mice (Aguinagalde et al., 2015).

BROAD SCOPE EFFICACY

There is evidence that auranofin impact on infectious diseases extends beyond Gram-positive bacteria and includes parasites. Auranofin inhibits *E. histolytica,* a parasite that causes diarrhea, by targeting TrxR (Andrade and Reed, 2015; Parsonage et al., 2016). It also affects *Giardia lamblia* and *S. mansoni* (Andrade and Reed, 2015). It is from these parasitic interactions that we gain valuable insight into the physical interaction of auranofin with the TrxR target. The ability to inhibit both bacteria and parasites lend to the potential of elevating auranofin or other effective TrxR targeting compounds to become broad-spectrum anti-infectious therapeutic agents.

EBSELEN

Like auranofin, the antimicrobial activity for ebselen was also revealed in a high throughput screening effort to find compounds that inhibit *S. aureus* and was found to have greater impact on planktonic cells than biofilm (Torres et al., 2016). Ebselen, chemically known as 2-phenyl-1,2-benzisoselenazol-3(2H)-one, is a seleno-organic, non-toxic drug reported to have antiatherosclerotic, anti-inflammatory, and cytoprotective properties (Schewe, 1995). It was initially developed to mimic the structure of glutathione peroxidase (Müller et al., 1984), but also reacts with peroxynitrite and can inhibit enzymes such as lipoxygenases, NO synthases, NADPH oxidase, protein kinase C, and H^+/K^+-ATPase (Parnham and Sies, 2000). In mammalian cells, ebselen is a favorable substrate for TrxR dependent detoxification of hydroperoxides (Müller et al., 1984).

Under *in vitro* analysis, ebselen exhibited antibacterial activity against MRSA strains USA300, USA100, USA200, USA500, USA1000, USA1100, linezolid resistant, VRSA and mupirocin resistant strains of *S. aureus* (King et al., 2006; Thangamani et al., 2015a), helping to bolster the idea that there is *S. aureus* broad scope susceptibility regardless of strain or drug resistance characteristics. Indeed, the inhibitory activity against *S. aureus* was robust with an MIC at 0.5 mg/mL (Thangamani et al., 2015a). The observed antimicrobial activity extends to other Gram-positive bacteria such as *Streptococcus* and *Enterococcus*. Once again, *H. pylori* proved to be an exceptional Gram-negative

bacteria, exhibiting sensitivity to ebselen with an MBC at 3.13–12.5 mg/mL and an MIC at 3.13 mg/mL for various isolates (Lu et al., 2013). Additionally, *M. tuberculosis* demonstrated ebselen sensitivity with an MIC at 20 μg/mL, congruent to findings with auranofin (Lu et al., 2013). Susceptible bacteria did not easily develop resistance to ebselen as demonstrated by Gustafsson et al. (2016) who were unable to induce *S. aureus* or *B. subtilis* resistance after extended exposure. This could be due to the essential nature of the currently identified TrxR target or suggest the compound has a larger impact and affects other cellular systems.

By measuring Trx reduction in a colorimetric assay with DTNB, Lu et al. (2013) demonstrate that ebselen acts as a competitive inhibitor to *E. coli* TrxR. When ebselen was removed from the reaction through membrane filtration, 80% of TrxR activity was restored (Lu et al., 2013). However, unlike auranofin, which was effective at reducing bacterial growth and lysed *M. tuberculosis*, ebselen did not work via TrxB inhibition and likely affects alternative targets in this bacterium (Lin et al., 2016).

SHIKONIN

The napthoquinone shikonin is a Chinese herbal medicine, also known as Zicao, isolated from *Lithospermum erythrorhizon* roots, a plant known for wound healing and anti-inflammatory effects (Andujar et al., 2013; Duan et al., 2014; Lee et al., 2015). There are several Gram-positive bacteria with demonstrated sensitivity to shikonin: *S. aureus*, *E. faecium*, and *B. subtilis*, with MICs ranging from 0.3 to 6.25 mg/mL (Andujar et al., 2013). Shikonin also prevents *H. pylori* growth in a dose dependent manner, reaching 86% inhibition at 40 μM (Kuo et al., 2004).

Duan and colleagues report that shikonin is yet another compound that interacts with cytosolic TrxR. The compound targets the Sec residue of the Gly-Cys-Sec-Gly active site motif of the human TrxR and irreversibly inhibits the enzyme (Duan et al., 2014). This interaction inhibits TrxR activity without depleting the cellular accumulation of the enzyme (Duan et al., 2014). Shikonin activity can be inhibited by the inclusion of N-acetyl-L-cysteine, a known antioxidant and a precursor to GSH, which neutralizes ROS as part of the alternate glutathione synthase pathway, or through the over expression of TrxR itself (Duan et al., 2014). Thus, shikonin appears to target the TS antioxidant activity as asserted by antagonistic effect when alternate cellular antioxidants are included. Although shikonin inhibits *S. aureus*, it does not reach the same impact as auranofin which exhibited lower MICs. The lesser inhibitory activity is likely due to impeded cellular entry due to factors that restrict shikonin passive entry. It is likely impeded by the cell membrane but inclusion of membrane permeabilization agents such as Triton X-100 enhances antimicrobial activity against *S. aureus* (Lee et al., 2015). Entry challenges are affirmed when peptidoglycans is added and shows competitive inhibition (Lee et al., 2015).

Although it has been used in an animal models, there are distinct challenges that impede shikonin moving forward as a widely antimicrobial therapeutic agent such as poor solubility. Also, shikonin can elicit adverse toxic effects. Although shikonin presents challenges of advancing as an antimicrobial agent in a clinical setting, it does highlight TrxR as a viable antibacterial target and present scaffolding structure that can be built upon for improved activity. And, importantly, it provides an example of a natural product that targets TrxR.

ALLICIN

Another natural plant derived compound that exerts antimicrobial effects is allicin, a biologically active oxygenated sulfur compound present in freshly crushed garlic extract that is chemically known as thio-2-propene-1-sulfinic acid *S*-allyl ester (Ankri and Mirelman, 1999). In 1944, Cavallito and Bailey (1944), first identified allicin and reported the antibacterial activity of diluted allicin against Gram-positive and Gram-negative bacteria. Later, in 1970, the antifungal activity of allicin was revealed (Feldberg et al., 1988). It was further identified to have antiparasitic activity against *E. histolytica* and *G. lamblia* (Ankri and Mirelman, 1999).

Allicin exerts antibacterial activity against *S. aureus* in combination or synergistically with cefazolin/oxacillin and cefoperazone (Cai et al., 2007). When allicin is provided at 100 μg/mL it prevents *S. aureus* biofilm formation on implant materials like reticular polypropylene meshes used in hernia repair (Pérez-Köhler et al., 2015a,b). When biofilm inhibitory activity was tested in an *in vivo* rabbit model, allicin (delivered at 4 mg/L) significantly inhibited the formation of *S. epidermidis* biofilm formation (Zhai et al., 2014).

Like auranofin, allicin is also able to inhibit *H. pylori*, possibly due to the GSH-independent status of the microbes (Jonkers et al., 1999; Aydin et al., 2000; Koçkar et al., 2001). The MIC and MBC were both measured at 6 μg/mL against *H. pylori* (O'Gara et al., 2000). In a cohort consisting of 210 *H. pylori* positive patients, a group (n = 30) treated with standard care medications lansaprasol, clarithromycin, and amoxicillin experienced eradication in 66.6% of the group. When allicin was added to the treatment regimen at 4200 μg/day eradication reached 90% within the group (Koçkar et al., 2001).

Mycobacterium tuberculosis was also sensitive to allicin, exhibiting MICs ranging from 2.58 to 33.33 μg/mL among drug resistant and drug susceptible isolates (Dwivedi et al., 2019). With multiple types of microbes inhibited by allicin, it is not surprising that its mode action is promiscuous. Allicin undergoes a chemical reaction with thiol groups present in several enzymes including TrxR, RNA polymerase, and alcohol dehydrogenase (Ankri and Mirelman, 1999). Muller et al. (2016) measured total sulfhydryl concentrations and demonstrated a reduction using crude extracts from cells treated with allicin. Sulfhydryl levels were quantified with DTNB (described above) and showed that TrxR is one of the targeted enzymes.

CIDAL AND STATIC ACTIVITY

Natural and synthetic drugs exhibit two types of inhibitory effects on bacteria: bacteriostatic and bactericidal. The MIC is the

concentration at which a compound inhibits the visible growth of bacterial at 24 h under optimum condition. While the minimum bactericidal concentration (MBC) is defined as the point at which a compound causes 1,000 fold bacterial density reduction at 24 h under standardized growth conditions (Wald-Dickler et al., 2018). Bactericidal activity is defined when the ratio of MBC to MIC is $\leq$4 and bacteriostatic activity is defined as the MBC to MIC ratio is >4. Therefore, a drug which achieves reduction of >1,000 fold in density of bacteria at concentration eight-fold above the MIC is considered bacteriostatic (Pankey and Sabath, 2004; French, 2006; Nemeth et al., 2015; Wald-Dickler et al., 2018). Thus, effective bactericidal compound needs to have an MBC close to the MIC.

Auranofin has been reported to exhibit bactericidal activity against Gram-positive bacteria like *B. subtilis*, *C. difficile*, *E. faecalis*, *E. faecium*, *S. aureus* (including MRSA and VISA strains), *S. epidermidis, S. pneumoniae*, and *S. agalactiae*. Reports also suggest bactericidal activity of auranofin against *M. tuberculosis* (Harbut et al., 2015; Thangamani et al., 2016b; AbdelKhalek et al., 2019). The MBC to MIC ratio of shikonin is reported above >4 against various strains of *S. aureus*. This suggest that shikonin exhibits bacteriostatic activity (Vegara et al., 2011; Lee et al., 2015). Ebselen shows MBC to MIC ratio is <4 against Gram-positive bacteria like *B. subtilis*, *Enterococcus* spp. (including VRE), *S. epidermidis*, *S. aureus* (including MRSA, VRSA, and VISA strains), *S. pyogenes*, and *S. agalactiae* (Thangamani et al., 2015b; Gustafsson et al., 2016; AbdelKhalek et al., 2018). Apart from these three molecules, allicin is reported to inhibit *S. aureus* at >32 μg/mL. This suggest that allicin possess bacteriostatic activity. Thus, among these four molecules (auranofin, shikonin, ebselen, and allicin), auranofin is potentially the most active at inhibiting bacteria in a bactericidal capacity.

CONCLUSION

Although there are differences between auranofin, ebselen, shikonin, and allicin, together, these compounds strongly suggest TrxR is a valid antimicrobial target. Although all of the compounds commonly impact TrxR there is debate as to whether it is the sole target. Indeed, other cellular systems may be augmented.

Only auranofin has been used clinically (with FDA approval) and found to be non-toxic. Therefore, holding the greatest potential to be repositioned for antimicrobial therapy. Interestingly, studies suggest TrxR inhibitors could also have anti-cancer efficacy due to increased growth rates and elevated cellular ROS from increased mitochondrial respiration that accumulate during accelerated growth resulting in high levels of Trx and TrxR to reduce oxidative stressors (reviewed in Mohammadi et al., 2019). Clinical trials are ongoing using a TrxR inhibitor ethaselen to treat non-small cell lung cancers.

Focusing on the common target, each of these compounds have been shown to reduce TrxR enzymatic activity and the inhibition of bacterial growth has been demonstrated with *in vitro* and *in vivo* assays. Antimicrobial impact is best reflected in Gram-positive bacteria with the exception of a couple of GSH-independent microbes, namely *H. pylori* and *M. tuberculosis*. Multiple studies demonstrate that drug resistant microbes are susceptible to TrxR targeting compounds and resistance is not developed upon exposure. Among GSH-independent bacteria, the essential nature of TrxR makes it a very attractive target. Although this review is restricted to bacterial inhibition, TrxR also poses a potential target in fungi. Indeed, Missall and Lodge (2005) and Ianiri and Idnrum (2015) report the essential nature of fungal TrxR in *Cryptococcus neoformans* with failure to produce a mutant strain.

The quickest path forward to introducing TrxR as a novel antimicrobial target not yet tapped by current antibiotics is to progress one of the existing compounds as a repurposed drug. With low toxicity and good efficacy at low concentrations, the best candidate for this ascension is auranofin. However, the creation of new compounds specifically designed to target Gram-positive TrxR can initiate a new antimicrobial class.

AUTHOR CONTRIBUTIONS

BF and LF prepared the initial draft. EM provided insightful discussions and contributed to the writing. All authors contributed to the article and approved the submitted version.

FUNDING

LF and BF were supported by NIH grant P20 GM121344.

REFERENCES

AbdelKhalek, A., Abutaleb, N. S., Mohammad, H., and Seleem, M. N. (2018). Repurposing ebselen for decolonization of vancomycin-resistant enterococci (VRE). *PLoS One* 13:e0199710. doi: 10.1371/journal.pone.0199710

AbdelKhalek, A., Abutaleb, N. S., Mohammad, H., and Seleem, M. N. (2019). Antibacterial and antivirulence activities of auranofin against *Clostridium* difficile. *Int. J. Antimicrob. Agents* 53, 54–62. doi: 10.1016/j.ijantimicag.2018.09.018

Abutaleb, N. S., and Seleem, M. N. (2020). Auranofin, at clinically achievable dose, protects mice and prevents recurrence from *Clostridioides* difficile infection. *Sci. Rep.* 10:7701. doi: 10.1038/s41598-020-64882-9

Aguinagalde, L., Díez-Martínez, R., Yuste, J., Royo, I., Gil, C., Lasa, Í, et al. (2015). Auranofin efficacy against MDR Streptococcus pneumoniae and *Staphylococcus aureus* infections. *J. Antimicrob. Chemother.* 70, 2608–2617. doi: 10.1093/jac/dkv163

Andrade, R. M., and Reed, S. L. (2015). New drug target in protozoan parasites: the tole of thioredoxin reductase. *Front. Microbiol.* 6:975. doi: 10.3389/fmicb.2015.00975

Andujar, I., Recio, M., Giner, R., and Ríos, J. (2013). Traditional chinese medicine remedy to jury: the pharmacological basis for the use of shikonin as an anticancer therapy. *Curr. Med. Chem.* 20, 2892–2898. doi: 10.2174/09298673113209990008

Angelucci, F., Sayed, A. A., Williams, D. L., Boumis, G., Brunori, M., Dimastrogiovanni, D., et al. (2009). Inhibition of *Schistosoma mansoni*

thioredoxin-glutathione reductase by auranofin: structural and kinetic aspects. *J. Biol. Chem.* 284, 28977–28985. doi: 10.1074/jbc.M109.020701

Ankri, S., and Mirelman, D. (1999). Antimicrobial properties of allicin from garlic. *Microbes Infect.* 1, 125–129.

Arnér, E. S. J., and Holmgren, A. (2000). Physiological functions of thioredoxin and thioredoxin reductase. *Eur. J. Biochem.* 267, 6102–6109. doi: 10.1046/j.1432-1327.2000.01701.x

Aydin, A., Ersöz, G., Tekesin, O., Akçiçek, E., and Tuncyürek, M. (2000). Garlic oil and *Helicobacter pylori* infection. *Am. J. Gastroenterol.* 95, 563–564. doi: 10.1016/S0002-9270(99)00871-0

Bageshwar, U., VerPlank, L., Baker, D., Dong, W., Hamsanathan, S., Whitaker, N., et al. (2016). High throughput scree for *Escherichia coli* twin arginine translocation (Tat) inhibitors. *PLoS One* 11:e0149659. doi: 10.1371/journal.pone.0149659

Baker, L. M. S., Raudonikiene, A., Hoffman, P. S., and Poole, L. B. (2001). Essential thioredoxin-dependent peroxiredoxin system from *Helicobacter pylori*: genetic and kinetic characterization. *J. Bacteriol.* 183, 1961–1973. doi: 10.1128/JB.183.6.1961-1973.2001

Becker, K., Gromer, S., Heiner Schirmer, R., and Müller, S. (2000). Thioredoxin reductase as a pathophysiological factor and drug target. *Eur. J. Biochem.* 267, 6118–6125. doi: 10.1046/j.1432-1327.2000.01703.x

Bonilla, M., Denicola, A., Novoselov, S. V., Turanov, A. A., Protasio, A., Izmendi, D., et al. (2008). Platyhelminth mitochondrial and cytosolic redox homeostasis is controlled by a single thioredoxin glutathione reductase and dependent on selenium and glutathione. *J. Biol. Chem.* 283, 17898–17907. doi: 10.1074/jbc.M710609200

Cai, Y., Wang, R., Pei, F., and Liang, B. B. (2007). Antibacterial activity of allicin alone and in combination with β-lactams against *Staphylococcus* spp. and *Pseudomonas aeruginosa*. *J. Antibiot.* 60, 335–338. doi: 10.1038/ja.2007.45

Cavallito, C. J., and Bailey, J. H. (1944). Allicin, the antibacterial principle of allium sativum. I. Isolation, physical properties and antibacterial action. *J. Am. Chem. Soc.* 66, 1950–1951. doi: 10.1021/ja01239a048

Couto, N., Wood, J., and Barber, J. (2016). The role of glutathione reductase and related enzymes on cellular redox homoeostasis network. *Free Radic. Biol. Med.* 95, 27–42. doi: 10.1016/j.freeradbiomed.2016.02.028

Debnath, A., Ndao, M., and Reed, S. (2013). Reprofiled drug targets ancient protozoans. *Gut Microbes* 4, 66–71. doi: 10.4161/gmic.22596

Duan, D., Zhang, B., Yao, J., Liu, Y., and Fang, J. (2014). Shikonin targets cytosolic thioredoxin reductase to induce ROS-mediated apoptosis in human promyelocytic leukemia HL-60 cells. *Free Radic. Biol. Med.* 70, 182–193. doi: 10.1016/j.freeradbiomed.2014.02.016

Dwivedi, V. P., Bhattacharya, D., Singh, M., Bhaskar, A., Kumar, S., Fatima, S., et al. (2019). Allicin enhances antimicrobial activity of macrophages during *Mycobacterium tuberculosis* infection. *J. Ethnopharmacol.* 243:111634. doi: 10.1016/j.jep.2018.12.008

Eagle, H. (1948). A paradoxical zone phenomenon in the bactericidal action of penicillin in vitro. *Science* 107, 44–45.

Feldberg, R. S., Chang, S. C., Kotik, A. N., Nadler, M., Neuwirth, Z., Sundstrom, D. C., et al. (1988). In vitro mechanism of inhibition of bacterial cell growth by allicin. *Antimicrob. Agents Chemother.* 32, 1763–1768. doi: 10.1128/AAC.32.12.1763

Felson, D., Anderson, J., and Meenan, R. (1990). The comparative efficacy and toxicity of second-line drugs in rheumatoid. *Arthritis Rheum.* 33, 1449–1461.

Finkelstein, A. E., Walz, D. T., Batista, V., Mizraji, M., Roisman, F., and Misher, A. (1976). Auranofin. New oral gold compound for treatment of rheumatoid arthritis. *Ann. Rheum. Dis.* 35, 251–257. doi: 10.1136/ard.35.3.251

French, G. L. (2006). Bactericidal agents in the treatment of MRSA infections - The potential role of daptomycin. *J. Antimicrob. Chemother.* 58, 1107–1117. doi: 10.1093/jac/dkl393

Fuchs, B. B., Rajamuthiah, R., Souza, A. C. R., Eatemadpor, S., Rossoni, R. D., Santos, D. A., et al. (2016). Inhibition of bacterial and fungal pathogens by the orphaned drug auranofin. *Future Med. Chem.* 8, 117–132.

Gromer, S., Urig, S., and Becker, K. (2004). The thioredoxin system - from science to clinic. *Med. Res. Rev.* 24, 40–89. doi: 10.1002/med.10051

Gustafsson, T. N., Osman, H., Werngren, J., Hoffner, S., Engman, L., and Holmgren, A. (2016). Ebselen and analogs as inhibitors of Bacillus anthracis thioredoxin reductase and bactericidal antibacterials targeting Bacillus species, *Staphylococcus aureus* and *Mycobacterium tuberculosis*. *Biochim. Biophys. Acta Gen. Subj.* 1860, 1265–1271. doi: 10.1016/j.bbagen.2016.03.013

Harbut, M. B., Vilchèze, C., Luo, X., Hensler, M. E., Guo, H., Yang, B., et al. (2015). Auranofin exerts broad-spectrum bactericidal activities by targeting thiol-redox homeostasis. *Proc. Natl. Acad. Sci. U.S.A.* 112, 4453–4458. doi: 10.1073/pnas.1504022112

Hu, Y., Palmer, S., Munoz, H., and Bullard, J. (2014). High throughput screen identified natural product inhibitor of phenylalanyl-tRNA synthetase from *Pseudomonas aeruginosa* and *Streptococcus pneumoniae*. *Curr. Drug Discov. Technol.* 11, 279–292.

Ianiri, G., and Idnrum, A. L. (2015). Essential gene discovery in the Basidiomycete Cryptococcus neoformans for antifungal drug target prioritization. *mBio* 6:e02334-14. doi: 10.1128/mBio.02334-14

Ilari, A., Baiocco, P., Messori, L., Fiorillo, A., Boffi, A., Gramiccia, M., et al. (2012). A gold-containing drug against parasitic polyamine metabolism: the X-ray structure of trypanothione reductase from *Leishmania infantum* in complex with auranofin reveals a dual mechanism of enzyme inhibition. *Amino Acids* 42, 803–811. doi: 10.1007/s00726-011-0997-9

Jonkers, D., Van Den Broek, E., Van Dooren, I., Thijs, C., Dorant, E., Hageman, G., et al. (1999). Antibacterial effect of garlic and omeprazole on *Helicobacter pylori*. *J. Antimicrob. Chemother.* 43, 837–839. doi: 10.1093/jac/43.6.837

Karlenius, T. C., and Tonissen, K. F. (2010). Thioredoxin and cancer: a role for thioredoxin in all states of tumor oxygenation. *Cancers* 2, 209–232. doi: 10.3390/cancers2020209

Katzianer, D., Yano, T., Rubin, H., and Zhu, J. (2014). A high-throughput small-molecule screen to identify a novel chemical inhibitor of *Clostridium* difficile. *Int. J. Antimicrob. Agents* 44, 69–73.

Kean, W. F., Hart, L., and Buchanan, W. W. (1997). Auranofin. *Br. J. Rheumatol.* 36, 560–572.

Kim, W., Conery, A. L., Rajamuthiah, R., Fuchs, B. B., Ausubel, F. M., and Mylonakis, E. (2015). Identification of an antimicrobial agent effective against methicillin-resistant *Staphylococcus aureus* persisters using a fluorescence-based screening strategy. *PLoS One* 10:e0127640. doi: 10.1371/journal.pone.0127640

King, M. D., Humphrey, B. J., Wang, Y. F., Kourbatova, E. V., Ray, S. M., and Blumberg, H. M. (2006). Emergence of community-acquired methicillin-resistant *Staphylococcus aureus* USA 300 clone as the predominant cause of skin and soft-tissue infections. *Ann. Intern. Med.* 144, 309–317. doi: 10.7326/0003-4819-144-5-200603070-00005

Koçkar, C., Oztürk, M., and Bavbek, N. (2001). *Helicobacter pylori* eradication with beta carotene, ascorbic acid and allicin. *Acta Medica* 44, 97–100. doi: 10.14712/18059694.2019.92

Kuo, H.-M., Hsia, T.-C., Chuang, Y.-C., Lu, H.-F., Lin, S.-Y., and Chung, J.-G. (2004). Shikonin inhibits the growth and N-acetylation of 2-aminofluorene in *Helicobacter pylori* from ulcer patients. *Anticancer Res.* 24, 1587–1592.

Lee, Y. S., Lee, D. Y., Kim, Y. B., Lee, S. W., Cha, S. W., Park, H. W., et al. (2015). The mechanism underlying the antibacterial activity of shikonin against methicillin-resistant *Staphylococus aureus*. *Evid. Based Complement. Altern. Med.* 2015:520578. doi: 10.1155/2015/520578

Leng, B. F., Qiu, J. Z., Dai, X. H., Dong, J., Wang, J. F., Luo, M. J., et al. (2011). Allicin reduces the production of α-toxin by *Staphylococcus aureus*. *Molecules* 16, 7958–7968. doi: 10.3390/molecules16097958

Lin, K., O'Brien, K. M., Trujillo, C., Wang, R., Wallach, J. B., Schnappinger, D., et al. (2016). *Mycobacterium tuberculosis* Thioredoxin Reductase is rssential for thiol redox homeostasis but plays a minor role in antioxidant defense. *PLoS Pathog.* 12:e1005675. doi: 10.1371/journal.ppat.1005675

Lu, J., and Holmgren, A. (2014). The thioredoxin antioxidant system. *Free Radic. Biol. Med.* 66, 75–87. doi: 10.1016/j.freeradbiomed.2013.07.036

Lu, J., Vlamis-Gardikas, A., Kandasamy, K., Zhao, R., Gustafsson, T. N., Engstrand, L., et al. (2013). Inhibition of bacterial thioredoxin reductase: an antibiotic mechanism targeting bacteria lacking glutathione. *FASEB J.* 27, 1394–1403. doi: 10.1096/fj.12-223305

Missall, T. A., and Lodge, J. K. (2005). Thioredoxin reductase is essential for viability in the fungal pathogen *Cryptococcus neoformans*. *Eukaryot. Cell* 4, 487–489. doi: 10.1128/EC.4.2.487-489.2005

Mohammad, H., Abutaleb, N. S., and Seleem, M. N. (2020). Auranofin rapidly eradicates methicillin-resistant *Staphylococcus aureus* (MRSA) in an infected

pressure ulcer mouse model. *Sci. Rep.* 10:7251. doi: 10.1038/s41598-020-64352-2

Mohammadi, F., Soltani, A., Ghahremanloo, A., Javid, H., and Hashemy, S. I. (2019). The thioredoxin system and cancer therapy: a review. *Cancer Chemother. Pharmacol.* 84, 925–935. doi: 10.1007/s00280-019-03912-4

Moy, T. I, Ball, A. R., Anklesaria, Z., Casadei, G., Lewis, K., and Ausubel, F. M. (2006). Identification of novel antimicrobials using a live-animal infection model. *Proc. Natl. Acad. Sci. U.S.A.* 103, 10414–10419. doi: 10.1073/pnas.0604055103

Müller, A., Cadenas, E., Graf, P., and Sies, H. (1984). A novel biologically active seleno-organic compound-I. Glutathione peroxidase-like activity in vitro and antioxidant capacity of PZ 51 (Ebselen). *Biochem. Pharmacol.* 33, 3235–3239. doi: 10.1016/0006-2952(84)90083-2

Muller, A., Eller, J., Albrecht, F., Prochnow, P., Kuhlmann, K., Bandow, J. E., et al. (2016). Allicin induces thiol stress in bacteria through S -allylmercapto modification of protein cysteines. *J. Biol. Chem.* 291, 11477–11490. doi: 10.1074/jbc.M115.702308

Nemeth, J., Oesch, G., and Kuster, S. P. (2015). Bacteriostatic versus bactericidal antibiotics for patients with serious bacterial infections: systematic review and meta-analysis. *J. Antimicrob. Chemother.* 70, 382–395. doi: 10.1093/jac/dku379

O'Gara, E., Hill, D., and Maslin, D. (2000). Activities of garlic oil, garlic powder, and their diallyl constituents against *Helicobacter pylori*. *Appl. Environ. Microbiol.* 66, 2269–2273.

Ollinger, J., Kumar, A., Roberts, D., Bailey, M., Casey, A., and Parish, T. (2019). A high-throughput whole cell screen to identify inhibitors of *Mycobacterium tuberculosis*. *PLoS One* 14:e0205479. doi: 10.1371/journal.pone.0205479

Owings, J. P., McNair, N. N., Mui, Y. F., Gustafsson, T. N., Holmgren, A., Contel, M., et al. (2016). Auranofin and N-heterocyclic carbene gold-analogs are potent inhibitors of the bacteria *Helicobacter pylori*. *FEMS Microbiol. Lett.* 363, 1–6. doi: 10.1093/femsle/fnw148

Pankey, G. A., and Sabath, L. D. (2004). Clinical relevance of bacteriostatic versus bactericidal mechanisms of action in the treatment of Gram-positive bacterial infections. *Clin. Infect. Dis.* 38, 864–870. doi: 10.1086/381972

Parnham, M., and Sies, H. (2000). Ebselen: prospective therapy for cerebral ischaemia. *Expert Opin. Investig. Drugs* 9, 607–619. doi: 10.1517/13543784.9.3.607

Parsonage, D., Sheng, F., Hirata, K., Debnath, A., Mckerrow, J. H., Reed, S. L., et al. (2016). X-ray structures of thioredoxin and thioredoxin reductase from Entamoeba histolytica and prevailing hypothesis of the mechanism of auranofin action. *J. Struct. Biol.* 194, 180–190. doi: 10.1016/j.jsb.2016.02.015.X-ray

Pérez-Köhler, B., García-Moreno, F., Bayon, Y., Pascual, G., and Bellón, J. M. (2015a). Inhibition of *Staphylococcus aureus* adhesion to the surface of a reticular heavyweight polypropylene mesh soaked in a combination of chlorhexidine and allicin: an in vitro study. *PLoS One* 10:e0126711. doi: 10.1371/journal.pone.0126711

Pérez-Köhler, B., García-Moreno, F., Brune, T., Pascual, G., and Bellón, J. M. (2015b). Preclinical bioassay of a polypropylene mesh for hernia repair pretreated with antibacterial solutions of chlorhexidine and allicin: an in vivo study. *PLoS One* 10:e0142768. doi: 10.1371/journal.pone.0142768

Potamitou, A., Holmgren, A., and Vlamis-Gardikas, A. (2002). Protein levels of *Escherichia coli* thioredoxins and glutaredoxins and their relation to null mutants, growth phase, and function. *J. Biol. Chem.* 277, 18561–18567. doi: 10.1074/jbc.M201225200

Prasetyoputro, A., Jarrrad, A. M., Cooper, M. A., and Blaskovich, M. A. T. (2019). The Eagle effect and antibiotic-induced persistence: two sides of teh same coin? *Trends Microbiol.* 27, 339–354.

Rajamuthiah, R., Fuchs, B. B., Jayamani, E., Kim, Y., Larkins-Ford, J., Conery, A., et al. (2014). Whole animal automated platform for drug discovery against multi-drug resistant *Staphylococcus aureus*. *PLoS One* 9:e89189. doi: 10.1371/journal.pone.0089189

Schewe, T. (1995). Molecular actions of ebselen-an antiinflammatory antioxidant. *Gen. Pharmacol.* 26, 1153–1169. doi: 10.1016/0306-3623(95)00003-J

St. John, G., Brot, N., Ruan, J., Erdjument-Bromage, H., Tempst, P., Weissbach, H., et al. (2001). Peptide methionine sulfoxide reductase from *Escherichia coli* and *Mycobacterium tuberculosis* protects bacteria against oxidative damage from reactive nitrogen intermediates. *Proc. Natl. Acad. Sci. U.S.A.* 98, 9901–9906. doi: 10.1073/pnas.161295398

Thangamani, S., Mohammad, H., Abushahba, M. F. N., Sobreira, T. J. P., Hedrick, V. E., Paul, L. N., et al. (2016a). Antibacterial activity and mechanism of action of auranofin against multi-drug resistant bacterial pathogens. *Sci. Rep.* 6:22571. doi: 10.1038/srep22571

Thangamani, S., Mohammad, H., Abushahba, M. F. N., Sobreira, T. J. P., and Seleem, M. N. (2016b). Repurposing auranofin for the treatment of cutaneous staphylococcal infections. *Int. J. Antimicrob. Agents* 47, 195–201. doi: 10.1016/j.ijantimicag.2015.12.016

Thangamani, S., Younis, W., and Seleem, M. N. (2015a). Repurposing clinical molecule ebselen to combat drug resistant pathogens. *PLoS One* 10:e0133877. doi: 10.1371/journal.pone.0133877

Thangamani, S., Younis, W., and Seleem, M. N. (2015b). Repurposing ebselen for treatment of multidrug-resistant staphylococcal infections. *Sci. Rep.* 5:11596. doi: 10.1038/srep11596

Tharmalingam, N., Ribeiro, N., da Silva, D., Naik, M., Cruz, L., Kim, W., et al. (2019). Auranofin is an effective agent against clinical isolates of *Staphylococcus aureus*. *Future Med. Chem.* 11, 1417–1425.

Torres, N. S., Abercrombie, J. J., Srinivasan, A., Lopez-Ribot, J. L., Ramasubramanian, A. K., and Leung, K. P. (2016). Screening a commercial library of pharmacologically active small molecules against *Staphylococcus aureus* biofilms. *Antimicrob. Agents Chemother.* 60, 5663–5672. doi: 10.1128/AAC.00377-16

Trivedi, A., Singh, N., Bhat, S. A., Gupta, P., and Kumar, A. (2012). Redox biology of tuberculosis pathogenesis. *Adv. Microb. Physiol.* 60, 263–324. doi: 10.1016/B978-0-12-398264-3.00004-8

Uziel, O., Borovok, I., Schreiber, R., Cohen, G., and Aharonowitz, Y. (2004). Transcriptional regulation of the *Staphylococcus aureus* thioredoxin and thioredoxin reductase genes in response to oxygen and disulfide stress. *J. Bacteriol.* 186, 326–334. doi: 10.1128/JB.186.2.326

Vegara, S., Funes, L., Martí, N., Saura, D., Micol, V., and Valero, M. (2011). Bactericidal activities against pathogenic bacteria by selected constituents of plant extracts in carrot broth. *Food Chem.* 128, 872–873. doi: 10.1016/j.foodchem.2011.03.109

Wald-Dickler, N., Holtom, P., and Spellberg, B. (2018). Busting the myth of "static vs cidal": a systemic literature review. *Clin. Infect. Dis.* 66, 1470–1474. doi: 10.1093/cid/cix1127

Williams, C. H., Arscott, L., Muller, S., and Lennon, B. (2000). Thioredoxin reductase: two modes of catalysis have evolved. *Eur. J. Biochem.* 267, 6110–6117.

Windle, H. J., Fox, Á, Eidhin, D. N., and Kelleher, D. (2000). The thioredoxin system of *Helicobacter pylori*. *J. Biol. Chem.* 275, 5081–5089. doi: 10.1074/jbc.275.7.5081

Zhai, H., Pan, J., Pang, E., and Bai, B. (2014). Lavage with allicin in combination with vancomycin inhibits biofilm formation by *Staphylococcus epidermidis* in a rabbit model of prosthetic joint infection. *PLoS One* 9:e102760. doi: 10.1371/journal.pone.0102760

Zheng, C., Guo, S., Tennant, W. G., Pradhan, P. K., Black, K. A., and Dos Santos, P. C. (2019). The thioredoxin system reduces protein persulfide intermediates formed during the synthesis of thio-cofactors in *Bacillus subtilis*. *Biochemistry* 58, 1892–1904. doi: 10.1021/acs.biochem.9b00045

Conflict of Interest: The authors declare that the research was conducted in the absence of any commercial or financial relationships that could be construed as a potential conflict of interest.

frontiers in Microbiology

ORIGINAL RESEARCH
published: 19 May 2021
doi: 10.3389/fmicb.2021.681911

Effect of Temperature on Metronidazole Resistance in *Helicobacter pylori*

Meiliang Gong[1†], Yingjie Han[2,3†], Xuning Wang[4], Hongjin Tao[2], Fansen Meng[2], Baicun Hou[2], Benjamin B. Sun[5,6] and Gangshi Wang[2*]*

[1] Department of Laboratory Medicine, Second Medical Center, Chinese PLA General Hospital, Beijing, China, [2] Department of Gastroenterology, Second Medical Center, Chinese PLA General Hospital, National Clinical Research Center for Geriatric Diseases, Beijing, China, [3] Department of Oncology, Fifth Medical Center, Chinese PLA General Hospital, Beijing, China, [4] Department of Surgery, First Medical Center, Chinese PLA General Hospital, Beijing, China, [5] British Heart Foundation Cardiovascular Epidemiology Unit, Department of Public Health and Primary Care, University of Cambridge, Cambridge, United Kingdom, [6] Royal Free Hospital, London, United Kingdom

Efficacy of *Helicobacter pylori (H. pylori)* eradication therapy has declined due to rapid rises in antibiotic resistance. We investigated how increased temperature affected *H. pylori* (NCTC 11637) growth and its sensitivity to metronidazole *in vitro*. We performed transcriptomic profiling using RNA-sequencing to identify differentially expressed genes (DEGs) associated with increased temperature. Transcriptional pathways involved in temperature-driven metronidazole resistance changes were analyzed through bioinformatic and literature curation approaches. We showed that *H. pylori* growth was inhibited at 41°C and inhibition was more apparent with prolonged incubation. Resistance to metronidazole was also reduced—minimum inhibitory concentration for metronidazole decreased from > 256 μg/ml at 37°C to 8 μg/ml at 41°C after culturing for 3 days. RNA-sequencing results, which were highly concordant within treatment conditions, revealed more than one third of genes (583/1,552) to be differentially expressed at increased temperatures with similar proportions up and down-regulated. Quantitative real-time PCR validation for 8 out of 10 DEGs tested gave consistent direction in gene expression changes. We found enrichment for redox and oxygen radical pathways, highlighting a mechanistic pathway driving temperature-related metronidazole resistance. Independent literature review of published genes associated with metronidazole resistance revealed 46 gene candidates, 21 of which showed differential expression and 7 out of 9 DEGs associated with "redox" resistance pathways. Sanger sequencing did not detect any changes in genetic sequences for known resistance genes *rdxA, frxA* nor *fdxB.* Our findings suggest that temperature increase can inhibit the growth and reduce *H. pylori* resistance to metronidazole. Redox pathways are possible potential drivers in metronidazole resistance change induced by temperature. Our study provides insight into potential novel approaches in treating antibiotic resistant *H. pylori*.

Keywords: *Helicobacter pylori*, temperature, transcriptomics, antibiotic resistance, metronidazole

OPEN ACCESS

Edited by:
Jong H. Kim,
Agricultural Research Service, United States

Reviewed by:
Alba Trespalacios, Pontifical Javeriana University, Colombia
Xiaoming Wang, Nanjing Agricultural University, China

***Correspondence:**
Benjamin B. Sun
bs446@medschl.cam.ac.uk
Gangshi Wang
wanggangshi@hotmail.com

[†] These authors have contributed equally to this work

Specialty section:
This article was submitted to Antimicrobials, Resistance and Chemotherapy, a section of the journal Frontiers in Microbiology

Received: *17 March 2021*
Accepted: *23 April 2021*
Published: *19 May 2021*

Citation:
Gong M, Han Y, Wang X, Tao H, Meng F, Hou B, Sun BB and Wang G (2021) Effect of Temperature on Metronidazole Resistance in Helicobacter pylori. Front. Microbiol. 12:681911. doi: 10.3389/fmicb.2021.681911

Abbreviations: BP, biological process; CC, cellular component; CFU, colony forming units; DEGs, differentially expressed genes; *E*-test, Epsilometer test; GC, gastric cancer; GO, Gene Ontology; *H. pylori*, *Helicobacter pylori*; KEGG, Kyoto Encyclopedia of Genes and Genomes; MF, molecular function; MIC, minimum inhibitory concentration; PBS, phosphate-buffered saline; PCR, polymerase chain reaction; Pfam, protein families database.

INTRODUCTION

Helicobacter pylori (H. pylori) infection has been established as the main cause of various gastroduodenal diseases including chronic gastric inflammation, peptic ulcer disease and gastric cancer (GC) and it is classified as a class I carcinogen (Ishaq and Nunn, 2015). *H. pylori* resides in human gastric mucosa and affects nearly half of the human population worldwide with prevalence exceeding 80% in certain regions such as parts of Asia (Hooi et al., 2017). Eradication of *H. pylori* has been shown to reduce GC incidence across a range of risk groups (Takenaka et al., 2007; Kosunen et al., 2011).

The standard triple therapy, consisting of a proton pump inhibitor combined with clarithromycin and amoxicillin or metronidazole, has been the mainstay of treatment for *H. pylori* infection over the last two decades. However, rising antibiotic resistance has made standard triple therapy less effective—bismuth and non-bismuth based quadruple therapies have also been introduced depending on efficacy and resistance patterns locally (Graham and Fischbach, 2010). Resistance to clarithromycin and metronidazole also varies between regions across the world and have hampered the elimination of *H. pylori* (Kim et al., 2015). In China, the resistance rate for clarithromycin is around 50% whilst resistance to metronidazole ranges from 41.6 to 95.4% in Southeast China (Su et al., 2013; Thung et al., 2016). Various mechanisms have been shown to affect *H. pylori* antibiotic resistance under physiological conditions (Hu et al., 2016; Alba et al., 2017). Point mutations in 23S rRNA and changes in efflux pump systems have been shown to confer resistance to macrolides such as clarithromycin (Francesco et al., 2011). In addition, reduced activities in nitroreductase (rdxA), flavinoxido reductase (frxA) and ferrodoxin-like enzymes (frxB) lead to reduced activation of metronidazole (Francesco et al., 2011).

Changes in environmental conditions lead to alterations in transcriptomic profiles of *H. pylori* (Thompson et al., 2003; De la Cruz et al., 2017). Previous evidence has demonstrated local nanoparticle heating inhibits *H. pylori* growth and virulence as a potential alternate approach to treating *H. pylori* infections (Wu et al., 2019; Zhi et al., 2019). Whilst temperature differences have led to changes leading to increased antibiotic resistance in other bacteria species (Liang et al., 2016; Loughman et al., 2016; De Silva et al., 2018), the effects of temperature on antibiotic resistance and transcriptomic changes in *H. pylori* have not been investigated previously.

In this study, we examine the effect of changes in temperature on the growth of *H. pylori* and its sensitivity to metronidazole using a reference resistant strain. In addition, we investigate perturbations in transcriptomic profiles underlying changes in temperature-driven antibiotic susceptibility.

MATERIALS AND METHODS

Bacterial Strain and Culture Conditions

H. pylori type strain NCTC 11637 (Lock et al., 2001) was used for this study and 16S rRNA identification was used to verify the strains. Bacteria was cultured on Karmali Agar Base (CM0935, Oxoid, United Kingdom) supplemented with 5% sterile defibrinated sheep blood (Beijing XLF Medical Sales Co. Ltd, China) for 3–5 days at 37°C, under microaerophilic conditions: microaerobic gas mixture composed of 5% oxygen, 10% carbon dioxide, and 85% nitrogen (GEN bag microaer, BioMérieux, France). *H. pylori* were subcultured three times before each experiment.

Comparison of *H. pylori* Growth at Different Temperatures

H. pylori NCTC 11637 was cultured at 37 and 41°C to evaluate the effects of elevated temperature on bacteria growth. Bacteria was resuspended in phosphate-buffered saline (PBS) to 8 different dilutional concentrations (0.5, 0.25, 0.125, 0.0625, 0.03125, 0.015, 0.0075, 0.003 McFarland). 90 mm plates seeded with 0.1 ml of bacterial suspensions were incubated at 37°C as controls. In the treatment group, 0.1 ml bacterial suspensions at the 8 dilution concentrations were seeded on 3 sets of 8 plates. After inoculation, the 3 sets of plates (each set consists of 8 plates of different bacterial concentrations) were incubated at 41°C for 1, 3, and 5 days, respectively, and then incubated at 37°C for a further 3 days. Colonies in each plate were counted after the last incubation.

Antibiotics Susceptibility Testing

In vitro minimum inhibitory concentrations (MICs) of four antibiotics (amoxicillin, clarithromycin, metronidazole, tetracycline) against *H. pylori* NCTC 11637 were tested. All experiments were performed in triplicate. The MICs of amoxicillin, metronidazole and tetracycline against *H. pylori* were determined via the Epsilometer test (E-test) using an E-strip (BioMerieux SA, France) and the Kirby-Bauer method was used for clarithromycin sensitivity. *H. pylori* NCTC 11637 was cultured as described above, and the third-generation colonies were selected and suspended in PBS to the turbidity of a 2 McFarland standard. Then, 0.1 ml of the bacterial suspension was evenly coated on Karmali Agar Base. Each agar plate was left to dry for 15 min before E-strip was affixed and the plates were incubated as described above. MICs were defined as the lowest concentration that allowed no visible growth after 72 h of incubation at 37°C. The clinical breakpoints for amoxicillin, clarithromycin, metronidazole, and tetracycline are defined as: >0.125, >0.5, >8, and >1 mg/L, respectively, as per European Committee on Antimicrobial Susceptibility Testing Breakpoints version 8 (European Committee on Antimicrobial Susceptibility Testing [ECUCAST], 2018).

RNA Extraction and Transcriptomic Analysis

H. pylori NCTC 11637 strain was divided into two groups in triplicate. The experimental group was treated at 41°C for 3 days. The control group was treated at 37°C for 3 days. The cells were harvested, and total RNA was extracted and purified using the Bacterial RNA kit (Omega Bio-tek, GA, United States) according to manufacturer protocols. Quality

control of each RNA sample was performed with Agilent 2100 Bioanalyzer (Agilent Technologies, Beijing, China). The cDNA libraries were constructed using NEBNext® Ultra™ RNA Library Prep Kit (New England Biolabs, Ipswich, MA, United States) and submitted for sequencing using IlluminaHiseq 4000. Library construction and sequencing were performed by Allwegene BioTech Co., Ltd. (Beijing, China). Raw reads were filtered using Trimmomatic v0.33 (Bolger et al., 2014) and mapped to the *H. pylori* NCTC 11637 genome (National Center for Biotechnology Information [NCBI], 2012) using Bowtie2 v2.2.6 (Langmead and Salzberg, 2012) with default parameters. Genes were quantified using HTSeq v0.6.0 (Anders et al., 2015). Differentially expressed genes (DEGs) were analyzed by DESeq2 v1.22.1 in R (Love et al., 2014). Genes with absolute $\log_2$ fold-changes > 1 and multiple testing adjusted (Benjamini–Hochberg procedure) $q < 0.05$ were considered as DEGs.

Gene Expression Using qRT-PCR

Quantitative real-time polymerase chain reaction (qRT-PCR) assays were performed using the same samples analyzed (3 controls at 37°C and 3 at 41°C for 3 days) as in the RNA-seq transcriptomic analyses. 10 genes with differential expression levels identified using RNA sequencing were selected for subsequent validation (5 of the most significantly associated genes and 5 associated with metronidazole resistance from bioinformatic screening as described in *Curation of resistance related genes*). Gene-specific primers (**Supplementary Table 1A**) were designed and purchased from Invitrogen (Beijing, China). Three technical replicates were performed for each biological sample. First strand cDNA was synthesized using PrimeScript™ RT reagent Kit with gDNA Eraser (Takara, Japan) according to manufacturer instructions. qRT-PCR reactions were performed using an ABI Prism 7500 Sequence Detection System (Perkin-Elmer Applied Biosystems, Foster City, CA). *H. pylori* 16S rRNA was used as housekeeping internal control. Gene expression and $\log_2$ fold-changes were analyzed using the $2^{-\Delta\Delta CT}$ algorithm (Livak and Schmittgen, 2001). After quality control, one biological sample at 37°C exhibited low readouts across all genes compared to the other 2 biological samples (which did not show low readouts in RNA-seq) and was excluded from analysis.

GO and KEGG Pathway Analysis

We mapped the genes to Entrez Gene symbols first. Gene Ontology (GO) enrichment analysis comprising cellular component (CC), molecular function (MF), and biological process (BP) were conducted for DEGs in R with GOSeq v1.26.0 and topGO v2.26.0 package, using the *H. pylori* 11637 reference strain annotated by Pfam (protein families database) (El-Gebali et al., 2019) as background. KOBAS v3.0 (Xie et al., 2011) was used to perform Kyoto Encyclopedia of Genes and Genomes (KEGG) pathway enrichment analysis for DEGs using *H. pylori* 26695 reference strain as background. The $p < 0.05$ adjusted for multiple testing (q-value) using the Benjamini-Hochberg method was used as significance thresholds for GO and KEGG pathway enrichment analyses. We also performed sensitivity analyses using absolute $\log_2$ fold-change > 1.5, $q < 0.05$ as cut-offs for DEGs.

Curation of Resistance Related Genes

Curation of All Mapped Genes Into Metronidazole Resistance Pathways

Metronidazole antibiotic resistance pathways in *H. pylori* based on four groups of broad mechanisms: (1) reduced activity of nitro-reductases, (2) increased activity of the oxygen radical scavenger system, (3) reduced uptake and increased efflux, and (4) increased activity of the DNA repair enzymes, were determined from current literature (Hu et al., 2016; Alba et al., 2017). All mapped genes ($n = 1{,}552$) were manually curated by two independent reviewers to determine whether each is related to one of the four mechanisms based on gene function and gene description. Genes with assignments which agree between the two reviewers were included.

Curation of Genes Associated With Metronidazole Resistance in Literature

Queries were made in PubMed using keywords "helicobacter pylori," "metronidazole," and "resist*" and subsequently manually curated to create a list of reported *H. pylori* metronidazole resistance genes. DEGs identified in this study were then mapped to the list of literature reported genes. Enrichment tests were performed by permutation testing (10,000 times).

Detection and Sequencing of rdxA, frxA, and fdxB

For both 37°C and 41°C conditions, conventional polymerase chain reaction (PCR) amplification was performed. Specific reagents, primers and conditions are detailed in **Supplementary Table 1B**. PCR, gel electrophoresis and DNA sequencing via Sanger sequencing method were performed following standard manufacturer protocols.

RESULTS

Increased Temperature Inhibits *H. pylori* Growth

The effect of elevated temperature on *H. pylori* (NCTC 11637 strain) growth was evaluated at 37°C (control group) and at 41°C for 1, 3, and 5 days. Growth of *H. pylori* was significantly inhibited after incubation at 41°C with inhibition more apparent with prolonged incubation (**Figure 1A**). At an inoculation concentration of 0.002 McFarland, bacterial colony count of the control group was 4,288 ± 184 CFU/ml. The counts decreased to 2,970 ± 462, 2,255 ± 575, and 1,990 ± 187 CFU/ml after 1, 3, and 5 days of treatment under 41°C, respectively ($p = 0.026$ [1 day], $p = 0.018$ [3 days], $p = 0.00011$ [5 days], compared with control group).

Temperature Change Increases Sensitivity of *H. pylori* to Metronidazole

We investigated the effect of increased temperature on sensitivities of the metronidazole-resistant *H. pylori* NCTC 11637 strain to metronidazole using the E-test strip. The minimum inhibitory concentration (MIC) for metronidazole

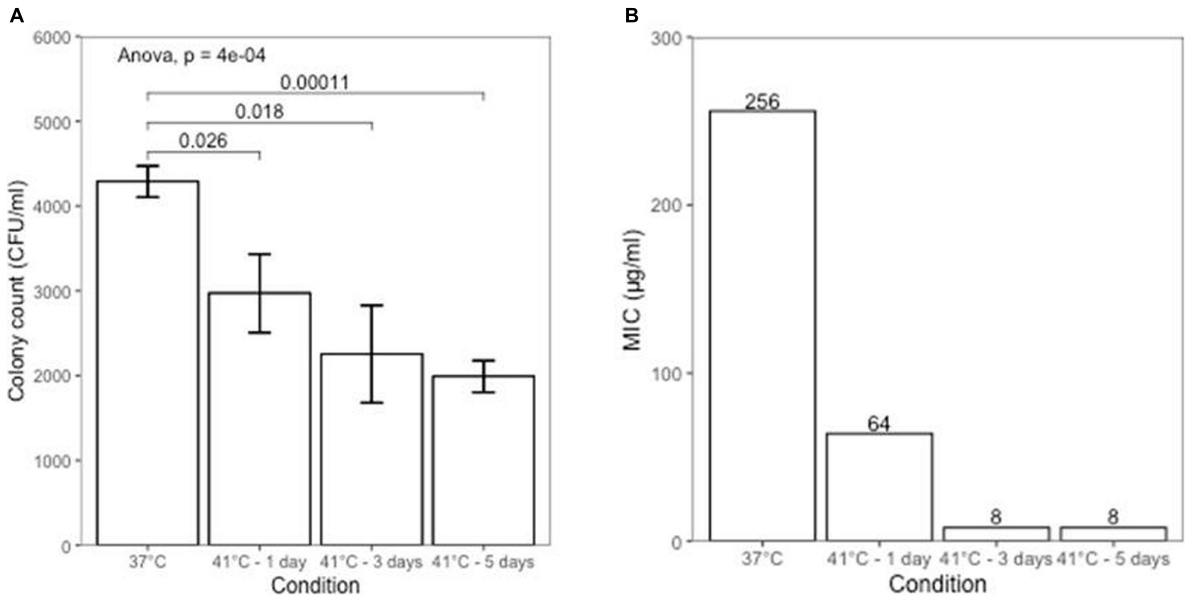

FIGURE 1 | (A) Growth inhibition of *H. pylori* at different temperature conditions. **(B)** Changes in metronidazole susceptibility at different temperature conditions.

under the 37°C culture condition (control group) was > 256 μg/ml. After culturing at 41°C for 3 days, MIC of *H. pylori* to metronidazole decreased to 8 μg/ml (**Figure 1B**), which is the breakpoint of metronidazole resistance. The NCTC 11637 strain was sensitive to clarithromycin, amoxicillin and tetracycline and this did not change under increased culture temperature conditions (**Supplementary Table 2**). There was no growth in the *H. pylori* subculture inoculation after returning from 41 to 37°C.

Transcriptome Analyses Identify Changes in Drug Resistance Genes

Identification of Differentially Expressed Genes by RNA-Sequencing

To study the transcriptomic changes which may drive decreased resistance to increased temperature, we used RNA sequencing to assess changes in gene expression between 37 and 41°C. Illumina paired-end sequencing of 6 samples (3 cultured at 37°C and 3 at 41°C) yielded a total of 252,222,378 clean reads. 70.9–80.1% reads of samples were mapped to the annotated *H. pylori* NCTC 11637 genome culminating in 1,552 mapped genes. Gene expression measurements were highly consistent between biological replicates within each temperature condition (Pearson's *r*: 0.97–0.99 within condition, **Figure 2A**). 583 out of 1,552 mapped genes were significantly differentially expressed at absolute $\log_2$ fold-change > 1 and $q < 0.05$ after incubation at 41°C for 3 days compared to 37°C, of which 292 were up-regulated and 291 were down-regulated (**Figures 2B,C** and **Supplementary Table 3**).

Gene Expression Measurements Using qRT-PCR

We selected 10 DEGs, 5 most significantly associated genes and 5 related to metronidazole resistance (Materials and Methods) for measurement using qRT-PCR. 8 out of the 10 DEGs showed consistent direction in log fold gene expression changes (**Figure 3**). All 5 of DEGs with the strongest statistical significance of association [HP17_RS13720 (HP1076), HP_RS12585 (HP0115), flgL, HP17_RS17120 (HP0630), and HP17_RS13130 (HP1286)] showed directionally concordant changes using qRT-PCR.

GO and KEGG Pathway Enrichment Analysis

To investigate molecular and functional pathway changes as result of increased temperature, GO and KEGG pathway enrichment analyses of DEGs were performed. Whilst no pathways were significantly enriched after adjusting for multiple testing, we found enrichment at nominal significance ($p < 0.05$) for drug, vitamin, superoxide and reactive oxygen species metabolic GO processes. Cellular component was enriched for ribosome, non-membrane-bounded organelle and cytoplasm components at nominal threshold. Molecular function enrichment included structural constituent of ribosome, oxidoreductase activity, superoxide dismutase activity and various symporter activities (**Supplementary Tables 4.1, 4.2**). Sensitivity analyses, using DEGs defined using more stringent thresholds of absolute $\log_2$ fold-change > 1.5 adjusted $q < 0.05$ showed similar results. Both analyses showed GO enrichment for reactive oxygen species and metabolic processes (**Supplementary Table 5**).

DEGs Are Enriched for Specific Metronidazole Resistance Pathways

All mapped genes were curated base on gene description and function into four broad metronidazole resistance pathways: (1) nitro-reductases, (2) oxygen radical scavenger, (3) drug uptake and efflux and (4) DNA repair related. 126 genes were related to

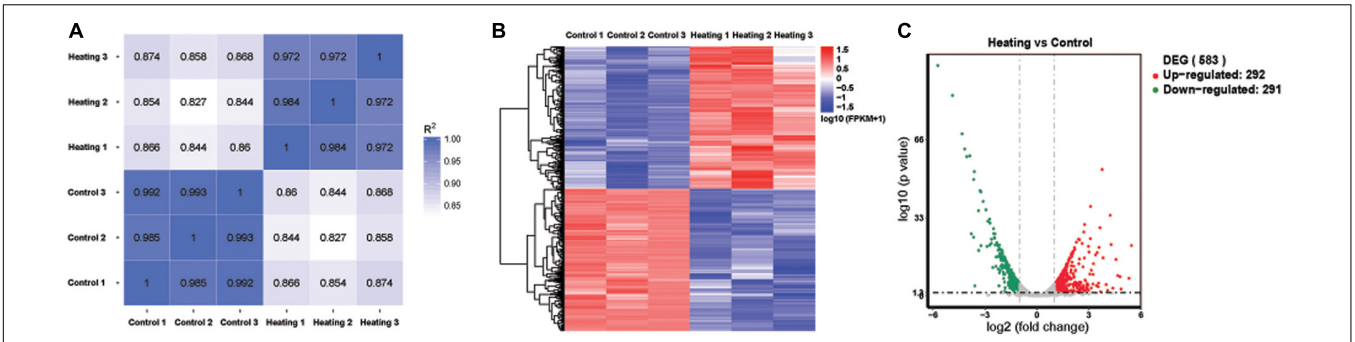

FIGURE 2 | Differentially expressed genes (DEGs) by RNA-seq. **(A)** Pearson's correlation heatmap of expression of all mapped genes **(B)** Hierarchical clustered heat map of significantly differentially expressed genes (583). **(C)** Volcano plot displaying DEGs. The vertical axis corresponds to the *q*-value, the horizontal axis displays the $\log_2$ fold-change. The red dots represent the up-regulated expressed transcripts (292), the green dots represent the down-regulated transcripts (291). Vertical and horizontal dashed lines indicate absolute $\log_2$ fold-change = 1 and adjusted $p = 0.05$, respectively.

one of the four pathways (**Supplementary Table 6** and **Table 1**). Nitro-reductase related pathways were enriched for DEGs under increased temperature condition at 41°C (permutation 10,000 times, empirical $p = 0.0038$). Oxygen radical scavenger pathways were borderline significant for enrichment of DEGs (empirical $p = 0.05$).

In addition, we performed independent literature search for published genes associated with metronidazole resistance. Our literature search revealed 46 gene candidates related to metronidazole resistance in *H. pylori* which were classified into 10 categories (**Supplementary Table 7**). These genes were all found within the 1,552 genes sequenced in our study. 21 of the 46 genes showed differential expression. Permutation testing did not reveal significant enrichment amongst resistance genes overall for DEGs (empirical $p = 0.15$). However, genes associated with "redox" resistance pathways were significantly enriched for DEGs with 7 out of 9 genes differentially expressed (empirical $p = 0.016$). Other pathways with more than 5 genes in each category did not show enrichment for DEGs.

Metronidazole is a prodrug which is first activated by nitro-reductase (mutated in resistant *H. pylori* NCTC 11637 strains; Debets-Ossenkopp et al., 1999) to produce oxygen radicals toxic to bacteria through DNA damage (Cederbrant et al., 1992; van der Wouden et al., 2001). We found that expression of NAD(P)H-dependent oxidoreductase (*rdxA [HP17_RS12480]*) was downregulated ($\log_2$ fold-change: −1.51, $p = 3.8 \times 10^{-5}$). In addition, we also found that superoxidase dismutase (*Sod [HP17_RS11110]*) expression, an important protein in detoxifying free oxygen radicals, was downregulated ($\log_2$ fold-change: −3.29, $p = 4.1 \times 10^{-45}$) and expression of its transcriptional repressor, ferric uptake regulator (*Fur* [HP17_RS13980]) (Tsugawa et al., 2011), was upregulated ($\log_2$ fold-change: 2.14, $p = 1.7 \times 10^{-8}$).

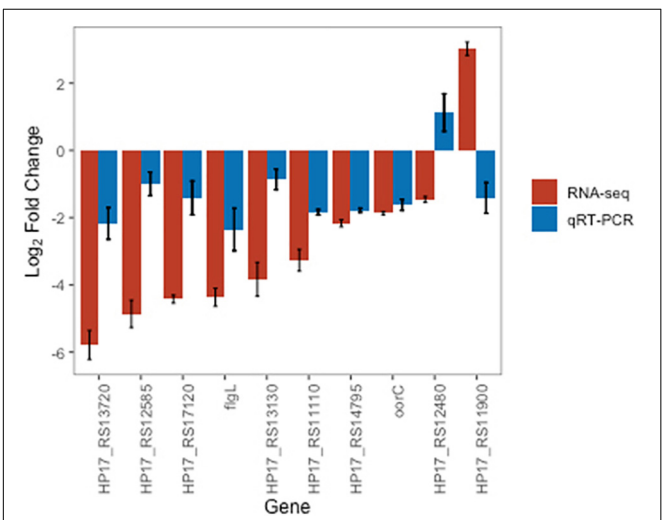

FIGURE 3 | Barplot showing $\log_2$ fold-changes at incubation of 41°C for 3 days compared to 37°C using RNA-Seq and qRT-PCR methods for 10 selected DEGs. Error bars indicate standard deviations from the mean. Genes ordered by RNA-Seq $\log_2$ fold-changes.

Key Resistance Gene Sequences Not Altered by Increased Temperature

We independently tested established *H. pylori* resistance genes *rdxA, frxA*, and *fdxB* through Sanger sequencing to see if increased temperature conditions led to structural changes in these genes. All three genes were successfully detected and amplified though PCR in both temperature conditions (**Supplementary Figure 1**). Sanger sequencing did not detect any changes in genetic sequences for *rdxA, frxA* nor *fdxB* (**Supplementary Figures 2–4**).

DISCUSSION

Our study showed that increased temperature inhibited the growth of metronidazole resistant *H. pylori* strain (NCTC 11637) consistent with previous reported changes in growth of sensitive *H. pylori* strains (26695 strain) under elevated temperatures (Jiang and Doyle, 1998). In addition, we present the novel finding that elevated temperature (41°C) increased sensitivities of the resistant strain to metronidazole which has not been reported previously. Studies have identified

TABLE 1 | Curation of DEGs into metronidazole resistance pathways (adjusted $p < 0.05$).

Resistance mechanism	Gene	Gene description	Log_2 (fold change)	Adjusted *p*-value
DNA repair (12/32 genes, enrichment $p = 0.57$)	HP17_RS15190	DNA (cytosine-5-)-methyltransferase	2.737	8.89E–31
	HP17_RS17710	DNA cytosine methyltransferase	2.476	7.30E–05
	HP17_RS14395	DNA polymerase III subunit delta'	2.209	1.39E–11
	HP17_RS13655	DNA translocase FtsK	−2.026	6.78E–18
	HP17_RS10090	DNA gyrase subunit A	−1.928	1.28E–16
	HP17_RS10700	DNA-binding response regulator	−1.904	5.06E–13
	HP17_RS12590	DNA topoisomerase I	1.893	1.46E–16
	HP17_RS15830	Thymidylate synthase (FAD)	−1.602	2.12E–11
	HP17_RS10880	DNA (cytosine-5-)-methyltransferase	1.473	7.16E–10
	HP17_RS14590	DNA-directed RNA polymerase subunit beta/beta'	1.174	2.01E–07
	HP17_RS16580	DNA starvation/stationary phase protection protein	−1.151	1.86E–07
	HP17_RS15450	DNA polymerase III subunit alpha	−1.045	1.11E–05
Drug transportation (25/78 genes, enrichment $p = 0.88$)	HP17_RS11900	Glucose/galactose MFS transporter	3.067	7.56E–25
	HP17_RS13150	Nicotinamide riboside transporter PnuC	3.043	6.80E–10
	HP17_RS11910	Glutamine ABC transporter substrate-binding protein	−2.846	3.78E–32
	HP17_RS16625	ABC transporter permease	2.690	1.28E–27
	HP17_RS13650	MFS transporter	−2.222	2.78E–17
	HP17_RS15125	Iron chelating transport ATP-binding protein	−2.040	1.09E–16
	HP17_RS14795	MFS transporter	−1.935	2.03E–10
	HP17_RS15130	Iron chelating ABC transporter permease	−1.932	5.41E–08
	HP17_RS16620	ABC transporter ATP-binding protein	1.922	1.14E–07
	HP17_RS10180	Lysine transporter	−1.874	9.77E–03
	HP17_RS16500	SulP family inorganic anion transporter	1.850	1.48E–02
	HP17_RS16985	MFS transporter	−1.794	1.49E–14
	HP17_RS16850	Autotransporter domain-containing protein	−1.754	1.86E–12
	HP17_RS17445	AI-2E family transporter	−1.582	6.10E–06
	HP17_RS15475	ABC transporter ATP-binding protein	−1.563	1.09E–06
	HP17_RS17915	ABC transporter ATP-binding protein	1.527	1.71E–05
	HP17_RS16110	ABC transporter substrate-binding protein	1.514	1.10E–06
	HP17_RS14930	ABC transporter ATP-binding protein	−1.473	9.38E–09
	HP17_RS09990	Ferrous iron transport protein B	−1.433	2.47E–09
	HP17_RS15230	Biopolymer transporter ExbD	1.261	7.33E–08
	HP17_RS11620	MATE family efflux transporter	1.222	1.01E–02
	HP17_RS13700	ABC transporter ATP-binding protein	1.139	8.19E–07
	HP17_RS14700	Molybdenum ABC transporter ATP-binding protein	−1.129	1.81E–03
	HP17_RS11565	ABC transporter ATP-binding protein	1.068	9.17E–06
	HP17_RS14520	ABC transporter ATP-binding protein	−1.009	1.74E–05
Nitro-reductase (10/13 genes, enrichment $p = 0.0038$)	HP17_RS17120	Flavodoxin family protein	−4.185	1.30E–62
	HP17_RS17325	2-oxoglutarate ferredoxin oxidoreductase subunit beta	−1.851	3.38E–16
	oorC	2-oxoglutarate:acceptor oxidoreductase	−1.849	1.07E–15
	HP17_RS11960	Flavodoxin	−1.664	9.96E–14
	HP17_RS15890	Pyruvate ferredoxin oxidoreductase subunit beta	−1.651	9.16E–14
	HP17_RS17330	2-oxoglutarate synthase subunit alpha	−1.632	3.93E–13
	HP17_RS12480	NAD(P)H-dependent oxidoreductase	−1.512	3.79E–05
	porC	Pyruvate flavodoxin oxidoreductase subunit gamma	−1.345	8.80E–08
	HP17_RS15705	Cytochrome c oxidase accessory protein CcoG	−1.239	6.23E–08
	HP17_RS15895	2-ketoisovalerate ferredoxin oxidoreductase subunit alpha	−1.161	1.68E–06
Oxygen-radical scavenging (3/3 genes, enrichment $p = 0.05$)	HP17_RS11110	Superoxide dismutase	−3.293	4.11E–45
	HP17_RS17265	3-methyladenine DNA glycosylase	1.904	1.31E–05
	HP17_RS13135	Thiaminase II	1.643	3.72E–04

thermoregulated antibiotic resistance in some species. *Francisella tularensis* showed increased resistance to gentamicin at ambient temperature (26°C) compared to mammalian body temperature (37°C) (Loughman et al., 2016). Temperature associated expression changes in antibiotic resistance were observed in *Acinetobacter baumannii* ATCC 17978 (De Silva et al., 2018).

This is the first study investigating gene expression changes with increased temperature in *H. pylori*. Transcriptomic profiling showed good internal consistency within treatment conditions and widespread changes in gene expression with more than one third of all genes differentially expressed. Previous literature showed transcriptomic changes in *H. pylori* with sudden decreased temperature (Han et al., 2009). Approximately equal proportion of DEGs was up and down-regulated similar to findings seen with decreased temperature.

Whilst no specific GO or KEGG pathways were enriched for DEGs after multiple testing correction, we found nominal statistical evidence indicating that metabolic processes may be enriched. Furthermore, permutation analyses based on annotation of genes for metronidazole resistance mechanisms and specific metronidazole resistance genes published in the literature showed enrichment for redox (oxygen radical scavenger) and nitro-reductase pathways. Metronidazole is a prodrug which is first activated by nitro-reductase to produce oxygen radicals toxic to bacteria through DNA damage (van der Wouden et al., 2001). Increased nitro-reductase activity in theory leads to reduced metronidazole resistance. We found reduced expression of nitro-reductases, such as NAD(P)H-dependent oxidoreductase (*rdxA*, *HP17_RS12480)* with heating. The *H. pylori* NCTC 11637 strain used in this study contains a transposon-induced deletion in *rdxA* which plays a key role conferring resistance (Debets-Ossenkopp et al., 1999), thus the NAD(P)H-dependent oxidoreductase produced by the mutated gene does not provide normal functions regardless of expression levels.

In addition we also found *Sod* expression to be downregulated with elevated temperature. Sod contributes to metronidazole resistance through mitigating oxygen radical related damage and increased Sod levels have been associated with development of metronidazole resistance (Wassmann and Bruchhaus, 2000; van der Wouden et al., 2001). Interestingly, we observed an increased expression of a negative transcription regulator of *Sod*, *Fur*, which may also contribute to decreased *Sod* expression. Therefore, another plausible mechanism by which higher temperature leads to reduced metronidazole resistance may be through decreased *Sod* expression which leads to increased susceptibility to superoxide damage. DEGs within other resistance pathways such as DNA repair, efflux pump complexes, bacterial flagellar mobility, changes in metabolism or potential novel pathways may also play a role in temperature induced reduction in metronidazole resistance. Lastly, we confirmed that key resistance genes, *rdxA, frxA,* and *fdxB,* are not mutated by increased temperature conditions, suggesting that resistance changes can be attributed to gene expression or protein function changes. Further studies would be needed to elucidate these functional mechanisms in detail. Our approach of studying transcriptomic changes associated with temperature-related antibiotic resistance can highlight perturbed gene pathways as well as suggest candidate genes and pathways as potential novel drug targets for antimicrobials.

Our study examined the effect of 41°C temperature on *H. pylori* growth, metronidazole resistance and transcriptomic changes. Further studies are needed to investigate the detailed mechanisms driving reduced resistance to metronidazole. Effects at other temperatures as well as using strains with different profiles and mechanisms of resistance to various other antibiotics commonly used in *H. pylori* eradication could also be explored. Whether *in vitro* effects of increased temperature are also reflected *in vivo* remain to be elucidated.

At present, antibiotics treatment combined with proton-pump inhibitors is the main approach to treating *H. pylori* infections. Unfortunately, efficacy has decreased, due to the rapid rise in resistance rates (Fallone et al., 2019). Emergence of multi-drug resistance strains further exacerbates the problem (Boyanova et al., 2019). *H. pylori* colonizes and grows in gastric mucosa in humans which makes local treatment possible. Since the stomach mucosa of mammal species can withstand temperatures as high as 46°C (Kang et al., 2004), raising local temperatures have been postulated to help eradicate *H. pylori in vivo* complementing antibiotic-based therapies. One way to achieve this may be through well-controlled local photothermal/magnetic thermal treatments using nanomaterials which have shown early promise in suppressing bacterial growths (Mocan et al., 2017; Chen et al., 2018), including *H. pylori* (Wu et al., 2019). It is recently reported that gold nanostars@*H. pylori*-antibodies nanoprobes could target and kill *H. pylori* in the stomach in model animals under near-infrared laser irradiation (Zhi et al., 2019). However, feasibility and safety of sustained localized thermal treatment within human gastric mucosa need to be ascertained in a clinical setting in order for it to become a viable strategy for *H. pylori* eradication.

In conclusion, growth of *H. pylori* and resistance to metronidazole was significantly inhibited when cultured *in vitro* at 41°C. Transcriptomic analyses showed differential gene expression changes in more than one third of the genes with evidence of enrichment pointing to redox pathways as potential drivers of temperature related reduction in metronidazole resistance. Expression changes for genes in other resistance pathways may also play a role in temperature induced metronidazole sensitivity. Our findings suggest a novel approach in treating metronidazole and multi-drug resistant *H. pylori in vivo*.

DATA AVAILABILITY STATEMENT

The original contributions presented in the study are publicly available. This data can be found here: https://www.ncbi.nlm.nih.gov/sra/PRJNA718481.

AUTHOR CONTRIBUTIONS

MG carried out *H. pylori* growth experiments and antibiotics susceptibility testing, and drafted the manuscript. YH performed

bioinformatic analysis and curation of related genes. XW participated in bioinformatic analysis. HT, FM, and BH participated in antibiotics susceptibility testing and gene expression analysis. BS and GW designed and conceived of the study, participated in its coordination, and wrote the manuscript. GW had primary responsibility for final content. All authors read and approved the final manuscript.

FUNDING

This study was supported by the National Science Foundation of China (grant no. 51471186) and the National Clinical Research Center for Geriatric Diseases (grant no. NCRCG-PLAGH-2019015). The funder had no role in the study design, data collection, data analysis, data interpretation, or writing of the article.

SUPPLEMENTARY MATERIAL

The Supplementary Material for this article can be found online at: https://www.frontiersin.org/articles/10.3389/fmicb.2021.681911/full#supplementary-material

Supplementary Figure 1 | Agarose gel electrophoresis of gene fragments of *H. pylori* NCTC 11637 amplified by PCR. **(A)** Lanes 1–6, PCR fragments of gene *rdxA*; **(B)** Lane 1, PCR fragments of gene *frxA* of *H. pylori* NCTC 11637 cultured in 37°C; Lane 2, PCR fragments of gene *frxA* of *H. pylori* NCTC 11637 cultured in 41°C; Lanes 3–5, PCR fragments of gene *fdxB* of *H. pylori* NCTC 11637 cultured in 37°C with primer pairs 1–3, respectively, Lanes 6–8, PCR fragments of gene *fdxB* of *H. pylori* NCTC 11637 cultured in 41°C with primer pairs 1–3, respectively.

Supplementary Figure 2 | The DNA sequence blast of *rdxA* gene in *H. pylori* 26695 and *H. pylori* NCTC 11637. The *H. pylori* 26695 is sensitive to metronidazole but *H. pylori* NCTC 11637 is resistant. Compared with *H. pylori* 26695, the structural variation of *rdxA* gene in *H. pylori* NCTC 11637 included point mutations and the insertion of mini-IS605, which caused *rdxA* inactivation and thus metronidazole resistance. 11637-*rdxA*-37: the *rdxA* gene sequence of *H. pylori* NCTC 11637 cultured in 37°C. 11637-*rdxA*-41: the *rdxA* gene sequence of *H. pylori* NCTC 11637 cultured in 41°C. 26695-*rdxA*: the *rdxA* gene reference sequence of *H. pylori* 26695. The dashed rectangle showed the start site of *rdxA* gene and the solid rectangle showed the termination site of *rdxA* gene. The figure showed that the 11637-*rdxA*-37 and 11637-*rdxA*-41 were exactly the same. The high light region showed the insertion of mini-IS605, one of the endogenous transposable elements, in *H. pylori* NCTC 11637.

Supplementary Figure 3 | The DNA sequence blast of *frxA* gene in *H. pylori* 26695 and *H. pylori* NCTC 11637. 11637-*frxA*-37: the *frxA* gene sequence of *H. pylori* NCTC 11637 cultured in 37°C. 11637-*frxA*-41: the *frxA* gene sequence of *H. pylori* NCTC 11637 cultured in 41°C. 26695-*frxA*: the *frxA* gene reference sequence of *H. pylori* 26695. The figure showed that the 11637-*frxA*-37 and 11637-*frxA*-41 were exactly the same.

Supplementary Figure 4 | The DNA sequence blast of *fdxB* gene in *H. pylori* 26695 and *H. pylori* NCTC 11637. 11637-*fdxB*-37: the *fdxB* gene sequence of *H. pylori* NCTC 11637 cultured in 37°C. 11637-*fdxB*-41: the *fdxB* gene sequence of *H. pylori* NCTC 11637 cultured in 41°C. 26695-*fdxB*: the *fdxB* gene reference sequence of *H. pylori* 26695. The figure showed that the 11637-*fdxB*-37 and 11637-*fdxB*-41 were exactly the same.

REFERENCES

Alba, C., Blanco, A., and Alarcon, T. (2017). Antibiotic resistance in *Helicobacter* pylori. *Curr. Opin. Infect. Dis.* 30, 489–497. doi: 10.1097/QCO.0000000000000396

Anders, S., Pyl, P. T., and Huber, W. (2015). HTSeq–a Python framework to work with high-throughput sequencing data. *Bioinformatics* 31, 166–169. doi: 10.1093/bioinformatics/btu638

Bolger, A. M., Lohse, M., and Usadel, B. (2014). Trimmomatic: a flexible trimmer for Illumina sequence data. *Bioinformatics* 30, 2114–2120. doi: 10.1093/bioinformatics/btu170

Boyanova, L., Hadzhiyski, P., Kandilarov, N., Markovska, R., and Mitov, I. (2019). Multidrug resistance in *Helicobacter* pylori: current state and future directions. *Expert. Rev. Clin. Pharmacol.* 12, 909–915. doi: 10.1080/17512433.2019.1654858

Cederbrant, G., Kahlmeter, G., and Ljungh, A. (1992). Proposed mechanism for metronidazole resistance in *Helicobacter* pylori. *J. Antimicrob. Chemother.* 29, 115–120. doi: 10.1093/jac/29.2.115

Chen, W., Wang, Y., Qin, M., Zhang, X., Zhang, Z., Sun, X., et al. (2018). Bacteria-driven hypoxia targeting for combined biotherapy and photothermal therapy. *ACS Nano* 12, 5995–6005. doi: 10.1021/acsnano.8b02235

De la Cruz, M. A., Ares, M. A., von Bargen, K., Panunzi, L. G., Martinez-Cruz, J., Valdez-Salazar, H. A., et al. (2017). Gene expression profiling of transcription factors of *Helicobacter pylori* under different environmental conditions. *Front. Microbiol.* 8:615. doi: 10.3389/fmicb.2017.00615

De Silva, P. M., Chong, P., Fernando, D. M., Westmacott, G., and Kumar, A. (2018). Effect of incubation temperature on antibiotic resistance and virulence factors of *Acinetobacter baumannii* ATCC 17978. *Antimicrob. Agents Chemother.* 62:e01514–17. doi: 10.1128/AAC.01514-17

Debets-Ossenkopp, Y. J., Pot, R. G., van Westerloo, D. J., Goodwin, A., Vandenbroucke-Grauls, C. M., Berg, D. E., et al. (1999). Insertion of mini-IS605 and deletion of adjacent sequences in the nitroreductase (rdxA) gene cause metronidazole resistance in *Helicobacter pylori* NCTC11637. *Antimicrob. Agents Chemother.* 43, 2657–2662. doi: 10.1128/AAC.43.11.2657

El-Gebali, S., Mistry, J., Bateman, A., Eddy, S. R., Luciani, A., Potter, S. C., et al. (2019). The Pfam protein families database in 2019. *Nucleic Acids Res.* 47, D427–D432. doi: 10.1093/nar/gky995

European Committee on Antimicrobial Susceptibility Testing [ECUCAST] (2018). *Clinical Breakpoints – Bacteria (V 8.0)*. Available online at: https://www.eucast.org/clinical_breakpoints/ (accessed January 6, 2018).

Fallone, C. A., Moss, S. F., and Malfertheiner, P. (2019). Reconciliation of recent *Helicobacter* pylori treatment guidelines in a time of increasing resistance to antibiotics. *Gastroenterology* 157, 44–53. doi: 10.1053/j.gastro.2019.04.011

Francesco, V. D., Zullo, A., Hassan, C., Giorgio, F., Rosania, R., and Ierardi, E. (2011). Mechanisms of *Helicobacter pylori* antibiotic resistance: an updated appraisal. *World J. Gastrointest. Pathophysiol.* 2, 35–41. doi: 10.4291/wjgp.v2.i3.35

Graham, D. Y., and Fischbach, L. (2010). *Helicobacter* pylori treatment in the era of increasing antibiotic resistance. *Gut* 59, 1143–1153. doi: 10.1136/gut.2009.192757

Han, Y. H., Liu, W. Z., Shi, Y. Z., Lu, L. Q., Xiao, S. D., and Zhang, Q. H. (2009). Gene expression profile of *Helicobacter* pylori in response to growth temperature variation. *J. Microbiol.* 47, 455–465.

Hooi, J. K. Y., Lai, W. Y., Ng, W. K., Suen, M. M. Y., Underwood, F. E., Tanyingoh, D., et al. (2017). Global prevalence of *Helicobacter pylori* infection: systematic review and meta-analysis. *Gastroenterology* 153, 420–429. doi: 10.1053/j.gastro.2017.04.022

Hu, Y., Zhang, M., Lu, B., and Dai, J. (2016). *Helicobacter pylori* and antibiotic resistance, a continuing and intractable problem. *Helicobacter* 21, 349–363. doi: 10.1111/hel.12299

Ishaq, S., and Nunn, L. (2015). *Helicobacter pylori* and gastric cancer: a state of the art review. *Gastroenterol. Hepatol. Bed Bench* 8(Suppl 1), S6–S14.

Jiang, X., and Doyle, M. P. (1998). Effect of environmental and substrate factors on survival and growth of *Helicobacter pylori*. *J. Food Prot.* 61, 929–933. doi: 10.4315/0362-028x-61.8.929

Kang, Y. M., Bielefeldt, K., and Gebhart, G. F. (2004). Sensitization of mechanosensitive gastric vagal afferent fibers in the rat by thermal and chemical stimuli and gastric ulcers. *J. Neurophysiol.* 91, 1981–1989.

Kim, S. Y., Choi, D. J., and Chung, J. W. (2015). Antibiotic treatment for *Helicobacter pylori*: is the end coming? *World J. Gastrointest. Pharmacol. Ther.* 6, 183–198. doi: 10.4292/wjgpt.v6.i4.183

Kosunen, T. U., Pukkala, E., Sarna, S., Seppala, K., Aromaa, A., Knekt, P., et al. (2011). Gastric cancers in Finnish patients after cure of *Helicobacter pylori* infection: a cohort study. *Int. J. Cancer* 128, 433–439. doi: 10.1002/ijc.25337

Langmead, B., and Salzberg, S. L. (2012). Fast gapped-read alignment with Bowtie 2. *Nat. Methods.* 9, 357–359. doi: 10.1038/nmeth.1923

Liang, Y., Guo, Z., Gao, L., Guo, Q., Wang, L., Han, Y., et al. (2016). The role of the temperature-regulated acyltransferase (PA3242) on growth, antibiotic resistance and virulence in *Pseudomonas aeruginosa*. *Microb. Pathog.* 101, 126–135. doi: 10.1016/j.micpath.2016.09.019

Livak, K. J., and Schmittgen, T. D. (2001). Analysis of relative gene expression data using real-time quantitative PCR and the 2(-Delta Delta C(T)) Method. *Methods* 25, 402–408. doi: 10.1006/meth.2001.1262

Lock, R. A., Cordwell, S. J., Coombs, G. W., Walsh, B. J., and Forbes, G. M. (2001). Proteome analysis of *Helicobacter pylori*: major proteins of type strain NCTC 11637. *Pathology* 33, 365–374.

Loughman, K., Hall, J., Knowlton, S., Sindeldecker, D., Gilson, T., Schmitt, D. M., et al. (2016). Temperature-dependent gentamicin resistance *of Francisella tularensis* is mediated by uptake modulation. *Front. Microbiol.* 7:37. doi: 10.3389/fmicb.2016.00037

Love, M. I., Huber, W., and Anders, S. (2014). Moderated estimation of fold change and dispersion for RNA-seq data with DESeq2. *Genome Biol.* 15:550. doi: 10.1186/s13059-014-0550-8

Mocan, L., Tabaran, F. A., Mocan, T., Pop, T., Mosteanu, O., Agoston-Coldea, L., et al. (2017). Laser thermal ablation of multidrug-resistant bacteria using functionalized gold nanoparticles. *Int. J. Nanomed.* 12, 2255–2263. doi: 10.2147/IJN.S124778

National Center for Biotechnology Information [NCBI] (2012). *Helicobacter pylori NCTC 11637 Genome Sequencing and Assembly*. Available online at: https://www.ncbi.nlm.nih.gov/bioproject/PRJNA76569 (accessed October 16, 2019).

Su, P., Li, Y., Li, H., Zhang, J., Lin, L., Wang, Q., et al. (2013). Antibiotic resistance of *Helicobacter* pylori isolated in the Southeast Coastal Region of China. *Helicobacter* 18, 274–279. doi: 10.1111/hel.12046

Takenaka, R., Okada, H., Kato, J., Makidono, C., Hori, S., Kawahara, Y., et al. (2007). *Helicobacter pylori* eradication reduced the incidence of gastric cancer, especially of the intestinal type. *Aliment Pharmacol. Ther.* 25, 805–812. doi: 10.1111/j.1365-2036.2007.03268.x

Thompson, L. J., Merrell, D. S., Neilan, B. A., Mitchell, H., Lee, A., and Falkow, S. (2003). Gene expression profiling of *Helicobacter pylori* reveals a growth-phase-dependent switch in virulence gene expression. *Infect. Immun.* 71, 2643–2655. doi: 10.1128/iai.71.5.2643-2655.2003

Thung, I., Aramin, H., Vavinskaya, V., Gupta, S., Park, J. Y., Crowe, S. E., et al. (2016). Review article: the global emergence of *Helicobacter pylori* antibiotic resistance. *Aliment Pharmacol. Ther.* 43, 514–533. doi: 10.1111/apt.13497

Tsugawa, H., Suzuki, H., Satoh, K., Hirata, K., Matsuzaki, J., Saito, Y., et al. (2011). Two amino acids mutation of ferric uptake regulator determines *Helicobacter pylori* resistance to metronidazole. *Antioxid. Redox. Signal.* 14, 15–23. doi: 10.1089/ars.2010.3146

van der Wouden, E. J., Thijs, J. C., Kusters, J. G., van Zwet, A. A., and Kleibeuker, J. H. (2001). Mechanism and clinical significance of metronidazole resistance in *Helicobacter pylori*. *Scand. J. Gastroenterol. Suppl.* 234, 10–14. doi: 10.1080/003655201753265055

Wassmann, C., and Bruchhaus, I. (2000). Superoxide dismutase reduces susceptibility to metronidazole of the pathogenic protozoan *Entamoeba histolytica* under microaerophilic but not under anaerobic conditions. *Arch. Biochem. Biophys.* 376, 236–238. doi: 10.1006/abbi.2000.1707

Wu, T., Wang, L., Gong, M., Lin, Y., Xu, Y., Ye, L., et al. (2019). Synergistic effects of nanoparticle heating and amoxicillin on *H. pylori* inhibition. *J. Magn. Magn. Mater.* 485, 95–104. doi: 10.1016/j.jmmm.2019.04.076

Xie, C., Mao, X., Huang, J., Ding, Y., Wu, J., Dong, S., et al. (2011). KOBAS 2.0: a web server for annotation and identification of enriched pathways and diseases. *Nucleic Acids Res.* 39, W316–W322. doi: 10.1093/nar/gkr483

Zhi, X., Liu, Y., Lin, L., Yang, M., Zhang, L., Zhang, L., et al. (2019). Oral pH sensitive GNS@ab nanoprobes for targeted therapy of *Helicobacter* pylori without disturbance gut microbiome. *Nanomedicine* 20:102019. doi: 10.1016/j.nano.2019.102019

Conflict of Interest: The authors declare that the research was conducted in the absence of any commercial or financial relationships that could be construed as a potential conflict of interest.

Advantages of publishing in Frontiers

OPEN ACCESS
Articles are free to read for greatest visibility and readership

FAST PUBLICATION
Around 90 days from submission to decision

HIGH QUALITY PEER-REVIEW
Rigorous, collaborative, and constructive peer-review

TRANSPARENT PEER-REVIEW
Editors and reviewers acknowledged by name on published articles

Frontiers
Avenue du Tribunal-Fédéral 34
1005 Lausanne | Switzerland

Visit us: www.frontiersin.org
Contact us: frontiersin.org/about/contact

REPRODUCIBILITY OF RESEARCH
Support open data and methods to enhance research reproducibility

DIGITAL PUBLISHING
Articles designed for optimal readership across devices

FOLLOW US
@frontiersin

IMPACT METRICS
Advanced article metrics track visibility across digital media

EXTENSIVE PROMOTION
Marketing and promotion of impactful research

LOOP RESEARCH NETWORK
Our network increases your article's readership